

DEVELOPMENT OF *IN SITU* GEL CONTAINING
ASIATICOSIDE-CYCLODEXTRIN COMPLEX FOR
PERIODONTAL TISSUE REGENERATION

Miss Hay Man Saung Hnin Soe



A Thesis Submitted in Partial Fulfillment of the Requirements
for the Degree of Master of Science in Pharmacy in Pharmaceutics
Department of Pharmaceutics and Industrial Pharmacy
Faculty of Pharmaceutical Sciences
Chulalongkorn University
Academic Year 2018
Copyright of Chulalongkorn University

การพัฒนาเอกสารเองที่มีสารประกอบเชิงซ้อนของเอเชียติโคไซด์-ไซโคลเดกซ์ทรินสำหรับการ
ฟื้นฟูเนื้อเยื่อปริทันต์



วิทยานิพนธ์นี้เป็นส่วนหนึ่งของการศึกษาตามหลักสูตรปริญญาเภสัชศาสตรมหาบัณฑิต
สาขาวิชาเภสัชกรรม ภาควิชาวิทยาการเภสัชกรรมและเภสัชอุตสาหกรรม
คณะเภสัชศาสตร์ จุฬาลงกรณ์มหาวิทยาลัย
ปีการศึกษา 2561
ลิขสิทธิ์ของจุฬาลงกรณ์มหาวิทยาลัย

Thesis Title	DEVELOPMENT OF <i>IN SITU</i> GEL CONTAINING ASIATICOSIDE- CYCLODEXTRIN COMPLEX FOR PERIODONTAL TISSUE REGENERATION
By	Miss Hay Man Saung Hnin Soe
Field of Study	Pharmaceutics
Thesis Advisor	Phatsawee Jansook, Ph.D.
Thesis Co Advisor	WANCHAI CHONGCHAROEN, Ph.D.

Accepted by the Faculty of Pharmaceutical Sciences,
Chulalongkorn University in Partial Fulfillment of the Requirement for
the Master of Science in Pharmacy

..... Dean of the Faculty of
Pharmaceutical Sciences
(Assistant Professor RUNGPETCH
SAKULBUMRUNGSIL, Ph.D.)

THESIS COMMITTEE

..... Chairman
(Associate Professor PARKPOOM
TENGAMNUAY, Ph.D.)

..... Thesis Advisor
(Phatsawee Jansook, Ph.D.)

..... Thesis Co-Advisor
(WANCHAI CHONGCHAROEN, Ph.D.)

..... Examiner
(Jittima Luckanagul, Ph.D.)

..... Examiner
(Assistant Professor Dusadee Charnvanich,
Ph.D.)

..... External Examiner
(Associate Professor Wandee Rungseevijitprapa)

เส มั่น ชวง นิน โช : การพัฒนาเจลก่อตัวเองที่มีสารประกอบเชิงซ้อนของเอเชียติโคไซด์-ไซโคลเดกซ์ทริน
 สำหรับการฟื้นฟูเนื้อเยื่อปริทันต์. (DEVELOPMENT OF *IN SITU* GEL
 CONTAINING ASIATICOSIDE-CYCLODEXTRIN COMPLEX FOR
 PERIODONTAL TISSUE REGENERATION) อ.ที่ปรึกษาหลัก : อ. ภก. ดร.ภาสวีร์
 จันทร์สุก, อ.ที่ปรึกษาร่วม : อ. ภก. ดร.วันชัย จงเจริญ

เอเชียติโคไซด์ เป็นสารที่มีฤทธิ์จากพืชสมุนไพรบัวบก (*Centella asiatica*) ช่วยในการกระตุ้นการสร้างคอลลาเจนไทป์วัน และช่วยในการเจริญเติบโตของเซลล์กระดูกอ่อนซี่รอบๆ ตัวฟัน อย่างไรก็ตาม เอเชียติโคไซด์มีค่าการละลายน้ำน้อยอาจส่งผลให้ลดชีวปริมาณออกฤทธิ์ได้ ดังนั้นวัตถุประสงค์ในการศึกษาครั้งนี้คือ การพัฒนาสูตรตำรับเจลก่อตัวเองเมื่อกระตุ้นด้วยอุณหภูมิบรรจุเอเชียติโคไซด์โดยใช้ไซโคลเดกซ์ทริน ทำการศึกษาการเพิ่มการละลายเอเชียติโคไซด์โดยใช้ไซโคลเดกซ์ทริน เลือกใช้ไฮดรอกซีโพรพิลบีต้า (HPβCD) และซัลโฟบิวทิลเอเธอร์บีต้า (SBEβCD) เนื่องจากสามารถเพิ่มการละลายเอเชียติโคไซด์ได้ ในการประเมินผลของพอลิเมอร์ต่อการเพิ่มการละลายของสารประกอบทุดิยภูมิของ เอเชียติโคไซด์/SBEβCD ใช้พอลิเมอร์เกาะติดเยื่อเมือก ไคโตซาน (Chitosan, CS) และพอลิเมอร์ก่อเจล พอลลอกซาเมอร์ 407 (poloxamer, P407) พบว่าช่วยเพิ่มการละลายในรูปแบบทุดิยภูมิได้ จากการประเมินสารประกอบเชิงซ้อนทุดิยภูมิและทุดิยภูมิ ในสภาวะสารละลายโดยเทคนิค ¹H-NMR และสภาวะของแข็งได้แก่ เทคนิค DSC FT-IR และ PXRD พบว่ามีอันตรกิริยาเกิดขึ้นและอาจเกิดสารประกอบเชิงซ้อนระหว่างเอเชียติโคไซด์และไซโคลเดกซ์ทริน สารประกอบเชิงซ้อนดังกล่าวสามารถเพิ่มอัตราการละลายของเอเชียติโคไซด์ได้เมื่อเทียบกับการใช้ตัวยาอย่างเดียว การศึกษาลักษณะทางสัณฐานวิทยาและขนาดอนุภาคโดยเทคนิค TEM และ DLS พบว่ามีการเกาะกลุ่ม (aggregates) ของอนุภาคนานาขนาดใหญ่ ซึ่งชี้ให้เห็นว่าการเพิ่มการละลายของเอเชียติโคไซด์นั้นมาจากการเกิดการเกาะกลุ่มของสารประกอบเชิงซ้อน หรือมีพฤติกรรมในลักษณะคล้ายไมเซลล์ การเตรียมอนุภาคนานาบรรจุเอเชียติโคไซด์ใช้เทคนิคไอโอดีนจิลเลชัน โดยใช้ SBEβCD เป็นประจุลบ และ CS เป็นประจุบวก พัฒนาสูตรตำรับเจลก่อตัวเองที่กระตุ้นด้วยอุณหภูมิบรรจุอนุภาคนานาของเอเชียติโคไซด์/SBEβCD/CS ในอัตราส่วนค่อน้ำหนักที่เหมาะสม เมื่อนำมาศึกษาคุณสมบัติทางเคมีกายภาพและทางเคมี ได้แก่ ลักษณะทางกายภาพ ความเป็นกรด-ด่าง ความหนืด อุณหภูมิและเวลาในการก่อเจล ความสามารถในการก่อเจล ปริมาณตัวยาสำคัญ การกักเก็บยาในอนุภาค พบว่าผลการประเมินอยู่ในช่วงที่ยอมรับได้ มีการเกาะติดเยื่อเมือกที่ดีและมีการปลดปล่อยสารออกฤทธิ์แบบเนิ่น สูตรตำรับค่อน้ำหนักให้ผลเชิงลบกับเซลล์กามาเมนต์ อย่างไรก็ตามปริมาณเอเชียติโคไซด์ที่ใช้ค่อน้ำหนักต่ำร่วมกับอยู่ในระบบสารประกอบเชิงซ้อนและแอนแคลพูเลชันซึ่งสามารถแสดงการเพิ่มปริมาณของคอลลาเจนไทป์วันในเซลล์ได้ ดังนั้นสูตรตำรับดังกล่าวจึงมีความเป็นไปได้ที่จะสามารถนำส่งเอเชียติโคไซด์สำหรับการฟื้นฟูเนื้อเยื่อปริทันต์

สาขาวิชา เกษษกรรม
 ปีการศึกษา 2561

ลายมือชื่อนิสิต
 ลายมือชื่อ อ.ที่ปรึกษาหลัก
 ลายมือชื่อ อ.ที่ปรึกษาร่วม

6076123833 : MAJOR PHARMACEUTICS

KEYWORD ASIATICOSIDE/ CYCLODEXTRIN/ IN SITU GEL/
D: PERIODONTITIS

Hay Man Saung Hnin Soe : DEVELOPMENT OF *IN SITU* GEL CONTAINING ASIATICOSIDE-CYCLODEXTRIN COMPLEX FOR PERIODONTAL TISSUE REGENERATION. Advisor: Phatsawee Phatsawee Jansook, Ph.D. Co-advisor: WANCHAI CHONGCHAROEN, Ph.D.

Asiaticoside (AS) is active herbal compound isolated from *Centella asiatica*. It has the potential benefit in promoting type I collagen (COL I) synthesis and osteogenic differentiation in human periodontal ligament cells. However, it has low aqueous solubility which may hamper the bioavailability. Thus, the main objective of this study was to develop the thermoresponsive *in situ* gels containing AS by using cyclodextrin (CD). To determine the solubility enhancement of AS, phase-solubility profiles were investigated and revealed that CDs enhanced the aqueous solubility of AS. Hydroxypropyl-beta-CD (HP β CD) and sulfobutyl-ether-beta-CD (SBE β CD) were selected due to highly solubilization enhancement of AS. The mucoadhesive polymer i.e., chitosan (CS) or thermogelling agent i.e., poloxamer 407 (P407) was added to investigate the effect of polymer to AS/SBE β CD binary complex. The resulted ternary systems synergistically improved the solubility of AS. Solution-state characterization (¹H-NMR) and solid-state characterization (DSC, FT-IR and PXRD) of binary complex (AS/HP β CD or AS/SBE β CD) as well as ternary complex (AS/SBE β CD/CS or AS/SBE β CD/P407) were performed. It indicated that there were some interactions and possibly formed AS/CD inclusion complex. The enhancement of AS dissolution was achieved in both binary and ternary system when compared with intact AS alone. The morphology and particle size were analyzed by TEM and DLS techniques. The large aggregate size provided the evidence that AS solubility was enhanced through the AS/CD aggregate formation or micelle-like behavior. AS loaded nanoparticles were prepared via ionic gelation using anionic SBE β CD and cationic CS. Thermally triggered *in situ* gels containing AS with the proper SBE β CD/CS weight ratio were developed. The physicochemical and chemical characterizations i.e., appearance, pH, viscosity, gelation temperature, gelation time, *in vitro* gelling capacity, drug content and entrapment efficiency were within acceptable range. *In vitro* mucoadhesion and the *in vitro* release studies revealed that nanoencapsulated *in situ* gels had excellent mucoadhesive property and performed the sustained release of AS. These formulations somewhat negative effect to ligament cells. However, the CD encapsulated platforms containing AS at low content could

Field of Study: Pharmaceutics

Student's Signature

Academic Year: 2018

.....
Advisor's Signature

Year:

.....
Co-advisor's Signature

.....

ACKNOWLEDGEMENTS

First and foremost, I would like to express my deepest gratitude to my thesis advisor, Phatsawee Jansook, Ph.D. for his valuable supervision, helpfulness, guidance, patience, kindness, understanding and encouragement throughout my study. He not only guided me for research but also taught to improve other weakness that are very beneficial for my lifelong career. His ultimate mentorship helped me effectively to improve my knowledge and to accomplish my research on time.

My sincere gratitude is extended to my thesis co-advisor, Wanchai Chongcharoen, Ph.D. for his kindness, advice and guidance.

I would like to thank my thesis committee for the valuable comments and suggestions to complete and succeed my thesis.

I would like to express much appreciation to Chulalongkorn University for CU-ASEAN Scholarship.

I would like to special thank to Agricultural Research Development Agency (ARDA) for financial support to finish this study.

I would like to manifest the gratefulness to every teachers and staffs in Department of Pharmaceutics and Industrial Pharmacy, Faculty of Pharmaceutical Sciences, Chulalongkorn University. They provided knowledge and generous supports for laboratory equipment and other facilities to perform research work effectively and smoothly.

Moreover, I would like to thank Master of Science program in cosmetic science in our department for kindly permitted to use Rheometer and Chulalongkorn University Centenary Academic Development Project for supporting powder X-ray diffractometer within CU.D.HIP to fulfill my research. In addition, I would like to thank Professor Dr. Prasit Pavasant from

Faculty of Dentistry for kindly donated Human Periodontal Ligament Cells. Furthermore, I would like to thank Jittima Luckanagul, Ph.D. and Sirikool Thamnum for their kind help to fulfill in vitro cytotoxicity and immunocytochemistry experiments.

I would like to pass my heartfelt thanks to all my lab members for their invaluable suggestions, encouragement and help throughout the research.

I am gratefully thanks to Ministry of Health, Myanmar and University of Pharmacy, Mandalay, Myanmar for giving permission to study a Master of Science (Pharmaceutics) program in Chulalongkorn University.

Above all, I would like to express my sincere thanks to my parents, my elder brother and my two elder sisters for their never-ending support and encouraging words, which are extremely valuable and precious for me to finish my study.

Finally, I wish to thank other persons whose names have not been mentioned here for their assistance and encouragement.

TABLE OF CONTENTS

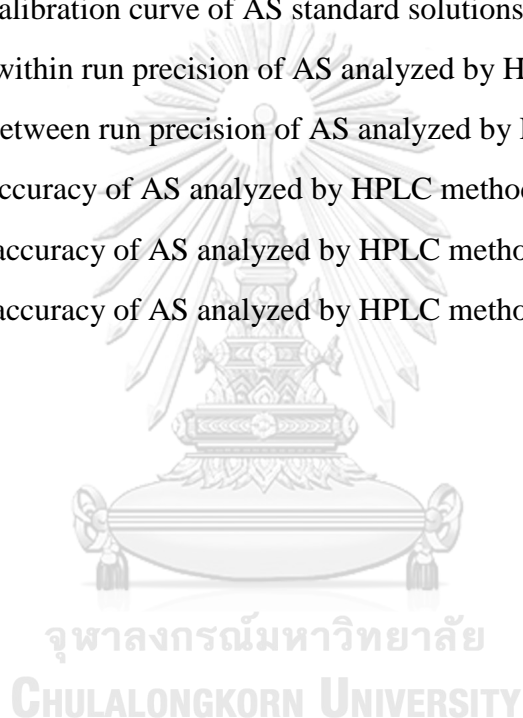
	Page
ABSTRACT (THAI)	iii
ABSTRACT (ENGLISH).....	iv
ACKNOWLEDGEMENTS.....	v
TABLE OF CONTENTS.....	vii
LIST OF TABLES	x
LIST OF FIGURES	xii
LIST OF ABBREVIATION.....	1
CHAPTER I INTRODUCTION.....	3
CHAPTER II LITERATURE REVIEW	9
1. Periodontal Diseases.....	9
2. Treatment of periodontal diseases	10
3. Periodontal wound healing and regeneration	11
4. Asiaticoside (AS).....	12
4.1 Physicochemical properties of AS	13
4.2 Mechanism of action in wound healing	14
5. Cyclodextrins (CDs).....	15
5.1 CD complexation and drug solubility.....	16
5.2 Effect of polymers to enhance CD solubilization.....	19
6. Local drug delivery systems for the treatment of periodontitis.....	20
7. In situ gelling system.....	22
8. Nanoparticles in periodontal drug delivery system	25
CHAPTER III MATERIALS AND METHODS	27
CHAPTER IV RESULTS AND DISCUSSION.....	47
1. pH-solubility profiles	47
2. Thermal stability of AS in aqueous solution.....	48

3.	Solubility determinations	49
3.1	The effect of CD on AS solubilization	49
3.2	The effect of water-soluble polymers on AS/SBE β CD complexation	52
4.	^1H -NMR determinations	54
5.	Solid-state characterization	61
5.1	DSC analysis.....	61
5.2	FT-IR spectroscopy	63
5.3	Powder X-Ray Diffraction (PXRD)	65
6.	<i>In vitro</i> release study	67
7.	Morphology, particle size and zeta potential analysis ...	69
8.	Preparation and characterization of drug-free and drug- loaded SBE β CD/CS nanoparticles	73
9.	Physicochemical and chemical characterizations	77
9.1	Appearance, pH, viscosity, and syringeability and injectability .	77
9.2	Gelation temperature, gelation time and <i>in vitro</i> gelling capacity	79
9.3	Particle size and size distribution, zeta potential and %EE.....	81
10.	Rheological study.....	83
11.	<i>In vitro</i> mucoadhesion.....	87
12.	<i>In vitro</i> release studies.....	89
13.	<i>In vitro</i> cytotoxicity.....	91
14.	Immunocytochemistry.....	93
CHAPTER V CONCLUSION.....		96
REFERENCES		98
APPENDIX.....		120
VITA.....		131

LIST OF TABLES

	Page
Table 1 Some physicochemical properties of natural cyclodextrins and selected cyclodextrin derivatives of pharmaceutical interest (modified from Ref. (21, 53)). ...	17
Table 2 The composition of thermoresponsive in situ gel formulations containing asiaticoside.....	40
Table 3 Percentage of AS remaining in pure water and aqueous solution containing 2.5% and 5% w/v SBE β CD after zero to three heating cycles in autoclave at 121 $^{\circ}$ C for 20 min. (Mean \pm S.D., n=3).....	48
Table 4 Percentage of AS remaining in pure water and aqueous solution containing 2.5% and 5% w/v SBE β CD after zero to three heating cycles in ultrasonic bath at 60 $^{\circ}$ C for 30 min. (Mean \pm S.D., n=3).....	49
Table 5 The values of the apparent stability constant ($K_{1:1}$) and the.....	52
Table 6 The values of apparent stability constant ($K_{1:1}$) and the complexation efficiency (CE) of AS/SBE β CD complex in aqueous.....	54
Table 7 The 1 H-chemical shifts of AS alone and in the presence of HP β CD.....	56
Table 8 The 1 H-chemical shifts of AS alone and in the presence of SBE β CD	58
Table 9 The 1 H-chemical shifts of AS alone and in ternary complex (AS/SBE β CD/CS).....	59
Table 10 The 1 H-chemical shifts of AS alone and in ternary complex (AS/SBE β CD/P407)	60
Table 11 Dissolution parameters of solid complexes	69
Table 12 Mean particle size and zeta potential of binary AS/CD, and ternary AS/SBE β CD/polymer complex aggregates.....	72
Table 13 Mean particle size, PDI and zeta potential values of drug loaded SBE β CD/CS micro- and nanoparticles	76

Table 14 pH, viscosity, syringeability and injectability of in situ gel formulations containing asiaticoside (Mean±S.D., n=3)	78
<i>Table 15 Gelation temperature ($T_{sol-gel}$), gelation time and in vitro gelling capacity of in situ gel formulations (n=3, Mean±S.D.).....</i>	<i>80</i>
Table 16 Particle size and size distribution (PDI), zeta potential and %EE of asiaticoside loaded in situ gel formulations	83
Table 18 Data of calibration curve of AS standard solutions (No.1).....	124
Table 19 Data of calibration curve of AS standard solutions (No.2).....	125
Table 20 Data of calibration curve of AS standard solutions (No.3).....	126
Table 21 Data of within run precision of AS analyzed by HPLC method	127
Table 22 Data of between run precision of AS analyzed by HPLC method	128
Table 23 Data of accuracy of AS analyzed by HPLC method (No.1).....	129
Table 24 Data of accuracy of AS analyzed by HPLC method (No.2).....	129
Table 25 Data of accuracy of AS analyzed by HPLC method (No.3).....	130



LIST OF FIGURES

	Page
Figure 1 Periodontal disease and pocket formation.....	10
Figure 2 Chemical structure of asiaticoside.....	13
Figure 3 Schematic presentation of parent cyclodextrins (54)	15
Figure 4 Graphical representations of A and B-type phase–solubility profiles (53). ..	19
Figure 5 Chemical Structure of P407.....	24
Figure 6 Chemical structure of CS.....	25
Figure 7 pH-solubility profile of asiaticoside	47
Figure 8 Phase-solubility profiles of asiaticoside in aqueous cyclodextrin solutions (a): β CD (●), (b): HP β CD (■), SBE β CD (◆), CM β CD (▲).....	51
Figure 9 Phase-solubility profiles of asiaticoside in aqueous SBE β CD solution containing (a) 0.01 mM CS and (b) 10 mM P407.	53
Figure 10 DSC thermograms of (a) pure AS, (b) pure HP β CD, (c) PM	62
Figure 11 FT-IR spectra of (a) pure AS, (b) pure HP β CD, (c) PM AS/HP β CD, (d) FD AS/HP β CD (e) pure SBE β CD, (f) PM AS/SBE β CD, (g) FD AS/SBE β CD, (h) FD AS/SBE β CD/CS, (i) FD AS/SBE β CD/P407	64
Figure 12 The PXRD spectra of (a) pure AS, (b) pure HP β CD, (c) PM AS/HP β CD, (d) FD AS/HP β CD, (e) pure SBE β CD, (f) PM AS/SBE β CD, (g) FD AS/SBE β CD, (h) FD AS/SBE β CD/CS, (i) FD AS/SBE β CD/P407.....	66
Figure 13 In vitro release study of AS, FD AS/SBE β CD, FD AS/HP β CD, FD AS/SBE β CD/CS and FD AS/SBE β CD/P407.	68
Figure 14 TEM photographs of AS saturated in 5% HP β CD or 2.5% SBE β CD solutions without and with polymers (5% P407 or 1% CS, all % w/w) (a) AS/HP β CD, (b) AS/SBE β CD, (c) AS/SBE β CD/P407, and (d) AS/SBE β CD/CS	73

Figure 15 Phase-diagram of SBE β CD/CS nanoparticle formation with three areas; clear solution (\circ), opalescent dispersion (\blacktriangle) and aggregates (\blacksquare)	74
Figure 16 G' and $\tan \delta$ vs frequency profile of in situ gel formulations at 37 °C; (a) F4-F6, (b) F7-F9, (c) F10-F12, (d) F13-F15.....	86
<i>Figure 17 Dynamic viscosity (η') vs frequency profile of in situ gel formulations at 37 °C; (a) F4-F6, (b) F7-F9, (c) F10-F12, (d) F13-F15.....</i>	<i>87</i>
Figure 18 Percentage of the AS remaining on the mucin coated semipermeable membrane.....	89
Figure 19 In vitro release profiles of AS in in situ gel formulations (F9, F12 and F15) through semi-permeable membrane MWCO 3,500 Da.....	90
Figure 20 MTT assay results on HPDLCs after 24 hr incubation with blank (B9, B12, B15) and asiaticoside loaded (F9, F12, F15) in situ gel formulations. Bar chart showed no statistically significant difference for cytotoxicity among groups compared in the cell treatment with 16.7 μ M of asiaticoside in each in primary cell culture media.....	92
Figure 21 The transmission light microscope picture shown regular cell morphology of HPDLCs at (a) 4X objective lens and (b) 10X objective lens.....	93
Figure 22 Photograph represented type I collagen (COL 1) synthesis in HPDLCs on the 24 hr treatment of AS loaded in situ gels by immunostaining assay; respectively; microscope images of HPDLCs at 10X objective lens, scale bars: 500 μ m	94
Figure 23 The HPLC chromatograms of (A) β CD, (B) HP β CD, (C) CM β CD, (D) SBE β CD, (E) CS, (F) P407, (G) SSF, (H) PBS, (I) BAC and mobile phase.	121
Figure 24 The HPLC chromatograms of AS standard solution (A) 12.5 μ g/mL, (B) 25 μ g/mL, (C) 50 μ g/mL, (D) 100 μ g/mL, (E) 200 μ g/mL, (F) 400 μ g/mL, (G) 600 μ g/mL, (H) 800 μ g/mL, (I) 1000 μ g/mL and (J) 1% w/w AS loaded in situ gel dissolved in methanol:water (30:70 v/v).....	123
Figure 25 Calibration curve of AS standard solutions by HPLC method (No.1)	124
Figure 26 Calibration curve of AS standard solutions by HPLC method (No.2)	125
Figure 27 Calibration curve of AS standard solutions by HPLC method (No.3)	126

LIST OF ABBREVIATION

%	percentage
°C	degree Celsius
μg	microgram (s)
μl	microliter (s)
M	molarity
αCD	alpha-cyclodextrin
βCD	beta-cyclodextrin
γCD	gamma-cyclodextrin
HPβCD	hydroxypropyl-beta-cyclodextrin
CMβCD	carboxymethyl-beta-cyclodextrin
BAC	benzalkonium chloride
CD	cyclodextrin
CE	complexation efficiency
CS	chitosan
DSC	differential scanning calorimetry
DLS	dynamic light scattering
e.g.	for example
Eq.	equation
FT-IR	Fourier-transform infra-red spectroscopy
FD	freeze dried
HPLC	high performance liquid chromatography
¹ H-NMR	proton nuclear magnetic resonance
K	stability constant
Da	dalton

MWCO	molecular weight cut-off
nm	nanometer
PXRD	powder X-ray diffraction
PM	physical mixture
rpm	revolutions per minute
RSD	relative standard deviation
R ²	coefficient of determination
SBE β CD	sulfobutylether-beta-cyclodextrin
SSF	simulated salivary fluid
SD	standard deviation
TEM	transmission electron microscopy



CHAPTER I

INTRODUCTION

Periodontal disease is a term to describe the several pathological conditions in periodontal area and characterized by inflammation of gums, degeneration of periodontal ligaments, alveolar bones and dental cementum. It is mainly caused by anaerobic bacterial infection within periodontal pocket via formation of subgingival plaque (1). Periodontal pathogens produce bacterial endotoxins that can breakdown the extracellular matrices as well as host cell membranes to produce nutrients for their growth. As the mild disease condition, inflammation is occurred in the gingiva termed gingivitis but as it progresses to deeper tissues leading to periodontitis. In the later phase of the disease, gingival swelling, bleeding and bad breath are recognized; subsequently, the supporting collagen of the periodontium is degenerated. Later the alveolar bone resorps and gingival epithelium migration along the tooth surface, a 'periodontal pocket' is formed (2).

The epidemiology, etiology, pathogenesis and microbiology of periodontal pocket flora have been revised as the strategies for the management of intra-periodontal pocket disease progressions. Standard periodontal therapy includes scaling and root planning, flap surgery with and without bone grafts, root amputation, strict plaque control and so on (1, 3). Scaling and root planning are generally successful to a moderate content but the recurrence rate of periodontitis is high. The use of antibiotics is beneficial for the treatment of periodontitis, however there are several disadvantages i.e., inadequate antibiotic concentration at the site of the periodontal pocket and a rapid decline of the plasma antibiotic concentration reached to sub-therapeutic levels. Because of these several

drawbacks, the development of novel intra-pocket drug delivery systems for the treatment of periodontal diseases have been emerged (4).

Treatment with local devices directly into the periodontal pocket not only can increase the drug concentration at the site of action, but also can prevent the undesirable side effects (5). Currently, the advanced formulations for periodontitis treatment such as fibers, films, strips, microparticles, nanoparticles and gels have been developed to retain antibiotics in the periodontal pockets with the concentration higher than their minimal inhibitory concentration against bacteria (6-11). According to the etiology of periodontal diseases and anatomy of periodontal pockets, the local drug delivery system for periodontitis should be easy to administer into the pocket and remain in place for prolong period of time to maintain the effective concentration within the periodontal pocket. In addition, patient compliance should be improved and the device should be cost effective as well (12).

The numerous therapeutic agents and devices have been introduced into the market such as Actisite® fiber containing ethylene vinyl acetate with 25% w/w tetracycline hydrochloride. Although it has controlled released property with good clinical efficacy, patients are suffered discomfort during the placement and removal of fiber, and need anaesthesia (10). Recently, Periochip® has been marketed as a chlorhexidine digluconate film containing cross-linked hydrolysed gelatin and glycerine for local delivery. An initial burst release followed by a constant slow release was occurred about seven days (13). Synthetic biodegradable polymers have also been evaluated for sustained release of drug in the periodontal pocket. The combination of amoxicillin and metronidazole in the carrier polymer [poly (lactide-co-glycolide)] PLGA

showed an extended therapeutic efficacy of antimicrobial agents (14). Another *in situ* forming implant is Atridox®, the injectable system composed of biocompatible solvent N-Methyl-2-Pyrrolidone (NMP) with 10% w/w doxycycline hyclate. After injection, it can transform from solution state to solid state via solvent displacement mechanism and can sustain drug release more than seven days (15). The *in situ* implant containing the combination of 5% w/w secnidazole and doxycycline hydrochloride based on biodegradable polymer 25% w/w PLGA was developed to increase the spectrum of the antimicrobial activity against the microorganisms which causing periodontal diseases. The developed implant showed initial faster release rate with a promising antimicrobial activity against aerobic and anaerobic bacteria in comparison with marketed product Atridox® (16).

Although local drug delivery of antibiotics can provide effective treatment for periodontitis to some extent, the damaged periodontal wound is not completely healed and the soft tissue of periodontal area especially periodontal ligament is not being regenerated. Nowwarote et al., (2013) (17) had reported that asiaticoside (AS) might be an alternative therapeutic agent for periodontal tissue healing which has been shown to promote both soft and hard tissue formation and osteogenic differentiations of human periodontal ligament cells. Bonte et al., (1994) (18) also reported that AS can promote type I collagen production which is a major soft tissue component of the periodontal ligament in human dermal fibroblasts. AS is one of the major triterpene derivatives of *Centella asiatica*, which is plenty in Asian countries and well known as ‘Buabok’ in Thailand (19). However, AS has the very low aqueous solubility which may hamper the permeability

of AS through the biological membranes resulting in insufficient drug level at the periodontal pocket.

Several methods are used to increase the aqueous solubility of poorly soluble drugs. The complexation by cyclodextrins (CDs) as inclusion complex is the promising strategy to enhance the solubility of drugs. CDs are cyclic oligosaccharides of toroid structure and possessed hydrophilic outer surface and lipophilic central cavity. The most common parent CDs are α , β , and γ CD with 6, 7 and 8 glucopyranose units, respectively. CDs have ability to enhance the aqueous solubility of various poorly water-soluble drugs by inserting the lipophilic drug into central hydrophobic cavity (20). However, due to the limited aqueous solubility and complexing ability of the natural CDs, the CD derivatives were synthesized. The CD derivatives such as 2-hydroxypropyl- β CD (HP β CD) and sulfobutylether- β CD (SBE β CD) can dramatically improve their solubilities and becoming more interesting in pharmaceutical applications. CDs have the molecular weight of about 1,000 - 2,000 Da and possess the negative Log P, therefore, they are poorly absorbed through biological membranes (21).

In situ gels are developed as a novel drug delivery system in a liquid dosage form but once administered, they can form gel under physiological stimuli such as pH, temperature, solvent exchange, ultra violet (UV) irradiation and the presence of specific ions or molecules, etc. (22). Ease of application and reduced frequency of administration are advantages of these smart delivery system. Various natural and synthetic polymers such as chitosan, poloxamer 407, carbopol 934P, hydroxyethyl cellulose and polycarbophil are widely used for the preparation of *in situ* gel dosage form. They can be easily injected through a syringe into the periodontal

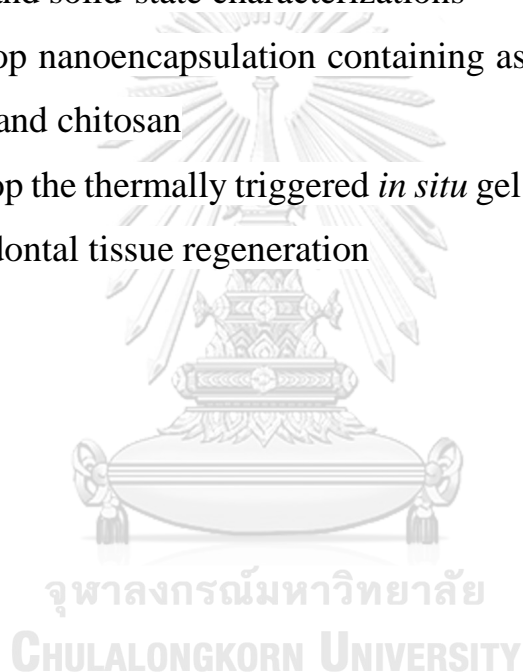
pocket where it solidifies *in situ* to deliver the therapeutic agent for a prolonged period (7, 23, 24).

It is known that the major problem of the periodontal treatment is the difficulty of the therapeutic drug level reached at the target site. It is due to the fact that periodontal pocket is the complex region with the constant flow of crevicular fluid. The delivered drug will be removed from the application site within the short period of time and consequently leading to suboptimal therapeutic effect. In present study, thermoresponsive *in situ* gelling systems will be investigated since they have superior advantages i.e., ease of application, low costs and can form gel via environmental stimuli after administration into the periodontal pocket. Nevertheless, they have some considerable drawbacks, for example, burst release of drug in small periodontal cavity that can negatively affect the drug release mechanism.

Microencapsulation technique has been widely used to retain the drug within the polymer matrix. The micro- and nanoparticles can be further incorporated into mucoadhesive or stimuli sensitive hydrogels to obtain synergistic controlled release of drug. In this study, polyanionic β CD derivatives (SBE β CD or carboxymethyl- β CD (CM β CD)) was selected and encapsulated with chitosan (CS) via ionic gelation technique. CS is the non-toxic, biocompatible and biodegradable polysaccharide with favorable mucoadhesive property (25). This platform will enhance the prolong residence time by interaction with negatively charge mucin in periodontal pocket. The solid and solution state characterizations of AS/CD complex will be performed. Then, the poloxamer based thermoresponsive *in situ* gel formulations containing AS will be developed. The physicochemical and chemical properties of these

formulations will be determined. In addition, the mucoadhesion properties, *in vitro* permeation, cytotoxicity and type I collagen synthesis will be evaluated. Thus, the main objectives of this work are as follows:

1. To study the cyclodextrin solubilization of asiaticoside by using parent cyclodextrin and its derivatives
2. To prepare the binary asiaticoside/cyclodextrin and ternary asiaticoside/cyclodextrin/ polymer complexes and evaluate by solution and solid-state characterizations
3. To develop nanoencapsulation containing asiaticoside/cyclodextrin complex and chitosan
4. To develop the thermally triggered *in situ* gel containing asiaticoside for periodontal tissue regeneration



CHAPTER II

LITERATURE REVIEW

1. Periodontal Diseases

Periodontal disease or periodontitis is highly prevalent periodontal tissue infections. Approximately 10% of the adult population is highly susceptible to severe periodontal disease (26-28). According to epidemiologic studies in the United States, in 0.2 % to 0.5% of children and young adults suffer from severe attachment loss. National Health and Nutrition Examination Survey (NHANES) also reported that the total prevalence of periodontitis in adults of 30 was 47.2 % (29).

The major causative pathogens which can render the periodontal diseases are *Porphyromonas gingivalis*, *Tannerella forsythensis* and the spirochete *Treponema denticola*. These organisms reside as plaques on the teeth and release the bacterial leucotoxins, collagenases, fibrinolysins and other proteases (30). The released endotoxins mostly affect the tissues surrounding the teeth and subsequently causing gingivitis as the early stage. Gingivitis is milder form that cannot defect the underlying supporting structure of the teeth and reversible. However, as the more severe case, swelling and bleeding of the gum is observed. When the inflammatory responses are induced, the matrix metalloproteinases (MMPs) are increasingly expressed and collagen is destroyed. Generally, the fibroblasts of periodontal ligament produce collagen and ground substances that can turn over. However, under the condition of periodontal disease, the periodontal ligament that supporting the tooth is degenerated. Later, as the gingival epithelial cells migrate along with the tooth, a space known as periodontal pocket is formed between the gingiva and tooth

(Figure 1). Then, the disease state is termed as periodontitis. The gingiva loss their attachments to the teeth and progressively causing the deep periodontal pocket. The destruction of connective tissue as well as of alveolar bone resulting in incompletely support for the teeth; unfortunately, the tooth loss (30, 31).

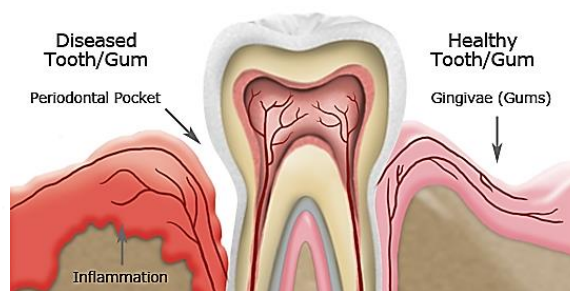


Figure 1 Periodontal disease and pocket formation
 (<https://www.arthurkentdds.com>)

2. Treatment of periodontal diseases

The periodontal pocket has been investigated as the ideal environment for the growth and proliferation of anaerobic pathogenic organisms (32). The aims of periodontal treatment include to inhibit disease progression, to prevent its recurrence and to preserve the teeth in a healthy status (30). The various therapies (nonsurgical and surgical) are performed according to the specific disease and severity.

For the clinical treatment of periodontal diseases, the conventional and the first-choice of therapy is plaque control. The treatment procedure is called scaling and root planing. Scaling is performed to remove the plaque and calculus (tartar) from the surface of tooth root in both supra and sub-gingival position. At the same time, root planing is carried out to remove bacterial toxins that adsorbed on cemental surface and limits

plaque recurrence. Although scaling and root planning can achieve good efficacy in initial periodontitis, this mechanical treatment alone is not enough in severe cases. The pathogenic organisms can recolonize and the recurrence of periodontitis can occur. Therefore, the antimicrobial therapy is used as an adjunct to scaling and root planning (33).

Another option is the surgical removal of calculus and subgingival biofilms together with the patient's oral hygiene practices to prevent bacterial recolonization. Bony defects can be surgically fixed in order to reduce periodontal pocket depth (34). In addition, systemic antimicrobial agents have been administered for the treatment of periodontitis. However, the drug concentration that reached to periodontal pocket is quite low and cannot provide the sufficient antimicrobial treatment leading to the risk of bacterial resistance (35). Because of these limitations, the localized administration of therapeutic agents has been given attention for the treatment of periodontitis (12).

3. Periodontal wound healing and regeneration

Although local antibiotic drug delivery systems can provide effective treatment for periodontal diseases to some extent, the wound healing of periodontium is not complete and the regeneration of periodontal soft tissue i.e., periodontal ligament is not being regenerated. The main function of periodontal ligament is to support the teeth as well as to regulate the cell reservoir for tissue homeostasis and regeneration. To consider the difficulties in with periodontal wound healing, repair and regeneration plays a key role as observed (36). For restoration of architecture and function of periodontium, several steps need to be

considered such as infected or degraded tissue elements must be eliminated, the pathogens should be free from wound healing site, progenitor cells should be populated and cell division should be adjacent to the wound. In addition, the repopulated cells must be able to differentiate and signaling factors to restore dynamic tissue homeostasis.

4. Asiaticoside (AS)

Centella asiatica, also known as Indian pennywort is perennial creeping herb, which is plenty in many Asian countries. This herb has been used in Ayurvedic and Chinese medicine for the treatment of skin diseases, gastro-intestinal tract and other psychotropic abnormalities (37), (38). It also has common name as ‘Buabok’ in Thailand. It has been reported that the plant extract contains major pentacyclic triterpene derivatives such as madecassoside, madecassic acid, asiaticoside, and asiatic acid (19).

One of the main components of the *Centella asiatica* (Linn.) namely asiaticoside (AS) is well known in possessing various pharmacological activities such as anxiolytic-like effect, antidepressant activity, neuroprotective effect, antipyretic and anti-inflammatory activities (39). It also has the potential benefits of wound healing activity by promoting collagen synthesis, enhancing the content of hydroxyproline, tensile strength, epithelialization as well as promoting fibroblast proliferation of the wounds (40). It has modulated the inflammatory response by inhibiting nitric oxide and tumor necrosis factor- α secretion from macrophages (41). In addition, it can provide the both soft and hard tissue regeneration for periodontal wound healing. Nowadays, therapeutic agents that used in periodontal tissues regeneration only facilitate hard tissue formation and

can lead to detrimental ankylosis. Nowwarote et al., (2013) revealed that AS might be an alternative therapeutic agent for periodontal tissue healing with the advantages of promoting both soft and hard tissue formation and osteogenic differentiations (17). In addition, it has been reported that AS can promote type I collagen synthesis which is a major soft tissue component of the periodontal ligament in human dermal fibroblasts (18). These properties of AS suggested that it could be useful in the treatment of periodontal wound healing.

4.1 Physicochemical properties of AS

Asiaticoside is the white odorless powder with the molecular weight of 959.12 Da and melting point 230-233 °C. Its chemical structure is similar to those of cholesterol, steroid and sex hormone (42) (Figure 2). Under hydrolytic condition, the glycoside portion of AS turned into asiatic acid. The aqueous solubility of AS is very low 0.67 mg mL^{-1} (43), so that the use of AS as active pharmaceutical component is quite limited even it possesses the potential benefits in wound healing process.

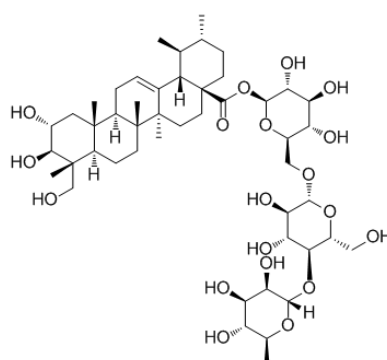


Figure 2 Chemical structure of asiaticoside

4.2 Mechanism of action in wound healing

AS was shown to increase production of collagen which promote angiogenesis and epithelialization when applied to skin wounds (40). AS was previously reported to promote type I collagen production in human dermal fibroblasts (18, 44, 45). Mechanistically, this occurred via activation of the Transforming Growth Factor-beta (TGF- β) receptor I kinase-independent Smad signaling pathway (46). The potential use of AS in tissue regeneration was previously investigated. The release of AS from electrospun gelatin and cellulose acetate fiber mats was studied and revealed that AS in fiber mats were stable up to 4 months after storage at room temperature or at 40°C (47). In addition, AS-loaded fiber mats promoted human dermal fibroblast attachment, proliferation, and extracellular matrix synthesis (47).

Apart from skin wound healing, periodontal wound healing requires the regeneration of both soft and hard tissues. In this regard, AS enhanced the synthesis of type I collagen, a major soft tissue component of the periodontal ligament. Furthermore, the ability of AS to promote osteogenic differentiation in human periodontal ligament cells (HPDLCs) suggests that it may be a viable treatment to promote hard tissue regeneration. Nowwarote et al., (2013) reported that AS induced type I collagen synthesis in HPDLs. The increased expression was occurred at both the mRNA and protein levels. In addition, AS decreased matrix metalloproteinase-1 (MMP-1) but increased tissue inhibitor of metalloproteinases-1 (TIMP-1) expression (17). AS promoted collagen homeostasis in HPDLCs by increasing its synthesis and attenuating its destruction. It has also been reported that fibronectin (FN) has a role in the early stage of osteogenesis and is also a critical element in bone

morphogenesis and differentiation process of calvarial osteoblastic cells (48, 49). Moreover, the normal osteogenic differentiation process of HPDLCs is marked by an increase in alkaline phosphatase (ALP) activity, N-linked glycoprotein synthesis i.e., osteopontin and mineralization (50, 51). AS also enhanced ALP enzymatic activity, osteoblast marker genes expression, and matrix mineralization and also stimulates HPDLCs differentiation toward the osteogenic lineage.

5. Cyclodextrins (CDs)

CDs are cyclic oligosaccharides, obtained from enzyme-catalyzed degradation of starch by glucosyltransferase (52). The molecular structure of CD resembles to a torus-like molecular ring, of which the inner cavity is hydrophobic, while the outer part is hydrophilic. α -cyclodextrin (α CD), β -cyclodextrin (β CD), and γ -cyclodextrin (γ CD) are parent CDs possessing 6, 7 and 8 glucopyranose units, respectively (Figure 3) (21). The primary hydroxyl groups are located on the narrow side of the torus and the secondary hydroxyl groups are located on the wider edge of CD structure (Figure 3). CDs have ability of enhancing aqueous solubility of various poorly water-soluble drugs by inserting the lipophilic moiety or molecule into central hydrophobic cavity (53).

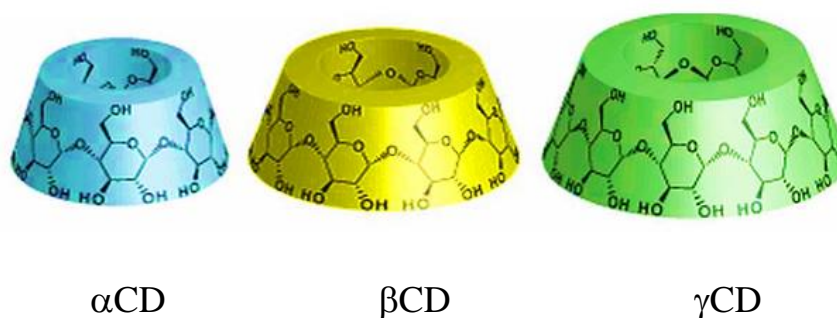


Figure 3 Schematic presentation of parent cyclodextrins (54)

Since the presence of intermolecular hydrogen bonds, native CDs are limited aqueous solubility and low affinity to form complex with lipophilic drugs, the CD derivatives were synthesized. Various β CD derivatives are modified such as randomly methylated- β CD (RM β CD), 2-hydroxypropyl- β CD (HP β CD) and sulfobutylether- β CD (SBE β CD) (Table 1).

5.1 CD complexation and drug solubility

Poorly water-soluble drugs have affinity to form complexation with CD in aqueous solution (21). Owing to the hydrophobic character of inner CD cavity, they can accommodate the lipophilic molecules into their inner cavity via inclusion complex formation and hence the solubility of the drug is significantly increased. When CD forms complexation with drug molecule, no covalent bonds are formed or broken. Generally, the complexes are in dynamic equilibrium with free molecules i.e., drug and CD in aqueous solution. The driving forces of the complexation include the release of water molecules from the cavity, electrostatic interactions, van der Waals' interactions, hydrophobic interactions, hydrogen bonding, the release of conformational and steric strains as well as charge-transfer interactions (53).

The number of physicochemical methods can be used to determine the drug/CD complex formation. The drug/CD complex in solution-state can be characterized by analytical methods such as UV/VIS absorbance (55), fluorescence spectroscopy (56), pH-potentiometric titration (57), nuclear magnetic resonance (NMR) (58) and permeation through different molecular weight cut-off (MWCO) of semipermeable membranes (59).

For the complex in solid-state, differential scanning calorimetry (DSC), powder X-ray diffraction (PXRD) and fourier-transform infrared spectroscopy (FT-IR) (60) are most commonly used to characterize the drug/CD complexation.

Table 1 Some physicochemical properties of natural cyclodextrins and selected cyclodextrin derivatives of pharmaceutical interest (modified from Ref. (21, 53)).

Cyclodextrin	Substitution ^a	MW (Da)	Solubility in water ^b (mg/ml)
α -cyclodextrin (α CD)	-	972	145
β -cyclodextrin (β CD)	-	1135	18.5
γ -cyclodextrin (γ CD)	-	1297	232
randomly methylated- β CD (RM β CD)	1.8	1312	>500
2-hydroxypropyl- β CD (HP β CD)	0.65	1400	>600
sulfobutylether- β CD (SBE β CD)	0.9	2163	>500

^aaverage number of substituents per glucopyranose repeat unit

^bsolubility in pure water at about 25°C

Phase-solubility analysis is the one of the traditional methods that can be used to investigate not only the effect of CD on the solubility of the drug and the apparent stability constant value but also the drug:CD stoichiometry of the equilibrium (53). According to the classification of Higuchi and Connors (1965), phase-solubility diagrams fall into two main types : A and B (61). Three sub-types are divided into A_L, A_P and A_N. A_L-type phase solubility profile is obtained when the solubility is linearly increased with respect to CD concentrations (Figure 4). When the curve positively deviates from linearity (i.e. CD is proportionally more effective

at higher concentrations), A_P -type profile is resulted. In contrast, when there is negative deviation from linearity (i.e. the CD is proportionally less effective at higher concentrations), A_N -type profile was achieved. A_L -type profiles are first order to CD and first or higher order with the drug (62, 63). A_P -type suggests that the complexation is first order with respect to the drug, but second or higher order with respect to the CD (64). A_N -type phase solubility profiles can be difficult to interpret. B-type phase-solubility profiles are indicative of the formation of complexes with limited water solubility (65). The most common type of CD complex is the 1:1 drug/CD complex (D/CD) in which one drug molecule (D) forms a complex with one CD molecule (CD):



$K_{1:1}$ is used to compare the affinity of drug to CD or CD derivatives. In the case of A_L -type phase solubility diagram, the slope is less than unity. The apparent stability constant ($K_{1:1}$) of the complex can be calculated from the slope and the intrinsic solubility (S_0) of the drug in the aqueous complexation media (i.e., drug solubility in the absence of CD).

$$K_{1:1} = \frac{\text{slope}}{S_0(1 - \text{slope})}$$

The complexation efficiency (CE) is the ratio of CD concentration in the complex and free state. For 1:1 drug/CD complexes, CE can be calculated from the slope of the phase solubility profiles (66):

$$CE = S_0 \cdot K_{1:1} = \frac{\text{slope}}{1 - \text{slope}}$$

According to the previous investigation, it is more reliable to compare CE than $K_{1:1}$ value for selecting CD or complexation conditions during formulation development.

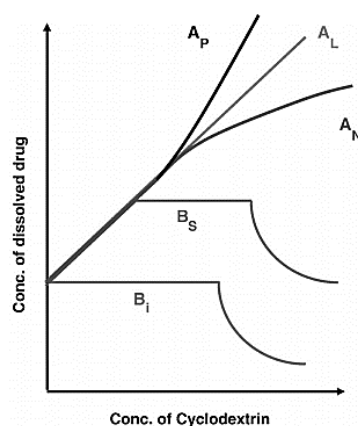


Figure 4 Graphical representations of A and B-type phase-solubility profiles (53).

5.2 Effect of polymers to enhance CD solubilization

Water-soluble polymers can help the solubility and dissolution of hydrophobic drugs by enhancing the wettability of particles (67). When the drug molecules are mixed together with CD and polymer in the solution, the ternary complex system was formed and it provides the synergistic enhancement in the drug solubilization rather than the use of CD and polymer individually (68). The water-soluble polymers can stabilize the micelles and other types of aggregates. They can also reduce CD mobility and increase the solubility of complexes by changing the hydration properties of CD molecules (21). The interaction between polymers and CDs or drug:CD complexes usually occur on the external surface of the CD molecule, form aggregates capable of solubilizing drugs and other hydrophobic molecules (52). According to literature reports, the ternary

system could form by heating method i.e., heating in an autoclave at 120 to 140 °C for 20 to 40 minutes or in sonicating bath more than 30 °C for 1 hour, (21). Recent studies reported that hydroxypropyl methylcellulose (HPMC) and poly vinyl pyrrolidone (PVP) increase the complexation of hydrocortisone, dexamethasone and naproxen with β CD (69). The synergistic increase in solubility of HPMC to the SBE β CD and carbamazepine complex had also been reported by Smith et al., (2005) (70).

6. Local drug delivery systems for the treatment of periodontitis

The periodontal pockets formed in diseased-state can act as a natural reservoir for local drug delivery system. The pocket is filled with gingival crevicular fluid (GCF). Hence, local periodontal delivery systems need to maintain the concentration of therapeutic agents in GCF higher than their minimum inhibitory concentration against bacteria. There are various systems that can be classified according to materials (biodegradable or non-biodegradable polymers) as well as device form (solid or semi-solid, adhesive or non-adhesive systems). The developed formulations include fibers, films, strips, microspheres, microcapsules, microparticles and gels. The local drug delivery system should have some satisfactory criteria in accordance with the etiology of disease conditions and anatomy of periodontal pocket such as (71):

1. It should easily be placed into the periodontal pocket and remained in place to maintain the local drug concentration.
2. The injectable delivery systems i.e., gels, microparticles and microspheres should be easy to administer.

3. The bioadhesive systems are preferred to ensure good retention of the device after placement.
4. To improve the patient compliance, the drug device should be easy to place and biodegradable, so that it can erode after period of time without any surgical procedure to remove residual device.
5. The targeted device should be sustained released to prolong therapeutic level at the site of administration.
6. The cost of device as well as the facility of production technique should be considered for drug research and development.

Despite the numerous local drug delivery systems have been developed, only a few products of these have been marketed. Actisite® is the first marketed fiber containing ethylene vinyl acetate with 25% w/w tetracycline hydrochloride. It can maintain the constant therapeutic level with prolonged release of drug for 9 days and showed good clinical efficacy (72). However, the main limitation of using this system is patient discomfort during the placement and removal of fiber and anesthesia is needed to perform the procedure (10). Periochip® is biodegradable insert containing chlorhexidine gluconate hydrolyzed in gelatin. It can sustain drug release over 7 days. However, Periochip® in conjunction with scaling and root planning therapy are limited and controversial (73).

Films are more widely used as intra-pocket delivery devices and superior to previous ones since it can easily be placed. In addition, the film dimension can be adjusted to insert well within the pocket with minimum pain. They can be prepared by solvent casting or direct milling and the loaded drug can be released by diffusion and/or matrix dissolution or erosion (74). Both synthetic biodegradable polymer i.e., PLGA and non-biodegradable ethyl cellulose films containing different types of antibiotics

that have been developed and the latter one can provide sustained release of drug. Although it has clinical benefits, this system possesses the drawback of low drug loading (74). Webber and Mathiowitz (1997) (74) studied PLGA film containing tetracycline to modulate the drug release but the amount of the drug which can load in the film was too low and only the small amount of antibiotic can reach minimum inhibitory concentration (MIC) when inserted once into periodontal pocket. The use of organic solvents during preparation can remain in the body as residue and possibly causing the toxicity to the patient. Therefore, in addition to solid devices, injectable gel formulations have been considered to use as local drug delivery system into the periodontal pockets.

Elyzol® is one of marketed gels containing 25% metronidazole. It can be easily administered into periodontal pocket with syringe. However, according to clinical studies, the poor retention of Elyzol® gel within periodontal pocket is still controversial for good clinical outcomes achievement (35). Minocycline gel (2% w/w) which has been marketed with trade names such as Dentomycin® or Periocline® or Parocline® seems to be good in clinical therapy. Dentomycin® has been reported to provide significant probing depth reduction and good clinical efficacy in attachment (72). However, all of the above gels still lack biodegradability and necessary to remove the residual gel after treatment.

7. In situ gelling system

In situ gels are polymeric formulations that can be in solution form before administration to the body but once administered it can form gel under physiological stimuli. The sol-gel transition takes place by the

different stimuli such as pH, temperature, solvent exchange, UV irradiation and the presence of specific ions or molecules, etc. (22). The marketed biodegradable injectable system is Atridox®. This system consists of 10% doxycycline hyclate based on biodegradable polymer PLA dissolved in a biocompatible solvent NMP. It is an *in situ* forming system and transfer from solution-state to solid-state after injection into periodontal pocket. This implant can sustain drug release over 7 days (75). However, the retention of implant and drug release control are important issues to be considered in the research and development for such devices.

Among *in situ* gelling systems, temperature modulation is advantageous for various routes of administration. It does not require organic solvents, co-polymerization agents, and externally applied trigger for gelation (76). The commonly used thermoreversible polymers are hydroxypropyl methylcellulose, methylcellulose, hydroxyethyl cellulose, N-isopropylacrylamide copolymers, poloxamer and its copolymers (76).

Poloxamer 407 (P407), commercially known as Pluronic® F127 “F” is a A-B-A type, non-ionic amphiphilic block copolymer, composed of polyethylene-oxide (PEO) (A) and polypropylene-oxide (PPO) units (B) (76). It is widely applied in pharmaceutical and cosmetic field because of its well compatibility, high solubilizing capacity, good releasing characteristics and low toxicity. In addition, it is well-known as thermoreversible gelling agent (77). Its amphiphilic character functions as surfactant, where concentrated poloxamer solution transforms thermoreversible gels. Figure 5 demonstrates the chemical structure of P407, with a central lipophilic propylene-oxide, bordered by two hydrophilic polyethylene-oxide chains.

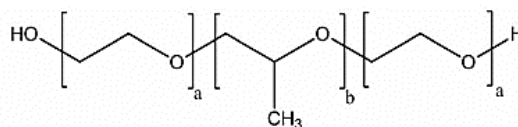


Figure 5 Chemical Structure of P407

P407 has been widely used to develop the hydrogel for various routes of administrations, for example, ocular (78), nasal (79), vaginal (80), transdermal (81), etc. and providing the depot of drug at the site of administration. The addition of mucoadhesive polymers such as carbopol, chitosan (CS), HPMC provide the significant mucoadhesive property and can prolong drug release. Recently, Bansal et al., (2018) conducted the development of intra-pocket periodontal *in situ* gel by using the combination of P407 and CS and the enhanced therapeutic outcome was observed with controlled released up to 48 hours along with additional mucoadhesive property (82).

CS is an amino polysaccharide and obtained from the alkaline deacetylation of chitin which is present in the exoskeleton of shrimps and crabs. The structural formula of chitosan is shown in Figure 6. CS comprises of glucosamine and *N*-acetylglucosamine units. CS is a biocompatible, biodegradable, non-toxic and possesses cationic charge. It is insoluble in water, but soluble in dilute acidic solution up to pH 6.2 (76, 83). The -OH and -NH₂ groups of CS can give rise to hydrogen bonding which can provide mucoadhesion (84). Because of its positive charged bearing capacity, the electrostatic interaction can occur and CS nanoparticles can be generated by ionically crosslinking the positively charge CS with negatively charged tripolyphosphate (TPP) (25). Moreover, it has wound healing activity and antimicrobial properties (85).

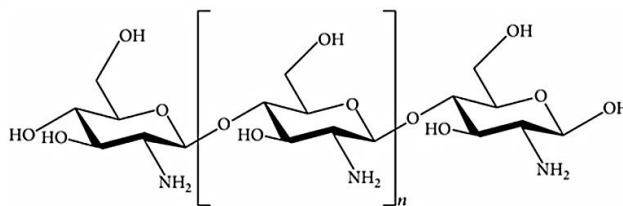


Figure 6 Chemical structure of CS

8. Nanoparticles in periodontal drug delivery system

Nanoparticle containing drug delivery systems are among the most popular fields of current research for periodontal treatment and regeneration. There are two main categories for the preparation of encapsulations such as physical techniques and physicochemical techniques. Physical techniques are known as spray drying (86) lyophilization (87), supercritical fluid techniques (88) and solvent evaporation (89), whereas physicochemical methods include coacervation (90), liposomes (91) and ionic gelation (92). Among the different techniques, ionic gelation has been widely proposed due to its ability for the fabrication of biocompatible system in biomedical field (92). Nanoparticles have also been developed to improve the effectiveness of drug delivery systems to overcome the premature and accidental expulsion of injected gels from the periodontal pockets. Polymer-based nanoparticles were prepared and incorporated into hydrogel matrix. The previous study formulated *Harungana madaascariensis* leaf extract (HLE) loaded PLGA nanoparticles by using interfacial polymer deposition following solvent diffusion method (11). It is the multicomponent system containing biodegradable nanoparticles and because of their small size, they can penetrate the periodontal pocket area under the gum line, reducing the

frequency of administration and uniform distribution of active agent over an extended period of time.



CHAPTER III

MATERIALS AND METHODS

Materials

The following materials were used as received;

- Acetonitrile HPLC grade (Burdick & Jackson, Korea)
- Asiaticoside (AS) (Xi'an Haoxuan Bio-Tech Co., Ltd, Xi'an, China)
- β -cyclodextrin (Wacker Chemie AG, Germany)
- Benzalkonium chloride (Sigma-Aldrich, USA)
- Carboxymethyl- β -cyclodextrin (CM β CD) (Wacker Chemie AG, Germany)
- Chitosan (Fluka Fine Chemical, Japan)
- Dialysis Membrane (Spectra/Por, Netherlands)
- Hydroxypropyl- β -cyclodextrin (HP β CD) (Roquette, France)
- Mucin from porcine stomach type II (Sigma-Aldrich, USA)
- Poloxamer 407 (Lutrol[®] F-127, P407) (BASF, Ludwigshafen, Germany)
- Potassium dihydrogen phosphate (Ajax Finechem Pty LTD, Australia)
- Sodium chloride (Ajax Finechem Pty LTD, Australia)
- Sulfobutylether- β -cyclodextrin (SBE β CD) (Roquette, France)

Equipments

- Analytical balance (MettlerToledo AG285, Germany)
- Autoclave (Hirayama, HICLAVE HVE-50, Japan)
- Differential scanning calorimetry (MettlerToledo, model DSC822 °STAR System, Germany)
- Fluorescent microscope (Axiovert 40CFL, Carl Zeiss, Gottingen, Germany)
- Fourier transform infrared spectroscopy (Thermo Scientific, model Nicolet iS10, USA)
- Freeze dryer (Labconco Lyophilizer, MO, USA)
- Haake MARS III rotational rheometer (Thermo Fisher Scientific, Schwerte, Germany)
- High speed refrigerator micro centrifuge (TOMY, MX-305, Japan)
- High performance liquid chromatography (HPLC) instrument equipped with the following :
 - Liquid chromatography pump (quaternary pump, Agilent 1260 Infinity II, G7111A)
 - UV-VIS detector (Agilent 1260 Infinity II, G7115A)
 - Auto sampler (Agilent 1260 Infinity II, G7129A)
 - C18 column (Shiseido, 5 µm, 250x4.6 mm ID reverse-phase column)
- Nanosizer (Zetasizer, Nano-ZS with software version 7.11, Malvern, UK)
- pH meter (MettlerToledo, sevenCompact, Germany)
- Powder X-ray Diffractometer (Rigaku, model MiniFlex II, Japan)
- Proton nuclear magnetic resonance spectroscopy (¹H-NMR, BRUKER, model AVANCE III HD, USA)

- Shaker Incubator (DLabTech, LSI-4018A, India)
- Transmission Electron Microscope (TEM JEOL, JEM-2100F, USA)
- Ultrasonic bath (GT sonic, China)
- Viscometer (Brookfield, Model DV-I Digital Viscometer RVTD-I, USA)



Methods

1. pH-solubility profiles

Excess amount of AS was added into pure water. The desired pH (in the range of 2 to 10) was adjusted by drop-wise titration with concentrated hydrochloric acid or sodium hydroxide solution. The formed suspension was agitated in mechanical incubating shaker at 30 ± 1 °C for 6 days and pH was readjusted, if necessary. After equilibration, the samples were filtered through 0.45 μm nylon filter, the filtrate was diluted with the mobile phase and the amount of dissolved drug was determined by reversed-phase high performance liquid chromatography method (HPLC).

2. Thermal stability of AS

The stability of AS in aqueous solution was evaluated by heating method (20). The small amount of AS was dissolved in pure water and aqueous SBE β CD solutions (2.5% or 5% w/v) that was divided into four sealed vials. The solution was equilibrated at 30 ± 1 °C for 24 hr under constant agitation. After equilibrium was attained, the samples were heated in autoclave at 121 °C for 20 min for zero, one, two and three heating cycles. The analogue sets were performed in sonicator at 60 °C for 30 min. The obtained solution in each sample was diluted with methanol: water (70:30 v/v) and subjected to analyze the AS concentration by HPLC.

3. Solubility determinations

3.1 Effect of CD on AS solubility

An excess amount of AS was added to aqueous solutions containing β CD (0-1.5% w/v) or SBE β CD, CM β CD and HP β CD (0-10% w/v). The

drug suspensions in sealed vials were heated in sonicator at 60 °C for 30 min and allowed to cool to room temperature. The suspension was equilibrated for 7 days at 30±1 °C under constant agitation. After equilibrium was reached, the suspension was filtered through 0.45 µm nylon filter and analyzed by HPLC. The phase-solubility diagrams were constructed by plotting the total dissolved AS concentration (M) against CD concentration (M). The apparent complexation constant ($K_{1:1}$) for AS/CD complex was determined according to phase-solubility method (2) and the complexation efficacy (CE) were calculated by Eq.1 (3):

$$CE = \frac{\text{Slope}}{1 - \text{Slope}} = \frac{[\text{drug/CD complex}]}{[\text{CD}]} = K_{1:1} \cdot S_0 \quad \text{Eq. 1}$$

where, S_0 is the intrinsic solubility of AS in the absence of CD

3.2 Effect of water-soluble polymers on solubility of AS/SBEβCD complexes

The phase-solubility of AS was determined in aqueous SBEβCD solutions (0-5% w/v) containing 0.01 mM CS or 10 mM P407. Briefly, CS solution was prepared by dissolving CS in 0.4% v/v acetic acid solution. In case of P407, it was dissolved in cold water for injection (WFI) and kept overnight in refrigerator at 4 °C to completely dissolved. The obtained polymer solutions were then added into the aqueous SBEβCD solutions. AS was added in excess amount and the phase-solubility was conducted as described above. The $K_{1:1}$ and CE values were calculated. The CE ratio between the presence and the absence of polymer was determined.

4. Quantitative analysis of AS

Calibration curve of AS

Accurate amount of AS 50.0 mg was weighed and placed into 50 mL volumetric flask, dissolved with methanol:water (70:30 v/v) and diluted to the desired volume to obtain 1 mg/mL AS as the stock solution. The solution was then further diluted to be a concentration range of 12.5 - 1000 µg/mL. Each concentration was subjected to HPLC analysis in triplicate. Peak area was recorded for all the solutions and the equation was calculated from the linear relationship between peak area of AS and their concentrations.

Sample preparation

The sample was appropriately diluted with methanol:water (30:70 v/v). A portion of sample was filtered through 0.45 µm nylon filter and subjected to HPLC analysis. The content of AS in the sample was calculated from calibration curve of AS.

HPLC condition

Quantitative determination of AS was performed by a reversed-phase HPLC component system from Agilent 1260 Infinity II consisting of Liquid chromatography pump (quaternary pump, G7111A), UV-VIS detector (G7115A), auto sampler (G7129A) with Chem Station software version (E.02.02) and Shiseido™ Capcell Pack C18 MG II S-5, C18, 250x4.5 mm ID with C18 guard cartridge column MGII 5 µm, 4x10 mm. The HPLC condition was as follows; mobile phase: acetonitrile: water (28:72 v/v); flow rate: 0.9 mL/min; oven temperature: ambient; UV detector wavelength: 220 nm; injection volume: 20 µL; and run time: 15 minutes.

5. Validation for the quantitative analysis of AS

Specificity

The specificity of analyte was investigated by injecting of AS and other components i.e., β CD, SBE β CD, CM β CD, HP β CD, CS, P407, benzalkonium chloride (BAC and mobile phase to demonstrate no interference in analyte elution. The components were properly diluted before determining by HPLC.

Linearity

Linearity was determined by injecting the series of AS standard solutions in the range of 12.5-1000 μ g/mL. Each concentration was done in triplicate and the calibration curves were constructed by plotting the peak area versus nominal concentration expressed in μ g/mL of AS. From each calibration curve, the slope, intercept and coefficient of determination (R^2) were evaluated.

Precision จุฬาลงกรณ์มหาวิทยาลัย

Within run precision

The within run precision was checked by analyzing five sets of three standard solutions of AS within one day. The coefficients of variation of the peak area responses (% CV) for each concentration were determined.

Between run precision

The between run precision was determined by comparing each concentration of AS standard solution which prepared and injected on

different days. The coefficients of variation of the peak area responses (% CV) from three standard solutions on different days was calculated.

Accuracy

The recovery of AS from blank formulation was assessed by spiking blank formulation (all components except the drug) with AS in triplicate at three level spanning 80-120% of amount of AS in the formulation. The average recovery and the coefficient of variation (% CV) were calculated.

6. Preparation and characterization of the binary AS/CD and ternary AS/CD/polymer complexes

6.1 Solution-state characterization by proton nuclear magnetic resonance (¹H-NMR) spectroscopy

The pure solid samples of AS, SBEβCD, HPβCD, P407 and CS as well as AS/CD binary complex (i.e., 1:1 molar ratio of AS/HPβCD or AS/SBEβCD) and AS/SBEβCD/polymer (10 mM P407 or 0.01 mM CS) ternary complexes were dissolved in 10% v/v D₂O in DMSO-*d*₆ and equilibrated at 30±1 °C for 24 hr. ¹H-NMR spectroscopy measurements were performed by using a 500 MHz ¹H-NMR spectrometer (BRUKER model AVANCE III HD, USA). The spectrum and chemical shift values were recorded as ppm. The residual solvent signal (DMSO-*d*₆ 2.50 ppm) was used as internal reference and the chemical shift values were calculated according to the following equation:

$$\Delta\delta^* = \delta_{(complex)} - \delta_{(free)} \quad \text{Eq. 2}$$

6.2 Solid-state characterization

Sample preparation

Aqueous solutions containing 1:1 molar ratio of the binary complexes i.e., AS/HP β CD and AS/SBE β CD ($m:n$; $D_m:CD_n$, where m and n represented the total moles of drug and CD, respectively) and AS/CD/polymer (10 mM P407 or 0.01 mM CS) ternary complexes were prepared by heating in the sonicator at 60 °C for 30 min. The samples were equilibrated at 30 \pm 1 °C for 7 days under constant agitation. After equilibrium was attained, the samples were centrifuged (Thermo Fisher Scientific, MA, USA) at 13000 rpm for 20 min. Then, the supernatant was withdrawn, frozen at -80 °C for 2 hr and lyophilized at -52 °C for 48 hr in a freeze-dryer (Labconco Lyophilizer, MO, USA), yielding a solid complex powder (FD). Identical physical mixtures (PM) were prepared by careful blending of ingredients in a mortar with pestle. The samples were characterized in solid-state as follows: intact, PM and FD of binary complexes (AS/HP β CD, AS/SBE β CD) and ternary complexes (AS/SBE β CD/P407, AS/SBE β CD/CS).

6.2.1 Differential scanning calorimetry (DSC)

DSC thermograms were determined in a differential scanning calorimeter (Mettler Toledo, DSC822 STAR^e System, Germany). The samples (3–5 mg) were placed in sealed aluminium pans and heated with flow rate of 10 °C/min from 30 to 300 °C under nitrogen. An empty aluminium pan was used as a reference.

6.2.2 Powder X-ray diffraction (PXRD)

The PXRD patterns were recorded by using Powder X-ray diffractometer (Rigaku model MiniFlex II, Japan), operated at a voltage of 30 kV and 15 mA current. The samples were analyzed as the 2θ angle range of 3° - 40° and the scanning rate of 2° per minute with the step size of 0.020° (2θ).

6.2.3 Fourier transform infra-red (FT-IR) spectroscopy

The samples were measured in a FT-IR spectrometer (Thermo Scientific model Nicolet iS10, USA) using the attenuated total reflectance (ATR) technique. The data were obtained in the range of 400 – 4000 cm^{-1} . The analysis was performed at room temperature.

6.3 In vitro release study

In vitro release study was performed by using a USP dissolution test apparatus type II (Vk 7010, Vankel Technology Group, NC, USA). Intact AS (20 mg) and FD samples of binary and ternary complexes equivalent to 20 mg of AS that obtained from section 6.2 were filled into transparent hard gelatin capsules No. 0. The capsules were hanged with stainless steel wires at the paddles and dipped into the cylindrical dissolution vessels containing 100 mL phosphate buffer saline (PBS), pH 7.4. The stirring speed was 100 rpm and the temperature of dissolution medium was maintained at $37\pm 0.5^\circ\text{C}$. Five milliliter aliquots of dissolution medium was withdrawn at various time intervals and replaced by the same amount of fresh medium. The collected samples were filtered through a $0.45\text{ }\mu\text{m}$ nylon filter and analyzed by HPLC. The experiment was carried out in

triplicate. The cumulative percentage release of AS against time was constructed to plot the drug release profile. Dissolution efficiency at 120 min (DE_{120}) was calculated according to Khan (1975) (93). The time required to release 50% of AS [$t_{50\%}$ (min)] together with the dissolution rate constant [K_1 (min^{-1})] were determined from the slope of linear plot of drug release profile.

7. Morphology, particle size and zeta potential analysis

The morphology, particle size and zeta potential of the drug/CD complex aggregates in aqueous complexation media were examined. AS was saturated in 5% w/v HP β CD or 2.5% w/v SBE β CD with and without CS (0.1% w/v) or P407 (5% w/v) and analyzed by using dynamic light scattering (DLS) and transmission electron microscopy (TEM).

7.1 DLS measurement

DLS technique was used to determine the particle size and zeta potential of AS/CD based aggregates in solutions and performed by using Zetasizer (Nano ZS, Malvern, UK, with software version 7.11). Sample was put in a cuvette and placed in the instrument. Measurements were carried out at 25 °C and 180° scattering angle. Particle size, size distribution and zeta potential were automatically calculated and analyzed by the software included within the system. Each measurement was done in triplicate.

7.2 TEM analysis

The morphology of AS/CD based aggregates were evaluated by TEM (JEOL, JEM-2100F, USA). Initially, the sample was placed on a formvar-coated grid. After blotting the grid with a filter paper, the grid was transferred onto a drop of negative staining. Aqueous 2% phosphotungstic acid solution or uranyl acetate was used as a negative stain for negatively charged and positively charged nanoparticles, respectively. The sample was air dried at room temperature and finally, the sample was examined with TEM.

8. Preparation of SBE β CD/CS nanoparticles

The drug-free nanoparticles containing SBE β CD and CS were prepared by ionotropic gelation according to the method of Calvo et. al with modification (25). Firstly, the various concentrations of CS (0.5-3% w/w) were prepared by dissolving CS in 0.4% v/v acetic acid solution. Then, the aqueous solutions of SBE β CD (0.5-5% w/w) was added dropwise (approximately 2 drops/min) into their different concentrations of CS at a weight ratio of 1:3 (w/w) via 27G needle under magnetic stirring at 500 rpm. The final concentrations of CS and SBE β CD in the preparations were from 0.375 to 2.25% w/w and from 0.125 to 1.25% w/w, respectively. The obtained preparations were continued stirring for 15 min at room temperature. After that, the appearance from visual observation was defined and recorded as clear, opalescent dispersion and turbid (aggregates). The aggregates referred to the preparations that were firstly observed in the appearance of suspension and then quickly sediment after

few minutes. The opalescent suspensions were determined as SBE β CD:CS nanoparticle formation. Of these ratios were subjected to load AS.

The AS loaded SBE β CD/CS nanoparticles were prepared by dissolving AS in SBE β CD solutions. The solution was then added drop-wise into CS solutions under the same conditions as drug-free SBE β CD/CS nanoparticle preparation. The particle size, size distribution and zeta potential were determined. Each preparation was done in triplicate.

9. Preparation of AS/SBE β CD/CS thermoresponsive *in situ* gel formulations

The composition of *in situ* gel formulations containing AS are displayed in Table 2. Briefly, thermo-gelling phase was prepared by dissolving 16% w/w P407 in water for injection (WFI), approximately 4 °C containing 0.02% w/w benzalkonium chloride (BAC) under continuous magnetic stirring. The obtained P407 gel solution was kept overnight in a refrigerator to obtain clear solution. The nanoencapsulation phase containing AS loaded NPs with various SBE β CD/CS ratios (F1-F3) was prepared as described in the method of drug-loaded SBE β CD/CS NPs. Then, the nanoencapsulation phase was transferred and mixed with thermo-gelling phase and stirred until the solution was homogenous. Finally, the preparation was filled up with WFI to the desired weight and kept at 4 °C for further analysis. In comparison, the non-encapsulated formulations comprised of AS/HP β CD complexes and the combination thereof (i.e., both encapsulated and non-encapsulated) were prepared. In case of non-encapsulated formulations, AS was dissolved in HP β CD solutions (F4-F6 and F10-F12) while the formulations containing both

systems (F7-F9 and F13-F15) the amount of AS was divided into two parts and was dissolved according to each platform prior to add into the gelling phase.

Table 2 The composition of thermoresponsive in situ gel formulations containing asiaticoside

^aweight ratio of SBE β CD/CS

Ingredients (% w/w)	Formulation ^a														
	F1	F2	F3	F4	F5	F6	F7	F8	F9	F10	F11	F12	F13	F14	F15
Asiaticoside	0.02	0.03	0.04	0.1	0.15	0.2	0.1	0.15	0.2	0.5	0.75	1	0.5	0.75	1
SBE β CD/CS ^b	1:2	1:1.5	1:1.2	-	-	-	1:2	1:1.5	1:1.2	-	-	-	1:2	1:1.5	1:1.2
HP β CD	-	-	-	0.5	0.75	1	0.5	0.75	1	2.5	3.75	5	2.5	3.75	5

^bEach formulation containing 16% P407 and 0.02% BAC, all %w/w and adjusted weight q.s. to 100 g with WFI

10. Physicochemical and chemical Characterizations

10.1 Appearance, pH, viscosity, and syringeability and injectability

The appearance of *in situ* gel formulations were subjected to visual observation. The pH of *in situ* gel was measured by using pH meter (Mettler Toledo, Seven Compact, Germany) at 25 °C. The viscosity was determined at 25 °C and 37 °C using Brookfield Digital Viscometer (Model DV-I Digital Viscometer RVT-D-I, USA). The syringeability and injectability of *in situ* gel formulations were investigated by using 27G needles which were commonly used in dental field (94). The syringeability of formulation was evaluated by withdrawing 1 mL of formulation in solution-state through 27G needle which attached to 1 mL syringe. The

injectability was determined by pressing the injector part of syringe with the gentle uniform force via 27G needle. The syringeability and injectability of the solution which passed through the syringe and needle was expressed as; (+) solution can be syringed and injected with strong force, (++) medium force, (+++) less force and (-) the solution cannot pass through the needle (95).

10.2 Gelation temperature, gelation time and in vitro gelling capacity

The gelation temperature was determined by test-tube inverting method (96). Two milliliters of the preparation were placed in test-tube which was immersed into water-bath at 25 °C. Then, the temperature of the water-bath was gradually increased in increment of 0.2 °C. The formulations were allowed to equilibrate at each temperature setting for 5 minutes. The gelation temperature was recorded when the absence of flow on inversion of the test-tube 90° was observed.

To investigate the gelation time, two milliliters of each formulation in solution-state was placed in the test-tube. Then the test-tube was immersed into the water-bath in which temperature was maintained at 37±0.5 °C. The time for gel formation was determined by investigating of the no flow of gel by tilting the test-tube 90° (97).

In vitro gelling capacity of formulation was evaluated on the basic of stiffness of the formed gel and the duration for which the formed gel remained. Two milliliters of simulated salivary fluid (SSF) was placed in test-tube and maintained at the temperature of 37±0.5 °C in the water-bath. One milliliter of formulation in sol form was pipetted and slowly released

to the surface of SSF in the test-tube. The time for gel formation and the time counted for the formed gel to be dissolved was noted and defined as (+) gelation after few minutes and disperse rapidly, (++) immediate gelation and remained for few hours, (+++) immediate gelation and remained for long period of time (97).

10.3 Particle size and size distribution and zeta potential analysis

The particle size and zeta potential of *in situ* gels were measured with DLS (Zeta sizer, Malvern Instruments Ltd, UK). The particle size distribution was reported as polydispersity index (PDI). The measurements were conducted at 25 °C. All experiments were performed in triplicate.

10.4 Total drug content and encapsulation efficiency (EE)

AS content in *in situ* gel formulation was determined by placing 1 g of *in situ* gel into 10 mL volumetric flask and dissolved with methanol:water (30:70 v/v). After proper dilution, the solution was filtered through 0.45 µm nylon filter and analyzed by HPLC. Each sample was done in triplicate.

The percentage of EE (%EE) of encapsulated *in situ* gel was determined by indirect method. The formulations were centrifuged at 10,000 rpm for 90 min (98). Then, the supernatant was withdrawn and the content of untrapped AS was dissolved, properly diluted with methanol:water (30:70 v/v) and then quantified by HPLC. The % EE was calculated as follow:

$$\%EE = \frac{\text{total amount of drug} - \text{amount of untrapped drug}}{\text{total amount of drug}} \times 100 \quad \text{Eq. 3}$$

11. Rheological study

The rheological study of *in situ* gel formulations was carried out with a HAAKE MARS III rotational rheometer (Thermo Fisher Scientific, Schwerte, Germany) using a Peltier unit to control the temperature. For oscillatory mode, a parallel plate (40 mm diameter, PP60Ti) geometry measuring system was employed, and the gap was set to 1 mm. Amplitude sweep was firstly done at 25 ± 0.1 °C and 37 ± 0.1 °C with constant frequency (1 Hz) to get linear viscoelastic region where stress was directly proportional to strain. Then, frequency sweep analysis was performed over the frequency range of 0.1-10.0 Hz. The storage modulus (G'), the loss modulus (G''), the dynamic viscosity (η') and the loss tangent ($\tan \delta$) were recorded.

12. *In vitro* mucoadhesion study

The mucoadhesive property of *in situ* gel formulations was determined by modified method (99). Firstly, semipermeable membrane was attached to the inside-bottom of glass vial by cyanoacrylate glue. Then, 0.1% w/v aqueous mucin solution (porcine stomach, Type II) was added into the vial to soak the membrane for about 2 hr. The excess mucin solution was removed from the surface of the membrane. Each formulation of 0.5 g was placed onto the center of the membrane and allowed it to form gel in oven at 37 °C for 15 min. Four milliliters of SSF which was previously degassed and pre-warmed at 37 °C was gradually added into the vial. The vials were shaken in the incubating shaker at 37 ± 0.5 °C, 50 rpm for 5 min. After the time reached, the liquid was pipetted off. Finally, the remaining *in situ* gel on the membrane was dissolved with methanol:water

30:70 v/v, filtered with 0.45 μm nylon filter and the amount of AS remained was analyzed by HPLC. Each formulation was done in triplicate.

13. *In vitro* release studies

The *in vitro* release of AS from *in situ* gel formulations through semipermeable membrane (MWCO 3,500 Da) was determined by modified Franz diffusion cell. The membrane was soaked overnight in the receptor medium, SSF pH 6.8 containing 2.5% w/v HP β CD before being mounted on the Franz diffusion cell. HP β CD was added to the receptor phase to allow sink condition. The donor compartment contained 1 g of tested formulation. The study was maintained at the temperature 37 ± 0.5 °C and the receptor phase (12 ml) was continuously stirred at 150 rpm during the experiment. A 150 μL aliquot of the receptor medium was withdrawn at various time intervals and replaced immediately with an equal volume of fresh receptor medium. The amount of AS in the receptor medium was analyzed by HPLC. Each experiment was conducted in triplicate.

จุฬาลงกรณ์มหาวิทยาลัย
CHULALONGKORN UNIVERSITY

14. Cytotoxicity Assay

Human periodontal ligament cells (HPDLCs) were obtained from Faculty of Dentistry, Chulalongkorn University. The HPDLCs were cultured in Dulbecco's modified Eagle's medium (DMEM, Gibco, NY, USA) containing 10% fetal bovine serum (Gibco), 2 mM L-glutamine (Gibco), 100 units/mL penicillin, and 100 mg/mL streptomycin in a humidified atmosphere with 5% carbon dioxide at 37 °C. Medium was changed every 48 hrs. All experiments were performed in serum-free medium and each experiment was carried out in triplicate (17). To study

the cell viability, 3-(4,5-dimethylthiazol-2-yl)-2,5-diphenyl tetrazolium bromide (MTT; Gibco) assay was performed. Briefly, the cells were seeded in 96-well tissue culture plates at a density of 10,000 cells/ml. Drug-free and AS loaded *in situ* gels with the serial dilutions as well as controls were added to the wells and incubated for 24 hr (100). After incubation, 200 μ L of MTT solution [5 mg/ml diluted in phosphate buffered saline (PBS)] was added to each well and incubated at 37 °C for 3 hr. Then MTT solutions were removed out of each well and 200 μ L of dimethyl sulfoxide (DMSO) was again added to each well. The plates were shaken until the formazan crystals were dissolved. The absorbance was determined at 570 nm with a microplate reader (Bio-Rad Model 550; Bio-Rad, Hercules, CA, USA). All reported values were the means of triplicate samples.

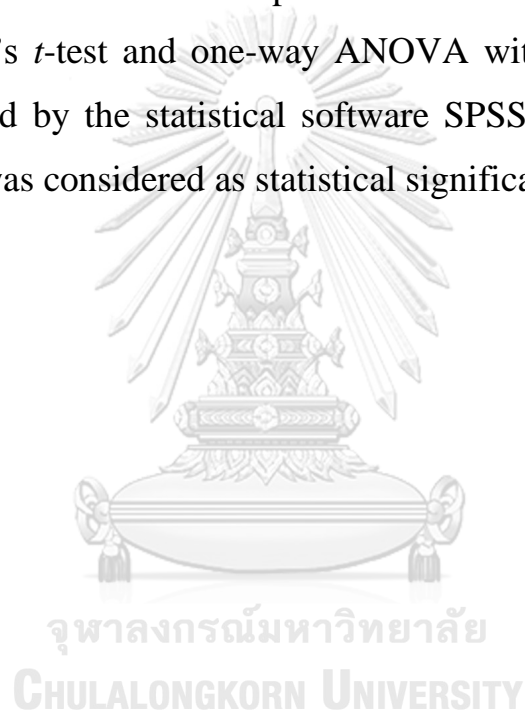
15. Immunocytochemistry

The HPDLCs were cultured in Dulbecco's modified Eagle's medium (DMEM, Gibco, NY, USA) containing 10% fetal bovine serum (Gibco), 2 mM L-glutamine (Gibco), 100 units/mL penicillin, 100 mg/mL streptomycin in a humidified atmosphere with 5% carbon dioxide at 37 °C. To study the immunocytochemistry, briefly, the cells were seeded in 96-well tissue culture plates at a density of 10,000 cells/ml. Drug-free and AS loaded *in situ* gels were added to the wells and incubated for 24 hr (100). After incubation, 150 μ L of media and sample solutions were removed out and washed with PBS. Then, HPDLCs were fixed by using 4% glutaraldehyde solution (Merck, Darmstadt, Germany). After 30 min, the cells were washed with PBS and blocked with FBS for 60 min. The cells were incubated with collagen I monoclonal antibody (5D8-G9) (thermo fisher scientific, U.S.A.), R-phycoerythrin goat anti mouse IgG (H+L)

(Invitrogen, U.S.A.) at a 1:100 dilution and kept overnight at 4 °C. After washing with PBS, the cells were counterstaining the nuclei with DAPI (0.1 mg/mL, Invitrogen) for 30 min, the cells were analyzed with a fluorescent microscope (17).

16. Statistical Analysis

All quantitative data were presented as means±standard deviation (S.D.). Student's *t*-test and one-way ANOVA with Tukey post-hoc test were determined by the statistical software SPSS, version 16.0. The *p*-value, $p < 0.05$ was considered as statistical significance.



CHAPTER IV

RESULTS AND DISCUSSION

1. pH-solubility profiles

The aqueous solubility of drug plays an important role on the pharmaceutical formulation development. One of the techniques for drug solubilization enhancement is the pH adjustment. The pH-solubility profile of AS was determined and shown in Figure 7. The solubility of AS was gradually increased from pH 2 to pH 4. At pH 4, the highest aqueous solubility of AS was attained and then leveled off to the lowest at pH 10. It indicated that the AS solubility was found to be 120 $\mu\text{g/mL}$ at physiological pH (pH 7.4). Since the high molecular weight of AS (959.12 Da) and the solubility of AS was relatively low, it may hamper the drug bioavailability.

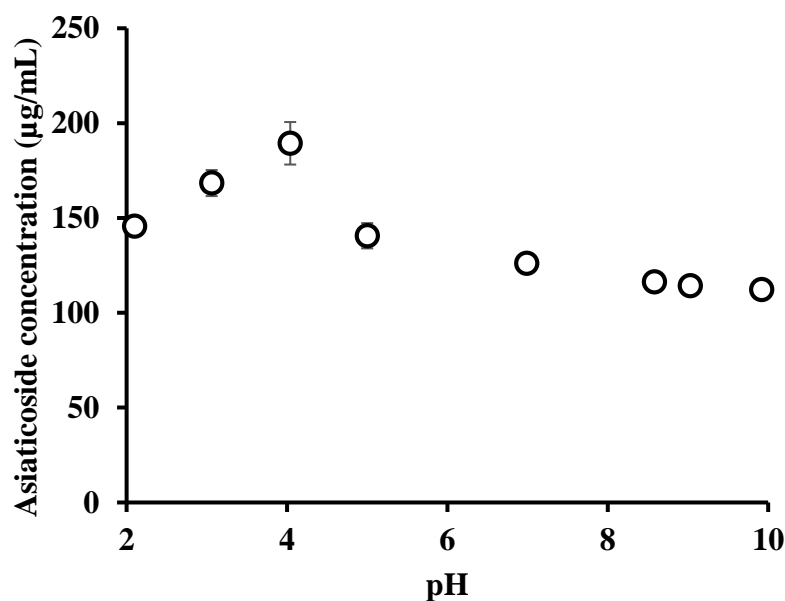


Figure 7 pH-solubility profile of asiaticoside

2. Thermal stability of AS in aqueous solution

It was believed that heating method can provide the more increasing of drug solubility through CD inclusion complex (101). Thus, the thermal stability study of AS was conducted according to Loftsson et al., (2005) (20). Table 3 and 4 display the percentage of AS remaining in pure water and aqueous solution containing 2.5% and 5% w/v SBE β CD after zero to three cycles of autoclave at 121 °C for 20 min and sonicate at 60 °C for 30 min, respectively.

The percentage loss of AS in pure water was significantly higher than those of aqueous SBE β CD solutions after passing through three heating cycles ($p < 0.05$) (Table 3).

Table 3 Percentage of AS remaining in pure water and aqueous solution containing 2.5% and 5% w/v SBE β CD after zero to three heating cycles in autoclave at 121 °C for 20 min. (Mean \pm S.D., n=3)

No. of cycles	Percentage of AS content in conc. change		
	pure water	SBE β CD (2.5% w/v)	SBE β CD (5.0% w/v)
cycle 0	100.00	100.00	100.00
cycle 1	95.92 \pm 2.28	99.01 \pm 1.00	97.38 \pm 1.68
cycle 2	94.76 \pm 2.71	97.75 \pm 0.59	95.93 \pm 1.99
cycle 3	89.05 \pm 2.01	94.61 \pm 0.87	94.67 \pm 3.23

The increasing AS/SBE β CD complex solubility via autoclaving gave the drug degradation about 5-10%. In contrast, AS content was less than 2% or unchanged in pure water or in SBE β CD solutions, respectively after three cycles of sonication (Table 4). It demonstrated that AS was relatively stable when using heating process through sonication method.

Table 4 Percentage of AS remaining in pure water and aqueous solution containing 2.5% and 5% w/v SBE β CD after zero to three heating cycles in ultrasonic bath at 60 °C for 30 min. (Mean \pm S.D., n=3)

No. of cycles	Percentage of AS content in conc. change		
	pure water	SBE β CD (2.5% w/v)	SBE β CD (5.0% w/v)
cycle 0	100.00	100.00	100.00
cycle 1	99.32 \pm 1.43	100.77 \pm 3.27	101.24 \pm 1.07
cycle 2	99.08 \pm 1.58	100.98 \pm 1.85	101.77 \pm 2.32
cycle 3	98.55 \pm 2.01	101.31 \pm 2.87	100.76 \pm 0.81

The recent accelerated stability studies have been reported that AS was decomposed when exposure to high temperature (102). It may be due to the hydrolysis of glycoside. The possible mechanism for hydrolysis of AS was proposed that AS was hydrolyzed and broken down to aglycone (asiatic acid), two sugar molecules and one rhamnose (103). Our investigation showed that AS degradation during the heating process by sonication was not more than 2%. Thus, this heating method was employed for further study.

3. Solubility determinations

3.1 The effect of CD on AS solubilization

AS is a low water-soluble compound that has intrinsic solubility i.e., the aqueous solubility in pure water approximately 0.7 mM (43). CDs can enhance the solubility of lipophilic compound via inclusion complex formation. It is well-known that, cavity size of β CD is the most suitable for complexation with many lipophilic drugs (101). However, because of the molecular rigidity and strong intermolecular hydrogen bonding in the

crystal state, native β CD resulted in poor aqueous solubility. Attachment of hydroxypropyl or sulfobutylether groups can favour the CD to interact with the surrounding water molecules and increase the aqueous solubility (104). In this study, β CD derivatives (HP β CD, SBE β CD and CM β CD) were included to investigate the CD solubilization of AS.

Figure 8 displays the phase-solubility diagrams of AS in aqueous CD solutions i.e., β CD, SBE β CD, HP β CD and CM β CD. All of the phase-solubility profiles represented the A_L -type according to Higuchi and Connors (1965) (105). The solubility of AS increased linearly as the concentration of CDs increased ($R^2 > 0.9$) and it was assumed that 1:1 AS:CD complexes were formed.

The apparent stability constant ($K_{1:1}$) and complexation efficiency (CE) of AS/CD complexes are shown in Table 5. The CD ranking regarding to $K_{1:1}$ and CE values was as follows: HP β CD > β CD > SBE β CD >> CM β CD. It indicated that AS has the highest affinity to HP β CD cavity in the complexing medium. Panichpakdee and Supaphol (2011) revealed that the solubility of AS was significantly increased about 20 times in the presence of HP β CD (43). In comparison of the negatively charged CDs (i.e., SBE β CD and CM β CD), SBE β CD has greater binding capacity than CM β CD. This may be due to that the significant distance of charged sulfonate moiety from the SBE β CD torus leading to enhance the binding potential with less steric interference when compared with carboxy-methyl substituent (CM β CD). In addition, the butyl moiety also acts as supplementary binding site for substrates (106, 107). Due to the limited aqueous solubility of native β CD and the very low CE of CM β CD, HP β CD

and SBE β CD were chosen for further study which represented to neutral and ionic β CD derivatives, respectively.

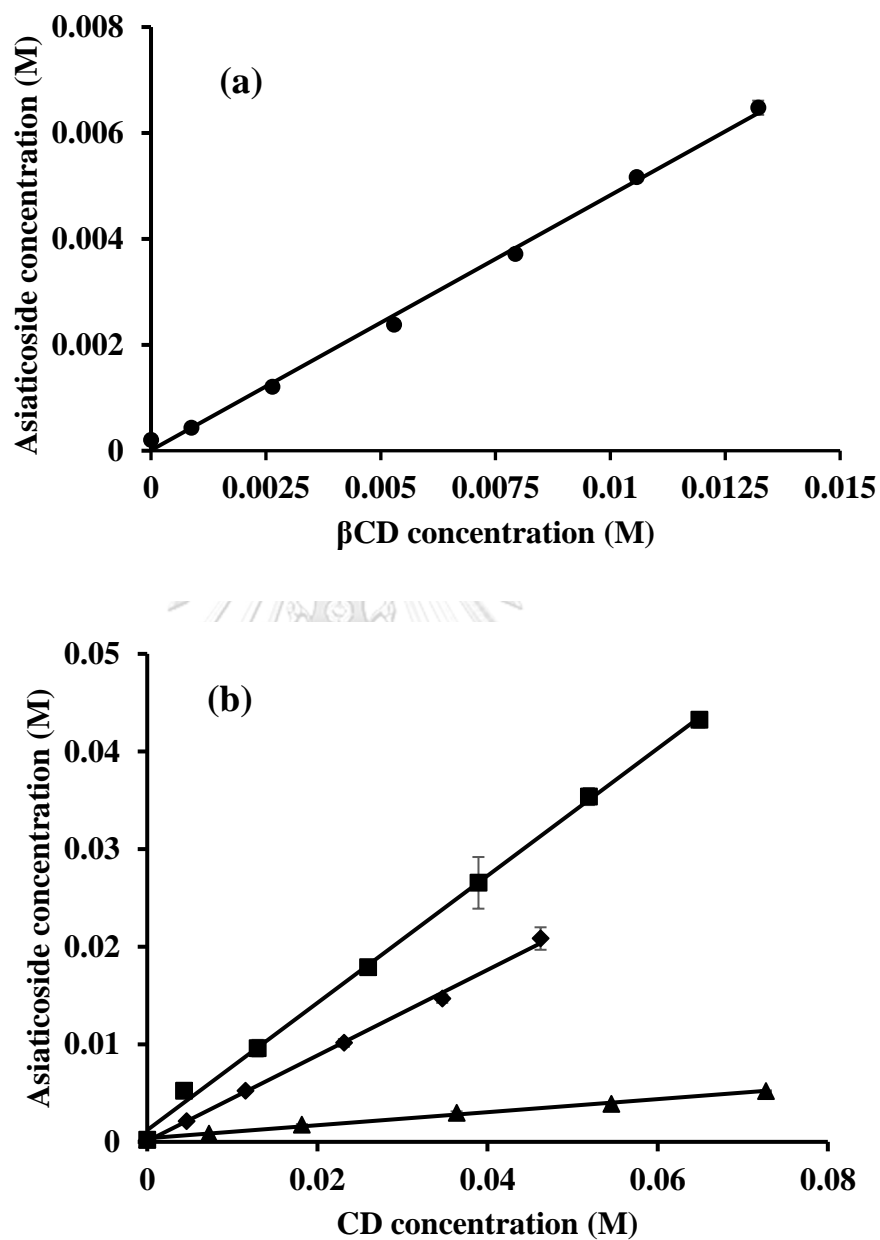


Figure 8 Phase-solubility profiles of asiaticoside in aqueous cyclodextrin solutions (a): β CD (●), (b): HP β CD (■), SBE β CD (◆), CM β CD (▲).

Table 5 The values of the apparent stability constant ($K_{1:1}$) and the complexation efficiency (CE) of AS/CD complexes in aqueous solutions at 30 ± 1 °C.

Cyclodextrin	Type	R ²	K _{1:1} (M ⁻¹)	CE
βCD	A _L	0.9979	4.55 x 10 ³	0.94
CMβCD	A _L	0.9923	3.55 x 10 ²	0.07
SBEβCD	A _L	0.9980	3.84 x 10 ³	0.78
HPβCD	A _L	0.9985	9.12 x 10 ³	1.85

3.2 The effect of water-soluble polymers on AS/SBEβCD complexation

Water-soluble polymers are able to form ternary complex via hydrophobic interaction, van der Waals dispersion forces or hydrogen bonds that can enhance the CD solubilization of drugs (108). In this study, the effect of water-soluble polymers (CS and P407) on SBEβCD solubilization of AS was investigated. CS is cationic polymer and P407 represents to non-ionic block copolymer. Figure 9 displays the phase-solubility profiles of AS/SBEβCD complex in the presence of CS (0.01 mM) or P407 (10 mM). The solubility of AS was increased with an increasing of SBEβCD concentration. It demonstrated that the phase-solubility profiles were A_L type and the stoichiometry of AS/SBEβCD complexation was not altered by addition of polymers.

Table 6 exhibits K_{1:1} and CE of AS/SBEβCD complex in the presence and absence of polymer (CS or P407). In case of the addition of CS, the values of K_{1:1} and CE were slightly increased with CE increment of 3.8%. CS could possibly form ternary complexes with AS/SBEβCD via electrostatic interaction (98, 109). In other words, SBEβCD/CS

nanoparticle formation could encapsulate AS resulted in increasing AS solubility. Interestingly, the synergistic effect of SBE β CD solubilization

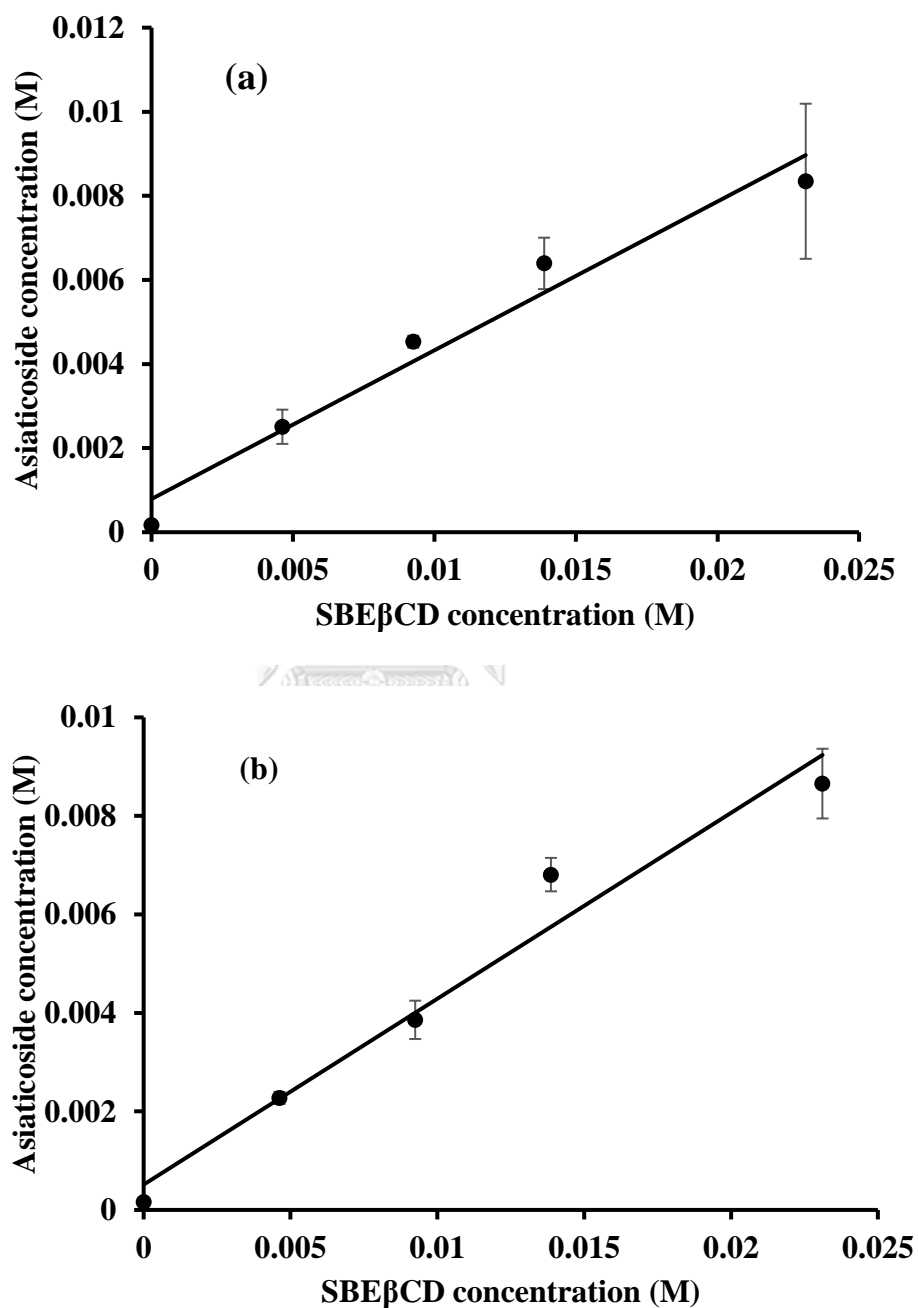


Figure 9 Phase-solubility profiles of asiaticoside in aqueous SBE β CD solution containing (a) 0.01 mM CS and (b) 10 mM P407.

Table 6 The values of apparent stability constant ($K_{1:1}$) and the complexation efficiency (CE) of AS/SBE β CD complex in aqueous solutions in the presence of polymers at 30 \pm 1 $^{\circ}$ C.

Cyclodextrin	Polymer ^a	Type	R ²	K _{1:1}	CE	% CE increment
SBE β CD	-	A _L	0.9980	3.84 x 10 ³	0.78	-
	0.01 mM CS	A _L	0.9637	4.95 x 10 ³	0.81	3.8 %
	10 mM P407	A _L	0.9654	6.18 x 10 ³	0.87	11.5 %

^aCS: Chitosan, P407: Poloxamer 407

of drug was observed with P407. The increment of solubilization when addition of P407 to AS/SBE β CD was approximately 12%. It has been reported that the addition of polymer to drug/CD complex as ternary complex, the extent of drug solubilization was higher than the binary complex (110). Moreover, water-soluble polymers are also known to form micellar type aggregates via the interaction with the outer surface of CD molecule or with drug/CD complex (53, 111). These results agreed with the study by Smith et al., (2005). They investigated the effect of hydroxypropyl methylcellulose (HPMC) on SBE β CD solubilization of carbamazepine (CBZ). The addition of HPMC to CBZ/SBE β CD binary complex resulted in enhancement of drug solubility. It facilitates SBE β CD amount reduction to be used in formulation (70).

4. ¹H-NMR determinations

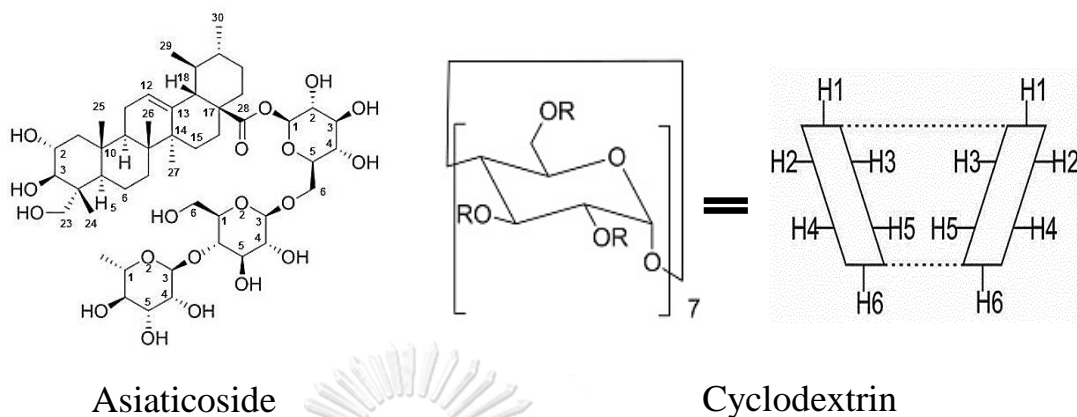
The information brought about by ¹H-NMR spectroscopy could be used to establish the inclusion modes of guest molecule into CD cavity. It is well-known that H-3 and H-5 protons of CDs are located in the inner

cavity of CDs and prominent chemical shifts of H-3 and H-5 are crucial for possible complex formation between drug and CD (58).

The chemical shift ($\Delta\delta^*$) of proton in CD cavity, the downfield shift of H-3 was +0.003 ppm and upfield shift of H-5 was -0.054 ppm in AS/HP β CD binary complex whereas in AS/SBE β CD complex, downfield shift of H-3 was +0.038 ppm and upfield shift of H-5 was -0.080 ppm. In literature, the upfield shifts occurred because of anisotropic magnetic effect induced by the presence of the aromatic group of guest molecule within the CD cavity (112). It was suggested that the significant upfield shifts of H-5 were observed in both CDs and assumed that AS molecule was inserted into the narrow side of CD cavities. Regarding to $\Delta\delta^*$ of CH₃-24, CH₃-25, CH₃-27 and CH₃-29 protons of AS, the significant upfield shifts within the binary AS/HP β CD and AS/SBE β CD were investigated (Table 7 and 8). The more chemical shift of CH₃-29 of AS was observed when it complexed with SBE β CD (-0.102 ppm) than HP β CD (-0.025 ppm). According to the observation by Panichpakdee and Supaphol (2011), the chemical shifts of CH₃-29 and CH₃-27 protons of AS and the inner-cavity proton of HP β CD were significantly shifted (43). Our investigation confirmed that the cyclohexane ring moiety of AS was inserted within high electron rich hydrophobic CD cavity.

The chemical shifts of ternary complexes of AS/SBE β CD/P407 and AS/SBE β CD/CS are summarized in Table 9 and 10. The incorporation of water-soluble polymers did not significantly change the chemical shift when compared with AS/SBE β CD binary complex.

Table 7 The ^1H -chemical shifts of AS alone and in the presence of HP β CD



HP β CD, R=CH₂CH(CH₃)OH or H;

SBE β CD, R=CH₂CH₂CH₂CH₂SO₃Na or H

1' 2' 3' 4'

^1H	δ_{free}	δ_{complex}	$\Delta\delta^* =$ $(\delta_{\text{complex}} - \delta_{\text{free}})$
AS			
H-12	5.264	5.205	- 0.059
H-1	5.174	5.150	- 0.020
CH ₃ -18	2.050	2.039	- 0.011
CH ₃ -27	1.151	1.066	- 0.086
CH ₃ -25	0.931	0.861	- 0.070
CH ₃ -29	0.854	0.829	- 0.025
CH ₃ -24	0.656	0.597	- 0.059
Rha-5	3.898	3.875	- 0.023

Table 7 The ^1H -chemical shifts of AS alone and in the presence of HP β CD
(Con't)

^1H	δ_{free}	δ_{complex}	$\Delta\delta^* =$ $(\delta_{\text{complex}} - \delta_{\text{free}})$
<i>HPβCD</i>			
H-1	4.872	4.864	- 0.008
H-2	3.396	- ^a	- ^a
H-3	3.813	3.816	+0.003
H-4	3.311	3.308	- 0.003
H-5	3.599	3.545	- 0.054
H-6	3.681	3.685	+0.004
CH ₃	0.955	0.975	+0.020

^aoverlapping of chemical shifts

Table 8 The ^1H -chemical shifts of AS alone and in the presence of $\text{SBE}\beta\text{CD}$

^1H	δ_{free}	δ_{complex}	$\Delta\delta^* =$ $(\delta_{\text{complex}} - \delta_{\text{free}})$
AS			
H-12	5.264	5.219	- 0.045
H-1	5.174	5.125	- 0.049
CH ₃ -18	2.050	2.043	- 0.007
CH ₃ -27	1.151	1.066	- 0.085
CH ₃ -25	0.931	0.854	- 0.077
CH ₃ -29	0.854	0.752	- 0.102
CH ₃ -24	0.656	0.598	- 0.058
Rha-5	3.898	3.864	- 0.034
SBEβCD			
H-1	4.880	4.858	- 0.022
H-2	3.400	3.368	- 0.032
H-3	3.784	3.822	+0.038
H-4	3.286	- ^a	- ^a
H-5	3.611	3.531	- 0.080
H-6	3.674	3.684	+0.010
H-4'	2.733	2.744	+0.011
H-2',H-3'	1.583	1.591	+0.008

^aoverlapping of chemical shifts

Table 9 The ^1H -chemical shifts of AS alone and in ternary complex (AS/SBE β CD/CS)

^1H	δ_{free}	δ_{complex}	$\Delta\delta^{*} =$ $(\delta_{\text{complex}} - \delta_{\text{free}})$
AS			
H-12	5.264	5.223	- 0.041
H-1	5.174	5.129	- 0.045
CH ₃ -18	2.050	2.042	- 0.008
CH ₃ -27	1.151	1.067	- 0.084
CH ₃ -25	0.931	0.857	- 0.074
CH ₃ -29	0.854	0.752	- 0.102
CH ₃ -24	0.656	0.600	- 0.056
Rha-5	3.898	3.858	- 0.040
SBEβCD			
H-1	4.88	4.868	- 0.012
H-2	3.400	3.383	- 0.014
H-3	3.784	3.808	+0.024
H-4	3.286	- ^a	- ^a
H-5	3.611	3.599	- 0.012
H-6	3.674	3.682	+0.008
H-4'	2.733	2.743	+0.010
H-2',H-3'	1.583	1.589	+0.006

^aoverlapping of chemical shifts

Table 10 The ^1H -chemical shifts of AS alone and in ternary complex (AS/SBE β CD/P407)

^1H	δ_{free}	δ_{complex}	$\Delta\delta^* =$ $(\delta_{\text{complex}} - \delta_{\text{free}})$
AS			
H-12	5.264	5.215	- 0.049
H-1	5.174	5.123	- 0.051
CH ₃ -18	2.050	2.044	- 0.006
CH ₃ -27	1.151	1.066	- 0.085
CH ₃ -25	0.931	0.856	- 0.075
CH ₃ -29	0.854	0.753	- 0.101
CH ₃ -24	0.656	0.598	- 0.058
Rha-5	3.898	3.862	- 0.036
SBEβCD			
H-1	4.880	4.859	- 0.021
H-2	3.400	3.363	- 0.037
H-3	3.784	3.821	+0.037
H-4	3.286	- ^a	- ^a
H-5	3.611	- ^a	- ^a
H-6	3.674	3.680	+0.006
H-4'	2.733	2.744	+0.011
H-2',H-3'	1.583	1.592	+0.009

^aoverlapping of chemical shifts

5. Solid-state characterization

5.1 DSC analysis

DSC is an important tool to investigate the interaction between host and guest molecule when the drug molecule included in CD cavity (60). It referred that when the drug molecule included in the CD cavity, the melting point might be shifted or disappeared. Figure 10 displays the DSC thermograms of intact AS, HP β CD, SBE β CD, the physical mixtures (PM) and freeze dried (FD) of binary (AS/HP β CD, AS/SBE β CD) and FD of ternary complexes (AS/SBE β CD/CS and AS/SBE β CD/P407). The DSC thermogram of AS displayed a broad endothermic peak in the temperature range of 50-130 °C due to dehydration during the heating process and sharp endothermic peak at 251.20 °C which corresponded to its melting point (Figure 10a). This observation was in accordance with the study of Panichpakdee and Supaphol (2011) (113). DSC curves of HP β CD and SBE β CD showed broad endothermic bands around 80 °C which attributed to the dehydration process (Fig. 10b and 10e respectively). Generally, DSC of amorphous CDs show broad endothermic peaks around 90-130 °C due to dehydration of CD molecule (60). In the thermogram of SBE β CD, the further decomposition peak was observed at 266.45 °C (114).

In case of PM of AS/HP β CD and AS/SBE β CD, AS melting peak was still observed in the thermograms but slightly shifted to lower temperature of 249.42 °C (Figure 10c) and 249.04 °C (Figure 10f), respectively. This may be due to the weak interaction of components or heat induced interaction during DSC operation (63). For FD samples of binary AS/HP β CD complex, the disappearance of an endothermic peak of

AS (251.20 °C) may be attributed to an amorphous state of AS and/or the formation of inclusion complex between AS and HP β CD in the solid-

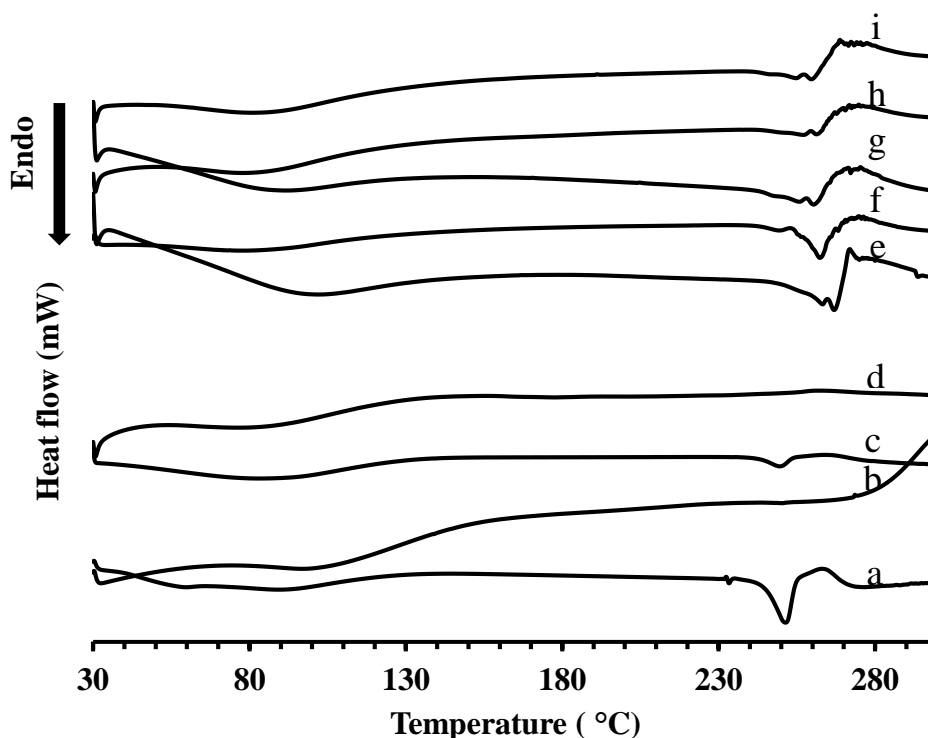


Figure 10 DSC thermograms of (a) pure AS, (b) pure HP β CD, (c) PM AS/HP β CD, (d) FD AS/HP β CD (e) pure SBE β CD, (f) PM AS/SBE β CD, (g) FD AS/SBE β CD, (h) FD AS/SBE β CD/CS, (i) FD AS/SBE β CD/P407.

state (Fig. 10d) (113). For FD binary (AS/SBE β CD) and ternary (AS/SBE β CD/CS) complexes (Fig. 10g, 10h, 10i), the endothermic peak of AS disappeared and the endothermic peak at 266.45 °C shifted to 259.75, 261.41 and 259.90 °C respectively. The similar finding was observed in thermogram of FD samples of SBE β CD and Nateglinide (NTG) and concluded that there was possible interaction between NTG and SBE β CD (115).

5.2 FT-IR spectroscopy

FT-IR spectroscopy is the widely used technique to determine the interaction between CD and guest molecule in solid-state and the complexation of guest molecules can be observed from changes or shifts in absorption spectrums (24). Figure 11 shows the FT-IR spectra of AS, HP β CD, SBE β CD, PM and FD samples of their binary complexes and FD samples of AS/SBE β CD/polymer ternary complexes. The typical absorption bands of AS depicted as C=C stretching vibration at 1027.49 cm^{-1} , C-O-C stretching at 1448.60 cm^{-1} , C-C stretching at 1734.22 cm^{-1} , C-H stretching at 2905.64 cm^{-1} and broad peak of O-H stretching at 3355.71 cm^{-1} (Figure 11a) (116). The FT-IR spectra of HP β CD and SBE β CD showed a broad absorption band between 2983 and 3675 cm^{-1} due to OH-stretching vibration (Figure 11b and 11e). Figure 11c and 11f show the FT-IR spectra of AS in PM of both CDs. It indicated that there was no interaction of AS and CD with a simple superimposition of individual components as well as no substantial alternation. In case of the FT-IR spectra of FD samples, they did not show new bands which inferred that there were no chemical bonds between AS and CD. However, in the binary complexes (Figure 11d and 11g), the prominent characteristic peaks corresponding to the aromatic ring of AS i.e., C=C stretching, C-H stretching and C-C stretching were shifted to 1021.65, 2924.16, 1735.21 and 1078.95, 2921.75, 1733.73 cm^{-1} respectively. The O-H stretching of AS was also shifted to 3355.68 cm^{-1} and, 3373.48 cm^{-1} in both AS/HP β CD and AS/SBE β CD binary complexes, respectively.

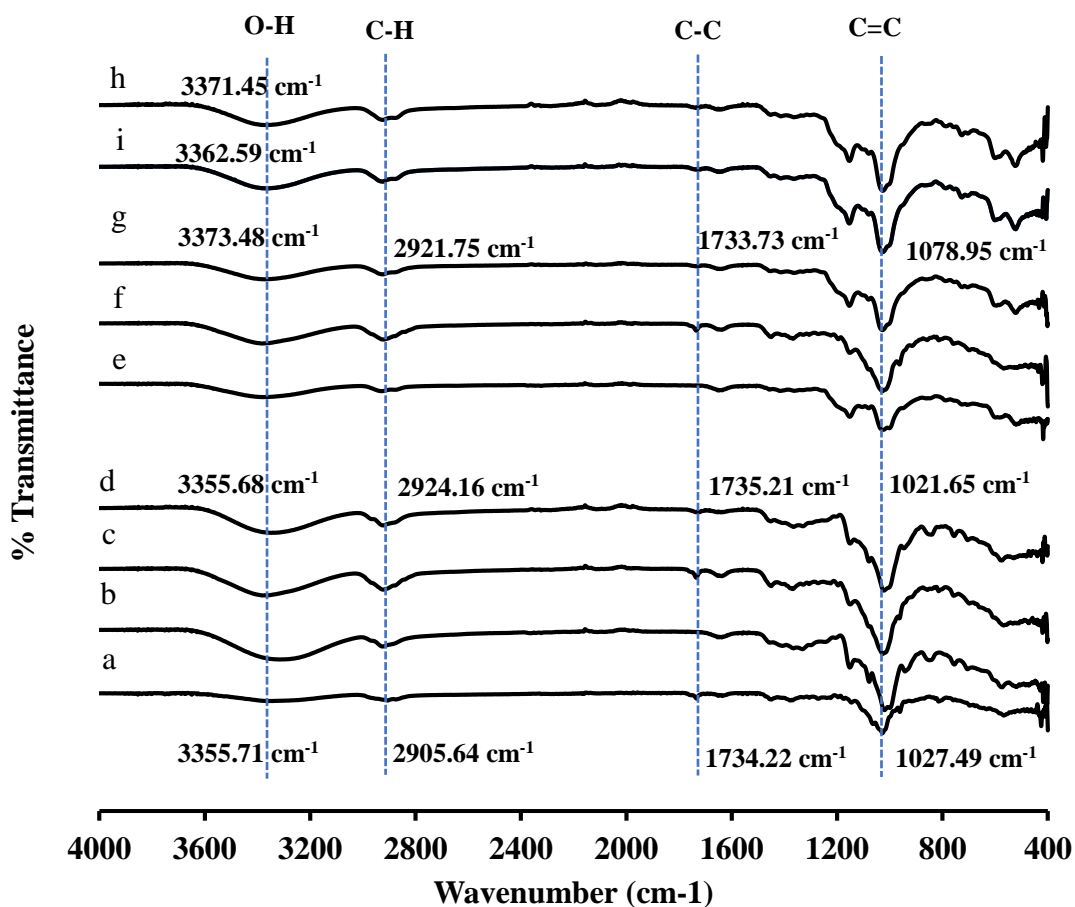


Figure 11 FT-IR spectra of (a) pure AS, (b) pure HPβCD, (c) PM AS/HPβCD, (d) FD AS/HPβCD (e) pure SBEβCD, (f) PM AS/SBEβCD, (g) FD AS/SBEβCD, (h) FD AS/SBEβCD/CS, (i) FD AS/SBEβCD/P407

Since the C=C, C-H and C-C bonds correspond to the aromatic ring of AS, there might be possible interactions between the benzene ring moiety of AS and hydrophobic cavity of CDs. This result was confirmed by the evidence of the ¹H-NMR data in which the significant chemical shifts of cyclohexane ring of AS and inner cavity of CDs were observed. The hydrogen bonding interaction of ternary complexes (AS/SBEβCD/CS and

FD AS/SBE β CD/P407) was also observed with significantly shifted O-H stretching vibration to 3362.59 and 3371.45 cm^{-1} respectively (Figure 11h and 11i). The existence of these spectral changes might be due to the dissociation of the intermolecular hydrogen bonds of AS through the formation of complexes via possible interactions between the functional groups of AS, CDs and polymers (68, 117). These findings were in agreement with the study of Jain et al., (2011) in which FT-IR spectrum shifts in O-H stretching of SBE β CD and C=C of carbamazepine (CBZ) were evidenced of interaction between CBZ and SBE β CD (118).

5.3 Powder X-Ray Diffraction (PXRD)

PXRD is the powerful method to detect CD complexation of compound in powder or crystalline states (60). Figure 12 depicts the X-ray diffraction patterns of AS, HP β CD, SBE β CD, PM and FD samples of their binary and ternary AS/SBE β CD/polymer complexes. The X-ray spectrum of AS represents the numerous sharp diffractions in the range of 4-25° 2 θ (Figure 12a). High intensity peaks were observed at 4.313, 13.870, 15.929, 16.632, 19.950, 21.557° indicating the high degree of crystallinity. For HP β CD and SBE β CD, their diffractograms did not show any sharp peak and only halo pattern were observed (Figure 12b and 12e) (119).

Simple overlapping of native diffraction patterns of AS and CD were observed in PM of AS/HP β CD and AS/SBE β CD and the sharp crystalline peaks of AS were scattered on the diffusion patterns of HP β CD and SBE β CD (Figure 12c and 12f). This indicated that there was no interaction

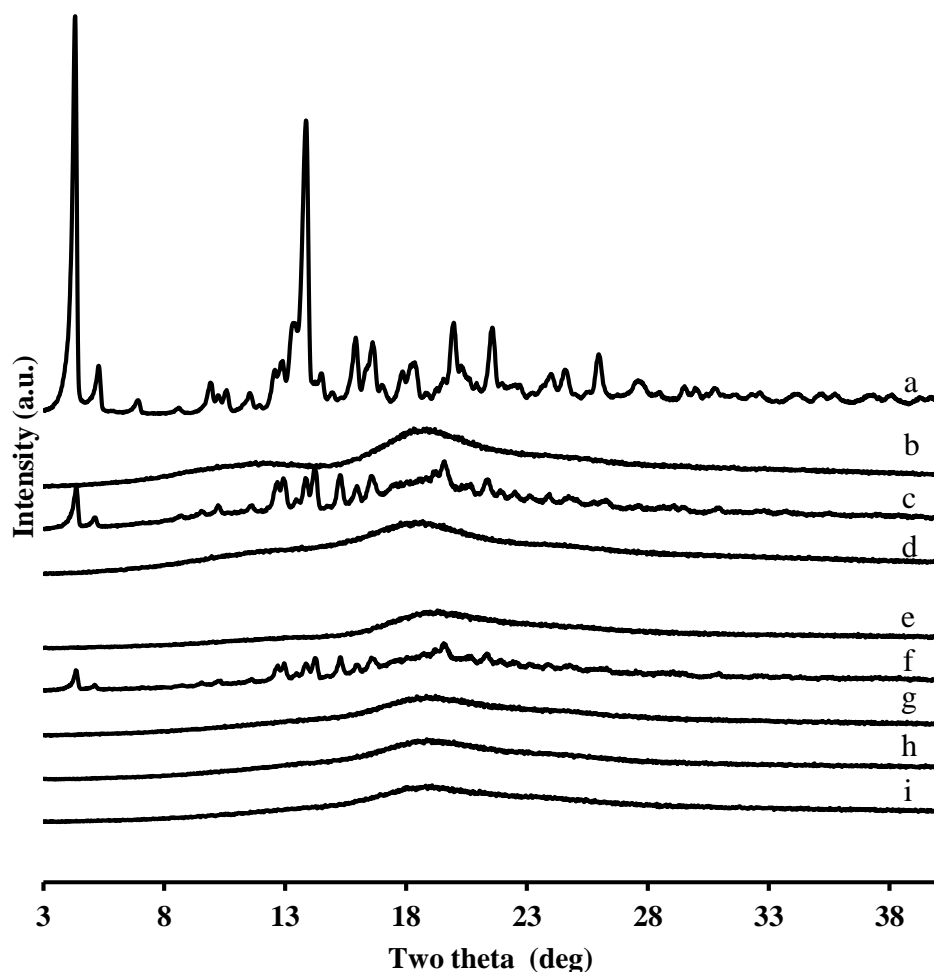


Figure 12 The PXR D spectra of (a) pure AS, (b) pure HP β CD, (c) PM AS/HP β CD, (d) FD AS/HP β CD, (e) pure SBE β CD, (f) PM AS/SBE β CD, (g) FD AS/SBE β CD, (h) FD AS/SBE β CD/CS, (i) FD AS/SBE β CD/P407

between the components. However, in FD samples of AS/CD binary complexes i.e., AS/HP β CD and AS/SBE β CD (Figure 12d and 12g) and ternary complexes (AS/SBE β CD/CS and AS/SBE β CD/P407) (Figure 12h and 12i), the corresponding AS peaks were completely disappeared. It represented that AS transformed from crystalline to amorphous state. It was probably due to the formation of drug/CD complexation. The similar

findings were observed in the study of FD complex of daidzein with HP β CD and SBE β CD by Deng et al., (2016). The results presented the transformation to amorphous patterns provided strong evidences of inclusion complexation between daidzein and both CDs (120).

6. *In vitro* release study

Figure 13 shows the AS dissolution profiles of free AS, binary (AS/HP β CD, AS/SBE β CD) and ternary (AS/SBE β CD/CS and AS/SBE β CD/P407) complexes. The dissolution efficiency at 120 min (DE_{120}), the time required to release 50% of the drug [$t_{50\%}$ (min)] together with the dissolution rate constant [K_1 (min^{-1})] were determined from the drug release profile and shown in Table 11. The AS/HP β CD and AS/SBE β CD binary complexes exhibited 69.93% and 61.77% drug release in 15 min, respectively; about 2-times higher in comparison to pure AS (35.53%). At 120 min, AS/HP β CD and AS/SBE β CD achieved 98.85% and 78.37%, while pure AS attained 50.45% at the same interval. The hydrophobic nature of AS prevented wetting in dissolution medium and resulted to poor dissolution rate.

All dissolution parameters i.e., K_1 , $t_{50\%}$ and DE_{120} of binary complexes (AS/HP β CD and AS/SBE β CD) demonstrated that they significantly improved the drug release or the drug dissolution rate when compared to intact AS alone. The enhancement of AS dissolution in binary complexes can be attributed based on high reduction of crystallinity, lower surface tension between poorly soluble drug and dissolution medium by CDs and greater solubilization of complexes (121). The similar dissolution

enhancement of nimodipine after complexation with HP β CD and SBE β CD was studied by Semchedine et al., (2014) (121).

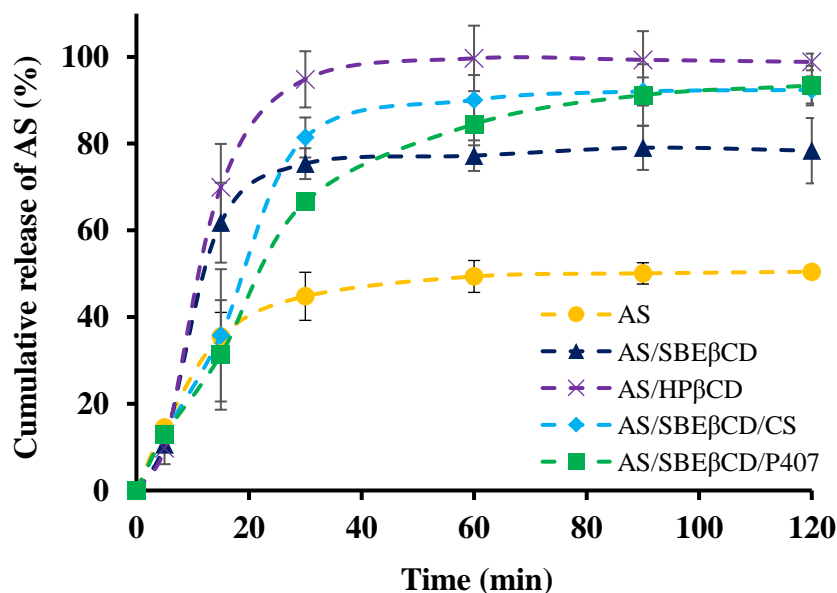


Figure 13 In vitro release study of AS, FD AS/SBE β CD, FD AS/HP β CD, FD AS/SBE β CD/CS and FD AS/SBE β CD/P407.

In the presence of polymers (CS or P407) as AS/CD/polymer ternary complexes, the slightly dissolution retardant was observed. $t_{50\%}$ of AS/SBE β CD/CS, was 20.3 min whereas that was longer in case of AS/SBE β CD/P407 (24.6 min). When the ternary complexes made in contact with dissolution medium, the polymers swelled and formed the hydrophilic layer resulting the slow drug diffusion rate, especially in case of P407. This is in accordance with the investigation of Jug and Bećirević-Laćan (2004) (122). It revealed that slow release effect of piroxicam was observed in the addition of HPMC as ternary complexation. In case of SBE β CD/CS, the electrostatic interaction between anionic SBE β CD and cationic CS enables the slow release of drug (34, 42). However, at 120 min

was attained, AS release rate of both ternary complexes were increased up to 93%. K_1 of binary complex was slightly higher than both ternary complexes, whereas there was only slight enhancement of DE_{120} in ternary complexes were observed. The higher dissolution rate in both binary and ternary complexes was achieved by possible amorphization of AS during freeze drying (123). The enhancement in dissolution of the FD complex could be derived from the formation of inclusion complexes in the solid-state which was confirmed by DSC, FT-IR and PXRD studies.

Table 11 Dissolution parameters of solid complexes

Sample	K_1 (min^{-1})	R^2	$t_{50\%}$ (min)	DE_{120}
AS	0.007±0.00	0.7058	80.03±7.79	27.82±0.47
AS/HP β CD	0.057±0.01	0.9070	12.94±0.74	54.54±1.20
AS/SBE β CD	0.051±0.01	0.8949	17.75±1.23	42.39±3.02
AS/SBE β CD/CS	0.039±0.01	0.9460	20.30±1.84	46.43±0.53
AS/SBE β CD/P407	0.031±0.01	0.9750	24.63±1.74	47.09±1.41

7. Morphology, particle size and zeta potential analysis

It is well-known that binary drug/CD as well as ternary drug/CD/polymer complexes can promote the solubilization of poorly water-soluble drugs via aggregate formation in aqueous solution. To evaluate the particle size of AS/CD binary complexes and AS/SBE β CD/polymer ternary complexes, DLS and TEM were applied.

Table 12 shows the particle size and size distribution and zeta potential of AS saturated in 5% w/w HP β CD or 2.5% w/w SBE β CD solutions in the presence and absence of polymers and the morphology of

their aggregates are displayed in Figure 14. For binary complexes i.e., AS/HP β CD and AS/SBE β CD, two different size populations were detected. The first population was smaller size aggregates which were 1-3 nm in diameter, represented to the AS/CD inclusion complexes and the second population referred to the formation of AS/CD complex aggregates of 300-450 nm in diameter. It has been reported that, the diameter of CD aggregates mostly occurs between 90 and 300 nm however size distribution can vary from 20 nm to a couple of μ m (124). In agreement with DLS, TEM images of binary complexes also displayed two different size populations (Figure 14a and 14b). The smaller aggregates possess the spherical in shape and the larger aggregate displays a cluster of small spherical shaped aggregates (125).

As expected, the aggregate size of ternary complexes (AS/SBE β CD/P407 and AS/SBE β CD/CS) was larger than that of binary system. The size of ternary AS/SBE β CD/P407 complex showed multicomponent of trimodal size distributions which existed as inclusion complexes, small and large aggregates formation (Table 12). The non-ionic polymer (P407) stabilize AS/SBE β CD binary complex by steric effect (126) and the resulted AS/SBE β CD/P407 ternary system was observed as the spherical shape aggregates (Figure 14c). In case of ternary AS/SBE β CD/CS complex, it exhibited monomodal size distribution with the particle size approximately 500 nm (Table 12). Polycationic CS electrostatically interacted with polyanionic SBE β CD to form ionically cross-linked SBE β CD/CS nanoparticles (109). These spherical shaped nanoparticles with irregular surface were observed by TEM image (Figure 14d). The appearance was in accordance with previous reports and the drug

was solubilized in SBE β CD as well as entrapped inside the shell of CS within the nanoencapsulation platforms (53, 110, 127). However, all the aggregates size appeared in TEM were smaller than the average size which observed in DLS measurement. This was probably due to the dehydration of sample during the preparation for TEM (109).

Water-soluble polymers and surfactants are known to have stabilizing effect on CD aggregates in aqueous solutions (68). In comparison between two ternary systems containing cationic polymer (CS) and non-ionic polymer (P407), the aggregate size of AS/SBE β CD/CS complex was smaller than that of AS/SBE β CD/P407, this may be due to the electrostatic interaction between anionic SBE β CD and cationic CS. Ryzhakov et al., (2016) revealed that as repulsive forces are strong the micelle size becomes small but it can become very large when the repulsive forces are weak as in the case with nonionic polymers (124). This was also supported by zeta potential values in which incorporation of CS as ternary system resulted higher zeta potential values of $+19.43 \pm 0.9$ mV than that of non-ionic P407 -0.42 ± 0.52 mV (126). It can also be seen that, the higher the zeta potential value, the greater the stability for nano-aggregate system. Although the zeta potential value of nano-aggregates in AS/SBE β CD/P407 ternary complex was low, its stabilization is regulated by van der Waals forces and hydrogen bonding interactions but there was competition of binding resulting unstable aggregates (124).

Table 12 Mean particle size and zeta potential of binary AS/CD, and ternary AS/SBE β CD/polymer complex aggregates

Cyclodextrin (% w/w)	Polymer (% w/w)	Mean particle size (nm; Mean \pm S.D.)	Zeta Potential (mV)
5% HP β CD	-	2.3 \pm 0.05 316.23 \pm 42.94	+6.82 \pm 3.97
2.5% SBE β CD	-	1.54 \pm 0.14 416.96 \pm 11.81	-1.27 \pm 0.54
	5% P407	5.17 \pm 0.69 31.76 \pm 4.60 2345.00 \pm 816	-0.42 \pm 0.52
	1% CS	527.86 \pm 18.41	+19.43 \pm 0.90

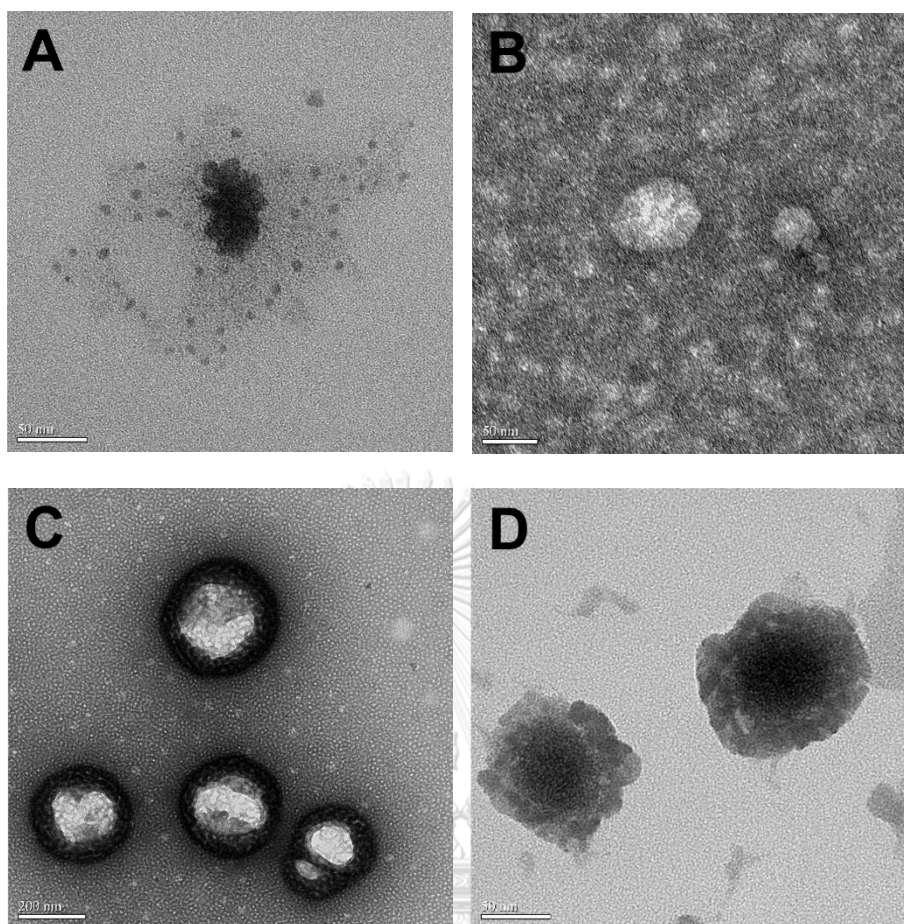


Figure 14 TEM photographs of AS saturated in 5% HP β CD or 2.5% SBE β CD solutions without and with polymers (5% P407 or 1% CS, all % w/w) (a) AS/HP β CD, (b) AS/SBE β CD, (c) AS/SBE β CD/P407, and (d) AS/SBE β CD/CS

8. Preparation and characterization of drug-free and drug-loaded SBE β CD/CS nanoparticles

The ratio between SBE β CD and CS is critical parameter for preparation of nanoparticles. Thus, prior to load AS into the nanoencapsulated platforms, the appropriate concentrations and the ratios

for drug-free nanoparticle formation was required to illustrate. The phase-diagram of the different concentrations of SBE β CD and CS which were used to prepare nanoencapsulation is shown in Figure 15. The appearance of each SBE β CD:CS ratio was classified into 3 categories: clear solution, opalescent suspension and aggregates.

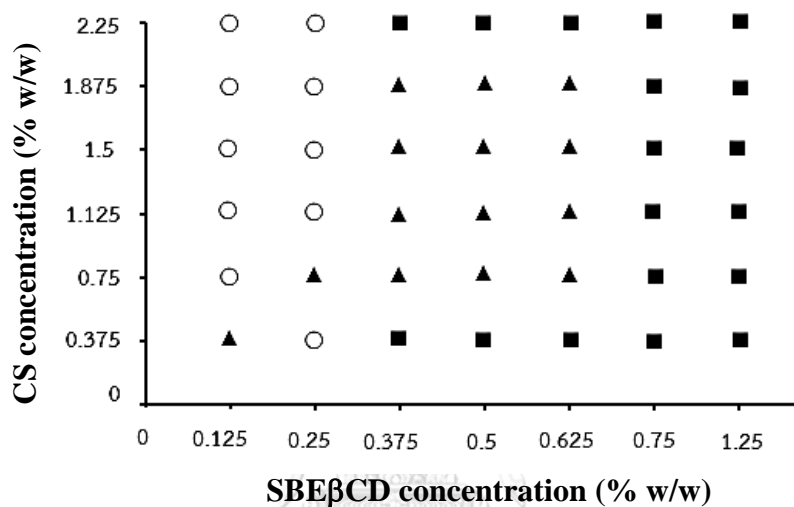


Figure 15 Phase-diagram of SBE β CD/CS nanoparticle formation with three areas; clear solution (O), opalescent dispersion (▲) and aggregates (■)

In most cases of low SBE β CD concentrations (0.125-0.25% w/w), the clear solution was observed. It indicated that the amount of anionic SBE β CD was too low to counteract the cationic CS resulted in the nanoparticles could not be formed or very low content of nanoparticles were obtained (109). When increasing the proper concentrations of SBE β CD (0.375-0.625% w/w) and CS (0.75-1.875% w/w), the opalescent suspensions were detected that represented the nanoparticles formation. Since the nanoencapsulations obtained from a high concentration of CS (1.875% w/w) with 0.375-0.625% w/w SBE β CD were viscous, they were

excluded from further study. The aggregation was observed when CS concentrations were out of the optimum range i.e., $<0.75\%$ and $>1.875\%$ w/w. Too high CS concentration i.e., 2.25% w/w the resulted preparation was viscous; thus, the nanoparticles was not formed. Whereas, too low CS concentration i.e., 0.375% w/w, shielding effect of positive charge of CS to counteract the high negative charge of SBE β CD ($>0.375\%$ w/w) was occurred which caused a decrease in the positive zeta potential values of the nanoparticles. Consequently, the reduction in the repulsive forces between the nanoparticles resulted in cross-bridge formation between nanoparticles and agglomeration of the nanoparticles was formed (109, 128).

From the results, the optimum concentration of SBE β CD and CS formed nanoparticles were $0.375\text{-}0.625\%$ w/w and $0.75\text{-}1.125\%$ w/w respectively. These concentrations were subjected to load AS via ionic gelation technique. The physicochemical characterizations i.e., mean particle size and size distribution (PDI) and zeta potential values of AS loaded micro- and nanoparticles are shown in Table 13.

At the concentration of 0.75% CS with increasing SBE β CD concentrations from 0.375% to 0.625% w/w, the nanoparticles were obtained in the range of $700\text{-}760$ nm. The higher the concentrations of CS up to $1.125\text{-}1.5\%$ w/w, the larger particle size in micrometer range were obtained. The increased particle diameter was possibly attributed to increase the viscosity of the solution as well as the greater availability of the protonated amine group of CS to crosslink with SBE β CD (129, 130). Also, the increasing of SBE β CD concentrations from 0.375 to 0.625% w/w with constant CS concentration resulted in decreased particle size. PDI of

all SBE β CD:CS ratios were in the range of 0.1- 0.7, it indicated that relatively homogenous dispersion (131).

Table 13 Mean particle size, PDI and zeta potential values of drug loaded SBE β CD/CS micro- and nanoparticles

SBE β CD (% w/w)	CS (% w/w)	Mean particle size (nm)	PDI	Zeta Potential (mV)
0.375	0.75	759.20 \pm 6.57	0.32 \pm 0.06	+22.03 \pm 7.762
0.5	0.75	702.80 \pm 7.65	0.17 \pm 0.00	+25.6 \pm 0.854
0.625	0.75	691.66 \pm 8.34	0.18 \pm 0.03	+26.6 \pm 0.264
0.375	1.125	1467.66 \pm 28.29	0.68 \pm 0.21	+29.93 \pm 1.60
0.5	1.125	1464.33 \pm 12.58	0.22 \pm 0.01	+26.56 \pm 3.00
0.625	1.125	1118.66 \pm 8.62	0.25 \pm 0.01	+24.46 \pm 1.40
0.375	1.5	4020.33 \pm 469.00	0.68 \pm 0.10	+25.33 \pm 1.88
0.5	1.5	1950.33 \pm 21.57	0.30 \pm 0.02	+26.23 \pm 1.30
0.625	1.5	1458.66 \pm 23.71	0.28 \pm 0.01	+21.43 \pm 1.53

Regarding to the zeta potential values, all micro- and nanoencapsulations exhibited high positive charge values (21-30 mV) which represented to relatively stable. In other words, drug and SBE β CD were mainly entrapped inside the matrix and do not mask the inherent charge of CS on the surface (132).

Among the CS concentrations tested, only 0.75% w/w of it can form nanoparticles with SBE β CD via encapsulation process. This was in agreement with the investigation of Mahmoud et al., (2011) and they found that, increasing CS concentration leads to increase the particle size and the

viscosity of the system (109). Therefore, the concentrations of SBE β CD (0.375, 0.5, 0.625% w/w) and CS (0.75% w/w) were selected for preparation of *in-situ* gel formulation.

9. Physicochemical and chemical characterizations

9.1 Appearance, pH, viscosity, and syringeability and injectability

All formulations were investigated for their physical appearance and revealed that *in situ* gels containing AS/SBE β CD/CS NPs (F1-F3, F7-F9 and F13-F15) displayed opalescent preparation while the non-encapsulated *in situ* gels (F4-F6 and F10-F12) exhibited clear solution.

The pH values of the *in situ* gel formulations containing AS were within the range of 4.9-6.7 (Table 14). The formulations consisted of AS/SBE β CD/CS NPs were slightly acidic while the non-encapsulated formulations had the pH closely to the neutral pH. The pH of the solutions has strongly affected from acetic acid to dissolve CS. However, all *in situ* gel formulations were within the pH range for optimum stability (133).

The viscosity is one of the main parameters of *in situ* gel formulation for periodontal application. The formulation in solution state should ideally have a low viscosity to pass through the syringe while injecting. It should also have a high viscosity in order to remain in place at the application site after delivering into periodontal pocket (134). All the formulations have viscosity value in the range of 37.31 ± 2.49 to 60.46 ± 11.48 cPs at 25 °C. The low viscosity of formulation meets the criteria of ease of administration and easily spreadable to the minor gap of periodontal pockets (135). When the temperature was increased to 37 °C, the viscosity was significantly higher up to 250-folds (Table 14). As the temperature increased, micellar entanglement of P407 was promoted,

Table 14 pH, viscosity, syringeability and injectability of in situ gel formulations containing asiaticoside (Mean±S.D., n=3)

Formulation	pH	Viscosity (cPs)		Syringeability and injectability ^a
		25 °C	37 °C	
F1	4.95±0.06	54.97±3.92	802.78±28.38	+++
F2	4.92±0.01	46.49±2.38	848.98±40.82	+++
F3	4.93±0.01	59.31±9.34	921.73±10.87	+++
F4	6.74±0.07	37.31±2.49	8584.87±234.55	+++
F5	6.52±0.19	41.00±1.46	8686.44±167.50	+++
F6	6.66±0.03	34.28±2.79	9128.79±195.20	+++
F7	4.92±0.05	41.82±2.46	8489.84±199.60	+++
F8	4.91±0.01	42.11±3.55	8588.14±157.60	+++
F9	4.94±0.01	43.91±1.05	8604.52±216.30	+++
F10	6.57±0.07	48.70±5.27	8847.00±206.43	+++
F11	6.57±0.08	51.69±4.39	8758.53±205.90	+++
F12	6.54±0.03	49.48±6.41	8738.87±125.50	+++
F13	4.85±0.05	57.79±6.17	8824.06±163.40	+++
F14	4.84±0.04	60.46±11.48	9089.47±251.00	+++
F15	4.87±0.02	54.07±4.80	9348.33±246.30	+++

^a syringeability and injectability; (+) solution can be syringed and injected with strong force, (++) medium force, (+++) less force and (-) the solution cannot pass through the needle

leading to gel formation and an overall increase in bulk viscosity. However, after gelation at 37 °C, the viscosity of F1, F2 and F3 were almost 10 times lower than other formulations (p -value <0.05). The lower the viscosity, the higher chance to flow out of the formulation from the pocket after forming gel. Therefore, these three formulations were excluded for further studies.

The syringeability and injectability of each formulation was tested and revealed that all formulations in solution state were easily syringeable and injectable with less force through the 27 G needle equipped to 1 mL plastic syringe (Table 14).

9.2 Gelation temperature, gelation time and in vitro gelling capacity

In this study, all formulations were within the range of 30 °C to 33 °C (Table 15). The temperature of periodontal pockets is approximately 35-37 °C (136). Thus, gelation time or sol-gel transition temperatures ($T_{\text{sol-gel}}$) range suitable for periodontal *in situ* gel formulation is 25–37 °C (96). If $T_{\text{sol-gel}}$ is lower than 25 °C, a gel might be formed at room temperature which is difficult in manufacturing and application. On the other hand, $T_{\text{sol-gel}}$ exceeds to 37 °C, the preparation remains as a liquid state at the site of action resulting in the drainage of formulation. $T_{\text{sol-gel}}$ of formulations containing SBE β CD/CS NPs (F7-F9, F13-F15) was slightly higher than those of non-encapsulated formulations (F4-F6, F10-F12). Since the P407 gelation is based on micelles packing and entanglement, the effect of additives may interfere the micelle formation and causing changes in gelation mechanism (137). The increasing of $T_{\text{sol-gel}}$ might be due to acetic acid, which used to solubilize CS. The acid could weaken the hydrogen bonding force between densely packed unit of P407, resulting in an increase gelation temperature (138, 139). Another explanation was the possibility of the threading of CD onto the P407 chains or P407/CD aggregate formation resulted in the shift the critical micellar concentration to higher value (140, 141). Shaker et al. reported that the incorporation of

tamoxifen citrate/SBE β CD complex in the poloxamer gel exhibited the increment of $T_{sol-gel}$ (142).

Table 15 Gelation temperature ($T_{sol-gel}$), gelation time and in vitro gelling capacity of in situ gel formulations (n=3, Mean \pm S.D.)

Formulation	$T_{sol-gel}$ ($^{\circ}$ C)	Gelation time (s)	<i>In vitro</i> gelling capacity ^a
F4	30.10 \pm 0.20	75	++
F5	30.10 \pm 0.17	60	++
F6	30.16 \pm 0.21	50	++
F7	31.83 \pm 0.11	100	+++
F8	30.96 \pm 0.05	75	+++
F9	30.76 \pm 0.05	50	+++
F10	30.36 \pm 0.12	80	++
F11	30.06 \pm 0.11	50	++
F12	29.96 \pm 0.05	50	++
F13	32.36 \pm 0.11	90	+++
F14	31.90 \pm 0.20	80	+++
F15	31.46 \pm 0.05	75	+++

^a*in vitro* gelling capacity; (+) gelation after few min and disperse rapidly, (++) immediate gelation and remain for few hours, (+++) immediate gelation and remained for extended period

The gelation time is the time taken by the system to transform from solution-state to gel-state when exposed to body temperature. All *in situ* gels underwent rapid gelation within 50-100 sec and can yield the promising result as they quickly formed gel when expose to such condition (Table 15). The gelation time of non-encapsulated *in situ* gel was slightly

faster than that of encapsulated formulations. Nevertheless, both additives i.e., CS and SBE β CD used in this study with low concentrations that do not significantly alter the micellar properties of P407.

The *in situ* gel should undergo rapid sol to gel transition in SSF at 37 ± 1 °C and maintained for a period of time. *In vitro* gelling capacity was performed and found that all the *in situ* gel formulations immediately exhibited the gelation when they were in contact with SSF. Non-encapsulated formulations immediately formed gel but less stiff and dissolved within 4-6 hr (Table 15). Rapid erosion of non-encapsulated formulations was due to P407, the thermogelling agent which possessed weak mechanical strength as the major drawback (143). In order to facilitate the sustained release of the drug within the periodontal pocket, the formed gel should preserve its integrity without eroding or dissolving for an extended the period of time. Interestingly, the gelling capacity of P407 was enhanced and remained in SSF for about 24 hr in the presence of SBE β CD/CS NPs. The addition of CS increased the number of hydrogen bonds due to the presence of -NH₂ group that could improve the mechanical strength of the P407 gel (144).

9.3 Particle size and size distribution, zeta potential and %EE

Table 16 displays the particle size and size distribution, zeta potential and %EE of *in situ* gel formulations. The mean particle size of non-encapsulated *in situ* gelling formulations were detected in the range of 25-350 nm. Whereas, in addition of SBE β CD/CS NPs in the formulation, the particle size raised up to approximately 500 nm. Particle size distribution known as polydisperse index (PDI) values of formulations

were between 0.19 and 0.61. This indicated that the particle size was uniformly distributed ($PDI \leq 0.7$) (131).

The negatively zeta potential values of non-encapsulated formulations were relatively low while the markedly positive surface charge in encapsulated SBE β CD/CS formulations were within the range of +20 to +27 mV (Table 16). The positive charge of the particles was likely to prevent the NPs from aggregation. In these systems, the lower zeta potential values were obtained from the formulations containing lower SBE β CD/CS weight ratio (Table 16). On the other hand, the formulation consisting of higher SBE β CD while CS concentration was constant at 0.3% w/w, the zeta potential value was lower. These results are in accordance with the studies of Oyarzun-Ampuero et al., (2009) and Mahmoud (2011). They revealed that it might be caused by increased masking of free positive charged -NH₂ group of CS as the concentration of polyanion was increased (109, 145).

The entrapment efficiency (%EE) of *in situ* gel formulations containing SBE β CD/CS NPs were evaluated. %EE of F7-F9 were significantly higher than those of F13-F15 (high drug loaded formulations). Two-third and one to two-tenth of the total drug loaded was entrapped in the SBE β CD/CS NPs from F7-F9 and F13-15, respectively. Regarding to the latter formulations, it indicated that the drug molecules were predominately solubilized in non-encapsulated part i.e., aqueous HP β CD solutions.

Table 16 Particle size and size distribution (PDI), zeta potential and %EE of asiaticoside loaded in situ gel formulations

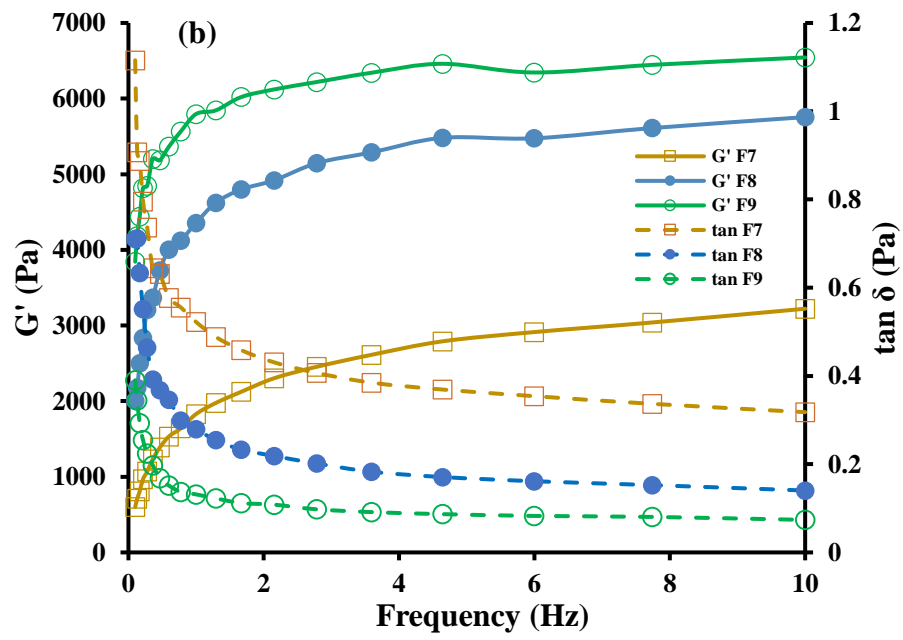
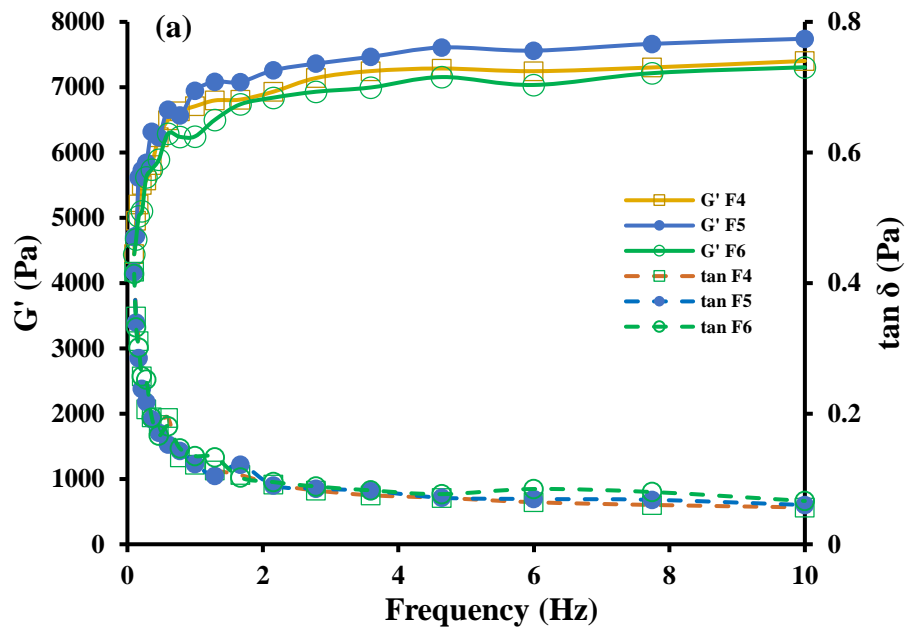
Formulation	Particle Size (nm)	PDI	Zeta Potential (mV)	%EE
F4	34.96±3.57	0.42±0.09	-0.38±0.57	-
F5	27.77±5.49	0.61±0.04	-4.54±0.78	-
F6	138.64±55.32	0.50±0.11	-12.70±2.19	-
F7	534.53±22.14	0.54±0.01	+26.33±0.11	62.26±1.04
F8	420.60±60.87	0.38±0.16	+21.40±1.05	63.15±2.24
F9	408.83±14.68	0.24±0.02	+20.13±0.35	63.16±0.15
F10	43.42±20.76	0.35±0.04	-5.76±1.46	-
F11	151.25±85.88	0.41±0.04	-2.74±0.34	-
F12	342.63±133.9	0.37±0.08	-0.78±0.49	-
F13	597.00±22.54	0.27±0.04	+26.83±0.35	9.26±4.78
F14	512.06±12.60	0.19±0.01	+25.20±1.77	19.33±6.36
F15	454.10±17.53	0.22±0.01	+19.93±0.49	10.61±5.11

10. Rheological study

Oscillatory rheological studies were performed by frequency sweep test from 0.1 to 10.0 Hz at a constant body temperature, 37 °C to investigate the viscoelastic and dynamical properties of formulations (146). Before determining frequency sweep, the applied stress throughout the study was firstly selected within the linear viscoelastic region. Figure 16 demonstrates the storage modulus (G') against applied oscillatory frequency of *in situ* gel formulations. Regarding to G' value of non-encapsulated (Figure 16a and 16c) and encapsulated SBE β CD/CS NPs (Figure 16b and 16d) *in situ* gels, the former formulations were

significantly higher than those of the latter formulations. These results agreed with the report of Şenyiğit ZA et al., (2015) that was G' values of formulations containing NPs were lower than those of without NPs (147). There was no significant difference in G' values of non-encapsulated *in situ* gels. It indicated that HP β CD concentrations did not influence on the elasticity of the formulations. However, in case of encapsulated AS/SBE β CD/CS NPs formulations, the G' values were significantly decreased in the *in situ* gels comprised of lower HP β CD concentration together with the higher SBE β CD/CS weight ratio (F7 and F13). This might be due to the intermolecular hydrogen bonding between HP β CD and excess amount of CS. Consequently, these *in situ* gels had a weak elasticity.

Another parameter to determine elastic property is loss tangent ($\tan \delta$). The value of phase angle ($\tan \delta$) is the measure of relative contribution of viscous components to mechanical properties of materials which was obtained from (G''/G'). As expected, all formulations presented frequencies independent at 37 °C which indicated that there were strong elastic characteristics with the value of phase angle ($\tan \delta$) < 1 (solid gel responses) (Figure 16). It indicated that the samples had formed a continuous network structure and these features are characteristic of a “strong gel” (148). The transformation of solution-state to elastic nature was previously determined by gelation temperature studies and all formulation exhibited gel-state beyond 30 °C. In addition, in most cases, $\tan \delta$ of non-encapsulated *in situ* gels were lower than the encapsulated ones. The reason of less elastic nature was already discussed in previous *in situ* gel characterizations in which the presence of additives may interfere the micelle formation of P407 and causing delay in gelation mechanism of encapsulated *in situ* gels.



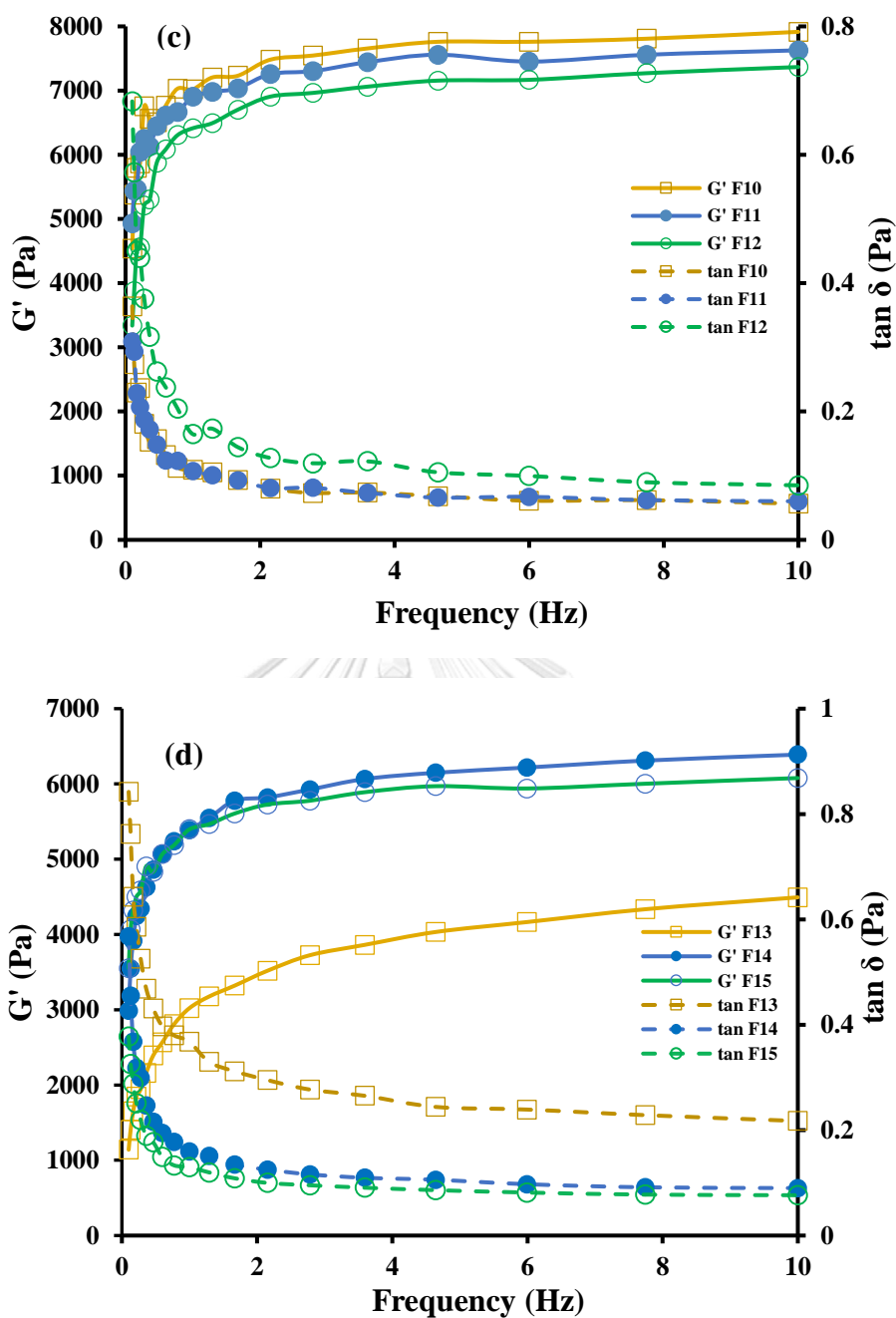


Figure 16 G' and $\tan \delta$ vs frequency profile of in situ gel formulations at 37 °C; (a) F4-F6, (b) F7-F9, (c) F10-F12, (d) F13-F15.

To investigate the flow resistance of the sample in the structured state, originating as viscous or elastic flow resistance to oscillating

movement, the dynamic viscosity (η') was determined. Interestingly, in most cases, the dynamic viscosity of encapsulated *in situ* gels was higher than that of non-encapsulated ones (Figure 17). In literature, it had been reported that the higher the dynamic viscosity, the greater resistance to flow in structured state and the more consistent gel was obtained.

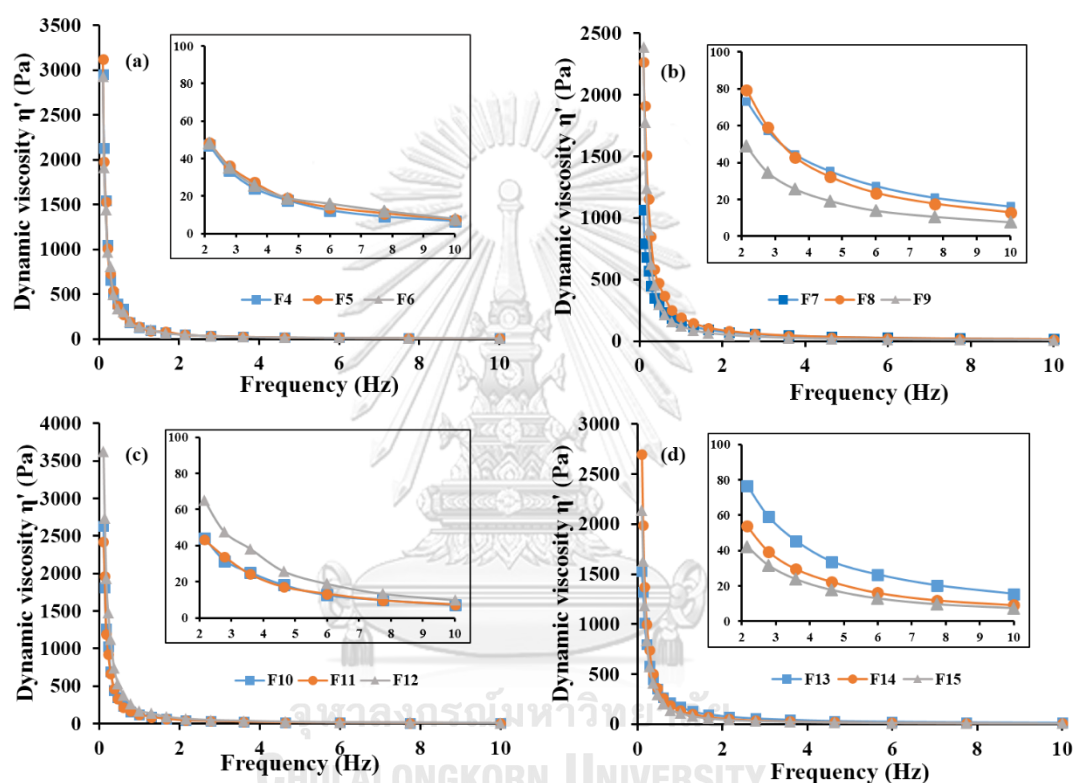


Figure 17 Dynamic viscosity (η') vs frequency profile of *in situ* gel formulations at 37 °C; (a) F4-F6, (b) F7-F9, (c) F10-F12, (d) F13-F15.

11. *In vitro* mucoadhesion

The flow and wash-off by salivary or gingival crevicular fluid in the periodontal pocket area is an obstacle for drug localized injection. One of the desirable properties of *in situ* gel formulations is excellent

mucoadhesion in order to prolong drug retention in the site of action (149). In this study, the mucoadhesion of *in situ* gel formulations was determined by analysis of the amount of drug retained on the mucin coated semipermeable membrane after agitated in the incubator at 37 ± 1 °C. The percentage of retained AS in the *in situ* formulations is presented in Figure 18. According to the results, the *in situ* gels containing SBE β CD/CS NPs were significantly retained the drug when compared with the formulations without encapsulated NPs ($p < 0.05$). The mucoadhesive characteristic of CS is attributed to several mechanisms. The most common mechanism is hydrogen bonding with glycoprotein of mucin due to presence of hydroxy and amine groups. The conformational flexibility of the linear CS molecule also contributes to the mucoadhesive effect (150). In addition, electrostatic interaction between positively charged, $-\text{NH}_2$ of CS and negatively charged sialic acid residue of the mucin is a crucial factor for mucoadhesion (151). Subsequently, it can result a continuous network of polymer and mucin interactions leading to strengthen a mucoadhesive joint. These results were in accordance with Thongborisute and Takeuchi (2008). It was reported that CS NPs probably had enough chain flexibility to interact with negatively charge mucin and facilitate the nanoparticle penetration into the branching sugars of mucin (135). Also, Gratieri et. al. investigated the effect of CS in P407 gels, the addition of CS improved the mucoadhesion about 1.5 and 3 times higher in comparison with the formulation containing P407 alone and control solution, respectively (152). Among the encapsulated *in situ* gels, the excellent mucoadhesive properties were observed in F9 and F15 which comprised the highest concentration of HP β CD. This was probably due to the additional hydrogen bonding formation by hydrophilic outer part of the CD molecule with $-\text{OH}$ of sugars

and other O- and N-containing groups of the protein backbone of mucin (153). The high mucoadhesion was also observed in F12, non-encapsulated *in situ* gels which contained the highest concentration of HP β CD despite of highly elastic nature. Therefore, the non-encapsulated *in situ* gel, F12 and encapsulated *in situ* gels, F9 (low drug loaded) and F15 (high drug loaded) were subjected to further *in vitro* permeation study.

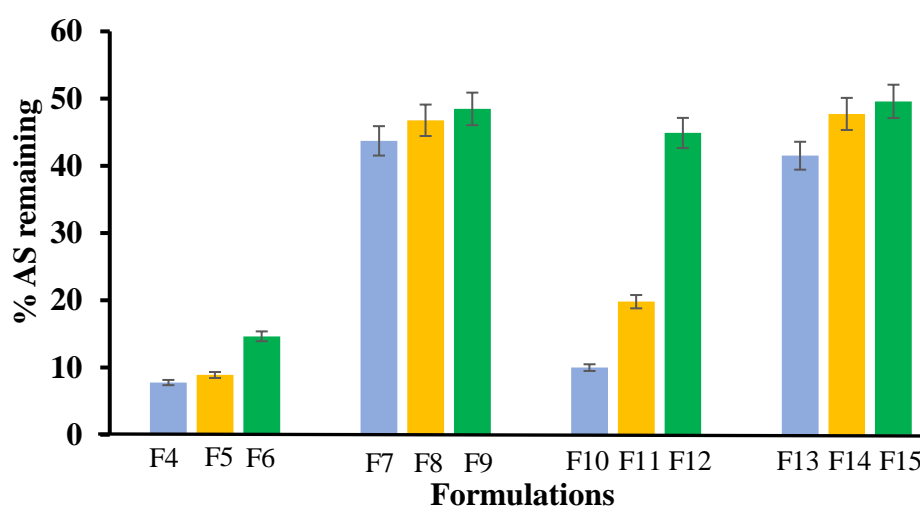


Figure 18 Percentage of the AS remaining on the mucin coated semipermeable membrane

12. *In vitro* release studies

The cumulative release profiles of AS in non-encapsulated (F12) and encapsulated (F9, F15) *in situ* gels are displayed in Figure 19. The MW of AS is 959.13 g/mol and CDs i.e., HP β CD and SBE β CD has MW of 1400 and 2163 Da, respectively. Thus, only free drug and 1:1 AS/CD complex can pass through the semipermeable membrane MWCO 3500 Da.

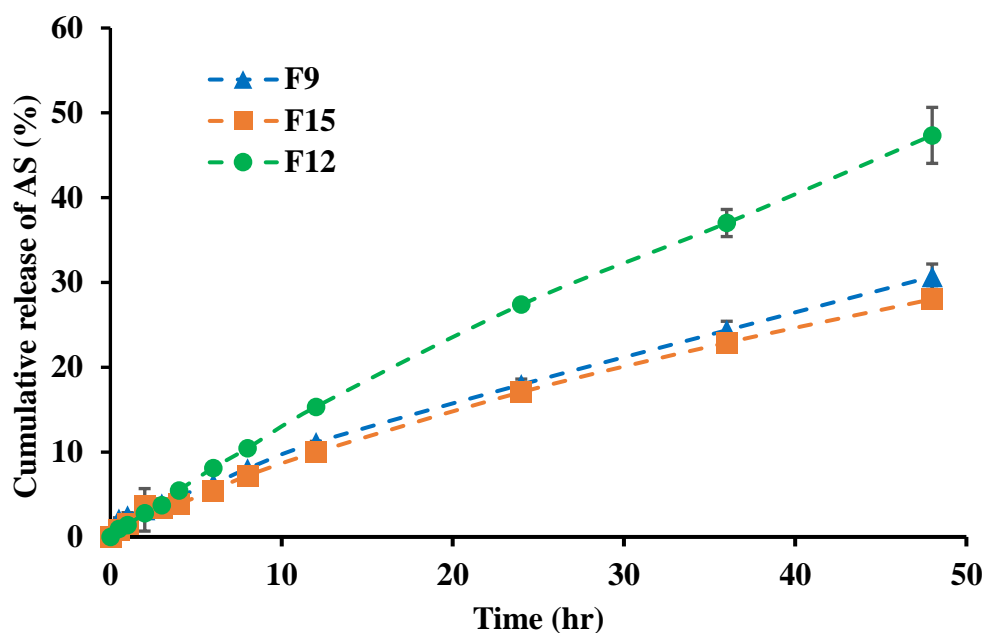


Figure 19 *In vitro* release profiles of AS in *in situ* gel formulations (F9, F12 and F15) through semi-permeable membrane MWCO 3,500 Da.

According to profiles, the slow release of AS was obtained in 48 hr and not reach to the plateau level. The drug release rate of F12 was significantly higher than those of F9 and F15. The drug release of non-encapsulated formulation, F12 was about 1.5 times and 1.6 times higher after 24 hr and at the end of 48 hr than those of encapsulated formulations (F9 and F15). Due to the drug was solubilized in the polymeric network and/or AS/HP β CD inclusion complex, the drug can permeate to the membrane without the dissolution or diffusion from the NPs. Although the gel strength of F12 was weakened when contact with SSF; however, it required to permeate the boundary of gel network consequently to sustain drug release (154). In case of F9 and F15, showed more sustained release of AS since the additional of NPs incorporated into hydrogel. The released profile was almost identical despite of F15 had the high drug loaded and

significantly lower in %EE. This observation may be explained in term of the viscosity and the particle size that influence on the release kinetics. Not only the higher viscosity value at 37 °C but also the larger particle size of F15 might be affected to slower drug release. Regarding to the platform, the multicomponent of the AS/CD inclusion complexes, complex aggregates, AS/SBE β CD/CS NPs etc. acted as the drug reservoir that sustain the drug release resulted in overall bioavailability enhancement.

13. *In vitro* cytotoxicity

HPDLCs were incubated with AS loaded formulations (F9, F12, F15) which were prior diluted to obtain 50 μ M of AS in each formulation. The blank samples (B9, B12, B15) with respect to their formulations were prepared with the same dilution. After incubating the treated samples in the 96-well plate for 24 h, the cell viability of tested samples was analyzed by MTT assay.

Figure 20 displays the viability of HPDLCs after exposure with different samples. When compared to the drug-free formulations, the drug in the *in situ* formulations had a slight negative effect to the cell viability for F9 and F12, but no statistical significance found across all groups. In comparison of AS loaded *in situ* formulations, the highest average cell survival among tested *in situ* gel formulations was F9. It might be due to the high %EE in F9 (63%) while that of F15 was 11% and F12 without entrapment. AS which was predominantly loaded in the SBE β CD/CS NPs might be slowly release from the polymeric matrix resulted in the lowest cytotoxicity among tested formulations. In addition, the *in vitro* release

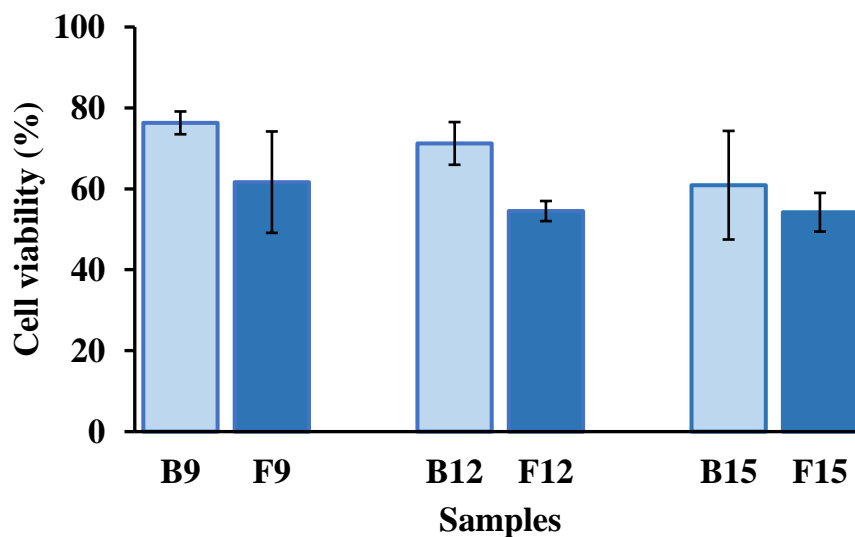


Figure 20 MTT assay results on HPDLCs after 24 hr incubation with blank (B9, B12, B15) and asiaticoside loaded (F9, F12, F15) in situ gel formulations. Bar chart showed no statistically significant difference for cytotoxicity among groups compared in the cell treatment with 16.7 μM of asiaticoside in each in primary cell culture media.

studies revealed that the cumulative release of AS in all three formulations were just within 30-150 μM in 24 hr. The literatures have been reported that AS at the concentrations 10-100 μM did not affect to the cell viability but its concentration more than 100 $\mu\text{g/mL}$, HPDLCs death was recorded (17, 155). As the results, all AS loaded formulations had slight negative effect on HPDLCs at the low AS concentration (the final treatment concentration of approximately 16.7 μM). However, Lu *et. al.* reported the effective concentration of the drug for enhanced cell proliferation and collagen synthesis was at a concentration of 30 $\mu\text{g/mL}$ (45). Altogether, we speculated that all 3 formulations might be more potent than the simple AS solution due to comprise of additives and/or the incorporation of nanoencapsulated platforms. Therefore, the formulations were subjected

for further investigation on the induction of cellular response regarding collagen synthesis with the treatment of our formulation.

14. Immunocytochemistry

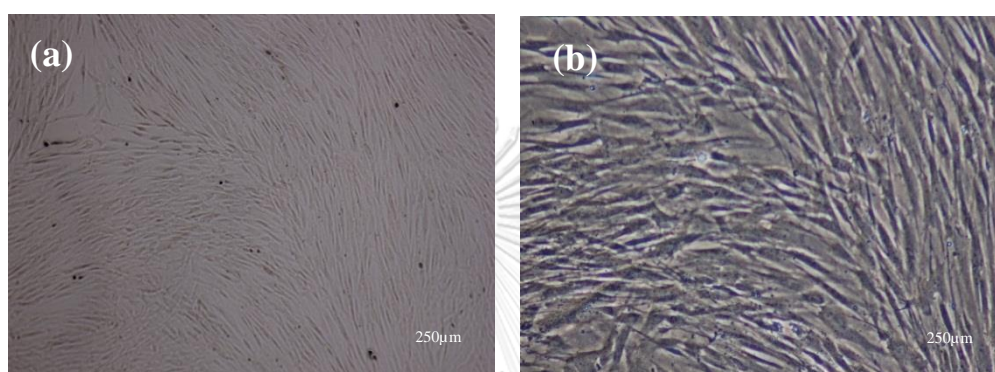


Figure 21 The transmission light microscope picture shown regular cell morphology of HPDLCs at (a) 4X objective lens and (b) 10X objective lens.

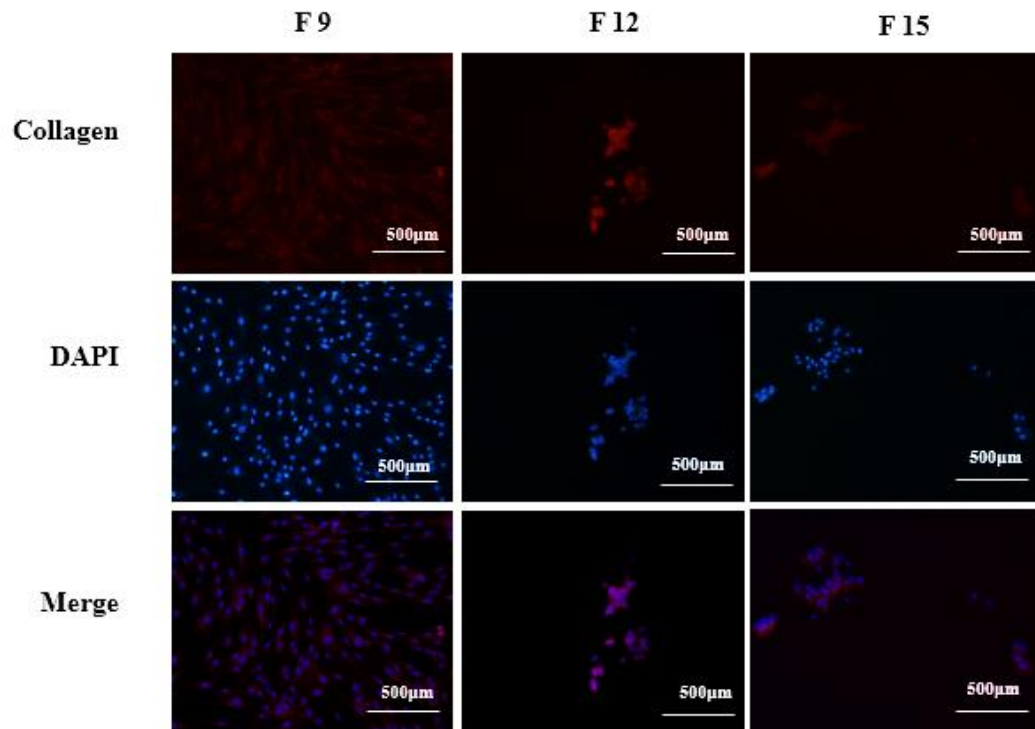
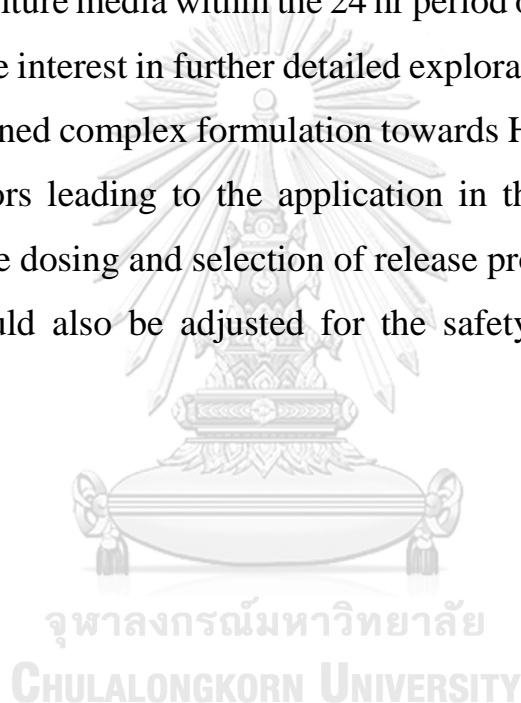


Figure 22 Photograph represented type I collagen (COL 1) synthesis in HPDLCs on the 24 hr treatment of AS loaded *in situ* gels by immunostaining assay; respectively; microscope images of HPDLCs at 10X objective lens, scale bars: 500 μm

Figure 21 displays the transmission light microscopic picture of regular HPDLCs at 4X objective lens and (b) 10X objective lens. The COL 1 synthesis level in HPDLCs after treatment with AS loaded *in situ* gels were determined by immunocytochemistry and illustrated in Figure 22. The predominantly COL 1 protein expression was observed in all formulations from the antibody staining specific to collagen 1 at the AS concentration of 16.7 μM . This could be considered as the potential of the formulation platforms in enhancing the AS efficacy when compared to the previous report (17, 45, 155). HPDLCs treated with F9 remained

unchanged morphology as spindle-like shape and spreading across tissue culture plate. Surprisingly, F12 and F15 displayed the cell aggregation with nodules to the cell response. It can be possibly explained in terms of the %EE and the release rate of AS in the formulations. F9 contained higher AS in ratio of NPs containing SBE β CD/CS NPs with the slow rate of AS while F15 and F12 had low AS entrapment in NPs and not contained NPs, respectively. The latter formulations bring about the immediate release of AS in the cell culture media within the 24 hr period of treatment. This result could initiate the interest in further detailed exploration on the effect of AS within the designed complex formulation towards HPDLCs in terms of the cellular behaviors leading to the application in the stem cell treatment. Furthermore, the dosing and selection of release profile possessed by each formulation could also be adjusted for the safety and pharmacological outcome.



CHAPTER V

CONCLUSION

Asiaticoside (AS) has poor aqueous solubility at the physiological pH. The solubility of AS was enhanced by complexation with cyclodextrin (CD) through heating method (sonication at 60 °C for 30 min). AS had the affinity to HP β CD and SBE β CD according to A_L type phase-solubility profiles, indicating formation of water-soluble complexes. The addition of polymers i.e., CS or P407 to AS/SBE β CD complex provided the synergistic solubilization effect. This might be due to formation of aggregate sizes of ternary complexes (AS/SBE β CD/CS or AS/SBE β CD/P407). Solution-state (¹H-NMR) and solid-state (DSC, FT-IR, PXRD) characterizations suggested that AS was deeply included into CDs and had the interactions with CDs in both binary and ternary complexes. Also, the dissolution of AS was significantly enhanced by binary AS/CD and ternary AS/CD/polymer complexation. The CD inclusion complex in the presence of polymer could markedly enhanced AS solubilization possible through aggregate formation or micellar-like effect. This can provide the information to develop the pharmaceutical formulations.

The *in situ* gel formulations containing AS without and with SBE β CD/CS NPs were developed. The appearance, pH and viscosity of all formulations were within the acceptable range. The gelation temperature of all formulations was below the body temperature and the gelation time was fast to transform into gel-state when contact with SSF. The *in vitro* gelation of encapsulated formulations in SSF remained longer with high mechanical strength when compared with non-encapsulated formulations.

The mean particle size of the *in situ* encapsulated gels were 400-600 nm and highly positive zeta potential values suggested that the formulations were physically stable. The significant mucoadhesive property was observed in the formulations containing high HP β CD concentration without and with encapsulated SBE β CD/CS NPs, suggested that these formulations could remain longer in the periodontal pocket. These sustained release formulations are based on the gel matrix formation at the physiological temperature especially the formulations comprised of NPs. The formulations were slightly negative effect to the HPDLCs even at low AS concentration. However, our promising *in situ* gel formulations containing AS could promote the collagen type I synthesis. They are the potential formulations that can be applied with lesser AS dose when compared to the AS solution which was reported in the literature. However, the quality, safety and the efficacy of these formulations should be further studied.

REFERENCES



จุฬาลงกรณ์มหาวิทยาลัย
CHULALONGKORN UNIVERSITY

1. Ahmad FJ, Iqbal Z, Jain N, Jain GK, Talegaonkar S, Ahuja A, Khar RK. Dental therapeutic systems. *Recent Patents on Drug Delivery & Formulation* 2008;2(1):58-67.
2. Vyas S, Sihorkar V, Mishra V. Controlled and targeted drug delivery strategies towards intraperiodontal pocket diseases. *Journal of Clinical Pharmacy and Therapeutics* 2000;25(1):21-42.
3. Genco RJ, Evans RT, Ellison SA. Dental research in microbiology with emphasis on periodontal disease. *The Journal of the American Dental Association* 1969;78(5):1016-36.
4. Greenstein G. Local drug delivery in the treatment of periodontal diseases: assessing the clinical significance of the results. *Journal of Periodontology* 2006;77(4):565-78.
5. Jain N, Jain GK, Javed S, Iqbal Z, Talegaonkar S, Ahmad FJ, Khar RK. Recent approaches for the treatment of periodontitis. *Drug Discovery Today* 2008;13(21-22):932-43.
6. Addy M, Langeroudi M. Comparison of the immediate effects on the sub-gingival microflora of acrylic strips containing 40% chlorhexidine, metronidazole or tetracycline. *Journal of Clinical Periodontology* 1984;11(6):379-86.
7. Akıncıbay H, Şenel S, Ay ZY. Application of chitosan gel in the treatment of chronic periodontitis. *Journal of Biomedical Materials Research Part B: Applied Biomaterials* 2007;80(2):290-6.
8. Esposito E, Cortesi R, Cervellati F, Menegatti E, Nastruzzi C. Biodegradable microparticles for sustained delivery of tetracycline to the periodontal pocket: formulatory and drug release studies. *Journal of Microencapsulation* 1997;14(2):175-87.

9. Golomb G, Friedman M, Soskolne A, Stabholz A, Sela MN. Sustained release device containing metronidazole for periodontal use. *Journal of Dental Research* 1984;63(9):1149-53.
10. Goodson JM, Holborow D, Dunn RL, Hogan P, Dunham S. Monolithic tetracycline-containing fibers for controlled delivery to periodontal pockets. *Journal of Periodontology* 1983;54(10):575-9.
11. Moulari B, Lboutounne H, Pellequer Y, Guillaume YC, Millet J, Pirot F. Vectorization of *Harungana madagascariensis* Lam. ex Poir. (Hypericaceae) ethanolic leaf extract by using PLG-nanoparticles: antibacterial activity assessment. *Drug Development Research* 2005 ;65(1):26-33.
12. Finkelman RD, Williams RC. Local delivery of chemotherapeutic agents in periodontal therapy: Has its time arrived? *Journal of Clinical Periodontology* 1998;25(11):943-6.
13. Goffin G. Efficacy of sustained local delivery of chlorhexidine Periochip as an adjuvant to scaling and root planning in the treatment of chronic periodontal disease. *International Journal of Dental Research and Reviews* 1998;18:1-8.
14. Ahuja A, Ali J, Rahman S. Biodegradable periodontal intrapocket device containing metronidazole and amoxycillin: formulation and characterisation. *Die Pharmazie - An International Journal of Pharmaceutical Sciences* 2006;61(1):25-9.
15. Johnson LR, Stoller NH. Rationale for the use of Atridox therapy for managing periodontal patients. *Compendium of Continuing Education in Dentistry* 1999;20(4):19-25.
16. Gad HA, El-Nabarawi MA, El-Hady SS. Formulation and evaluation of PLA and PLGA in situ implants containing

- secnidazole and/or doxycycline for treatment of periodontitis. *Pharmaceutical Sciences and Technology* 2008;9(3):878.
17. Nowwarote N, Osathanon T, Jitjaturunt P, Manopattanasoontorn S, Pavasant P. Asiaticoside induces type I collagen synthesis and osteogenic differentiation in human periodontal ligament cells. *Phytotherapy Research* 2013;27(3):457-62.
18. Bonte F, Dumas M, Chaudagne C, Meybeck A. Influence of asiatic acid, madecassic acid, and asiaticoside on human collagen I synthesis. *Planta Medica* 1994;60(2):133-5.
19. Azis HA, Taher M, Ahmed AS, Sulaiman WM, Susanti D, Chowdhury SR, Zakaria ZA. *In vitro* and *in vivo* wound healing studies of methanolic fraction of *Centella asiatica* extract. *South African Journal of Botany* 2017;108:163-74.
20. Loftsson T, Hreinsdóttir D, Másson M. Evaluation of cyclodextrin solubilization of drugs. *International Journal of Pharmaceutics* 2005;302(1-2):18-28.
21. Loftsson T, Jarho P, Masson M, Järvinen T. Cyclodextrins in drug delivery. *Expert Opinion on Drug Delivery* 2005;2(2):335-51.
22. Madan M, Bajaj A, Lewis S, Udupa N, Baig JA. *In situ* forming polymeric drug delivery systems. *Indian Journal of Pharmaceutical Sciences* 2009;71(3):242-51.
23. Bruschi ML, Jones DS, Panzeri H, Gremião MP, De Freitas O, Lara EH. Semisolid systems containing propolis for the treatment of periodontal disease: *in vitro* release kinetics, syringeability, rheological, textural, and mucoadhesive properties. *Journal of Pharmaceutical Sciences* 2007;96(8):2074-89.

24. Jones DS, Woolfson AD, Brown AF, O'Neill MJ. Mucoadhesive, syringeable drug delivery systems for controlled application of metronidazole to the periodontal pocket: *in vitro* release kinetics, syringeability, mechanical and mucoadhesive properties. *Journal of Controlled Release* 1997;49(1):71-9.
25. Calvo P, Remunan-Lopez C, Vila-Jato JL, Alonso MJ. Novel hydrophilic chitosan-polyethylene oxide nanoparticles as protein carriers. *Journal of Applied Polymer Science* 1997;63(1):125-32.
26. Bostanci N, Belibasakis GN. Periodontal Pathogenesis: Definitions and Historical Perspectives. In *Pathogenesis of Periodontal Diseases* 2018 (pp. 1-7). Springer, Cham.
27. Burt B. Position paper: epidemiology of periodontal diseases. *Journal of Periodontology* 2005;76(8):1406-19.
28. Papapanou PN. Epidemiology of periodontal diseases: an update. *Journal of the International Academy of Periodontology* 1999;1(4):110-6.
29. Califano JV. Position paper: periodontal diseases of children and adolescents. *Journal of Periodontology* 2003;74(11):1696-704.
30. Pihlstrom BL, Michalowicz BS, Johnson NW. Periodontal diseases. *The Lancet* 2005;366(9499):1809-20.
31. Page RC, Offenbacher S, Schroeder HE, Seymour GJ, Kornman KS. Advances in the pathogenesis of periodontitis: summary of developments, clinical implications and future directions. *Periodontology* 2000 1997;14(1):216-48.
32. Marsh PD. Host defenses and microbial homeostasis: role of microbial interactions. *Journal of Dental Research* 1989;68:1567-75.

33. Berezow AB, Darveau RP. Microbial shift and periodontitis. *Periodontology* 2000 2011;55(1):36-47.
34. Sanz I, Alonso B, Carasol M, Herrera D, Sanz M. Nonsurgical treatment of periodontitis. *Journal of Evidence Based Dental Practice*. 2012 Sep 1;12(3):76-86.
35. Schwach-Abdellaoui K, Vivien-Castioni N, Gurny R. Local delivery of antimicrobial agents for the treatment of periodontal diseases. *European Journal of Pharmaceutics and Biopharmaceutics* 2000;50(1):83-99.
36. Gottlow J, Karring T, Nyman S. Guided tissue regeneration following treatment of recession-type defects in the monkey. *Journal of Periodontology* 1990;61(11):680-5.
37. Dev S. Ancient-modern concordance in Ayurvedic plants: some examples. *Environmental Health Perspectives* 1999;107(10):783-9.
38. Jamil SS, Nizami Q, Salam M. *Centella asiatica* (Linn.) Urban—a review. *Indian Journal of Natural Products and Resources* 2007;6(2):158-170.
39. Xu CL, Wang QZ, Sun LM, Li XM, Deng JM, Li LF, Zhang J, Xu R, Ma SP. Asiaticoside: attenuation of neurotoxicity induced by MPTP in a rat model of Parkinsonism via maintaining redox balance and up-regulating the ratio of Bcl-2/Bax. *Pharmacology Biochemistry and Behavior* 2012;100(3):413-8.
40. Shukla A, Rasik AM, Dhawan BN. Asiaticoside-induced elevation of antioxidant levels in healing wounds. *Phytotherapy Research* 1999;13(1):50-4.
41. Nhiem NX, Tai BH, Quang TH, Van Kiem P, Van Minh C, Nam NH, Kim JH, Im LR, Lee YM, Kim YH. A new ursane-type

- triterpenoid glycoside from *Centella asiatica* leaves modulates the production of nitric oxide and secretion of TNF- α in activated RAW 264.7 cells. *Bioorganic & Medicinal Chemistry Letters* 2011;21(6):1777-81.
- 42.El-Hefnawi H. Treatment of keloid with asiaticoside. *Dermatology* 1962;125(6):387-92.
- 43.Panichpakdee J, Supaphol P. Use of 2-hydroxypropyl- β -cyclodextrin as adjuvant for enhancing encapsulation and release characteristics of asiaticoside within and from cellulose acetate films. *Carbohydrate Polymers*. 2011;85(1):251-60.
- 44.Lu L, Ying K, Wei S, Fang Y, Liu Y, Lin H, Ma L, Mao Y. Asiaticoside induction for cell-cycle progression, proliferation and collagen synthesis in human dermal fibroblasts. *International Journal of Dermatology* 2004;43(11):801-7.
- 45.Lu L, Ying K, Wei S, Liu Y, Lin H, Mao Y. Dermal fibroblast-associated gene induction by asiaticoside shown in vitro by DNA microarray analysis. *British Journal of Dermatology* 2004;151(3):571-8.
- 46.Lee J, Jung E, Kim Y, Park J, Park J, Hong S, Kim J, Hyun C, Kim YS, Park D. Asiaticoside induces human collagen I synthesis through TGF β receptor I kinase (T β RI kinase)-independent Smad signaling. *Planta Medica* 2006;72(04):324-8.
- 47.Suwantong O, Ruktanonchai U, Supaphol P. In vitro biological evaluation of electrospun cellulose acetate fiber mats containing asiaticoside or curcumin. *Journal of Biomedical Materials Research Part A* 2010;94(4):1216-25.

48. Moursi AM, Damsky CH, Lull J, Zimmerman D, Doty SB, Aota SI, Globus RK. Fibronectin regulates calvarial osteoblast differentiation. *Journal of Cell Science* 1996;109(6):1369-80.
49. Moursi AM, Globus RK, Damsky CH. Interactions between integrin receptors and fibronectin are required for calvarial osteoblast differentiation in vitro. *Journal of Cell Science* 1997;110(18):2187-96.
50. Berendsen AD, Smit TH, Schoenmaker T, Walboomers XF, Harris SE, Everts V, et al. Inorganic phosphate stimulates DMP1 expression in human periodontal ligament fibroblasts embedded in three-dimensional collagen gels. *Cells Tissues Organs* 2010;192(2):116-24.
51. San Miguel SM, Fatahi MR, Li H, Igwe JC, Aguila HL, Kalajzic I. Defining a visual marker of osteoprogenitor cells within the periodontium. *Journal of Periodontal Research* 2010;45(1):60-70.
52. Loftsson T, Duchene D. Cyclodextrins and their pharmaceutical applications. *International Journal of Pharmaceutics* 2007;329(1-2):1-1.
53. Loftsson T, Brewster ME. Pharmaceutical applications of cyclodextrins. 1. Drug solubilization and stabilization. *Journal of Pharmaceutical Sciences* 1996;85(10):1017-25.
54. Narayanan G, Boy R, Gupta BS, Tonelli AE. Analytical techniques for characterizing cyclodextrins and their inclusion complexes with large and small molecular weight guest molecules. *Polymer Testing* 2017;62:402-39.
55. Higuchi T, Connors KA. Phase-solubility techniques. *Advances in Analytical Chemistry & Instrumentation* 1965;4(2):117-212.

56. Cappello B, di Maio C, Iervolino M, Miro A. Combined effect of hydroxypropyl methylcellulose and hydroxypropyl- β -cyclodextrin on physicochemical and dissolution properties of celecoxib. *Journal of Inclusion Phenomena and Macrocyclic Chemistry* 2007;59(3-4):237-44.
57. Nagarsenker MS, Joshi MS. Celecoxib-cyclodextrin systems: characterization and evaluation of in vitro and in vivo advantage. *Drug Development and Industrial Pharmacy* 2005;31(2):169-78.
58. Patel JS, Patel RP. Preparation, characterization and in vitro dissolution study of Nitrazepam: Cyclodextrin inclusion complex. *Journal of Pharmacy & Bioallied Sciences* 2012;4(Suppl 1):S106.
59. Shen C, Yang X, Wang Y, Zhou J, Chen C. Complexation of capsaicin with β -cyclodextrins to improve pesticide formulations: effect on aqueous solubility, dissolution rate, stability and soil adsorption. *Journal of Inclusion Phenomena and Macrocyclic Chemistry* 2012;72(3-4):263-74.
60. Loftsson T, Hreinsdóttir D, Másson M. The complexation efficiency. *Journal of Inclusion Phenomena and Macrocyclic Chemistry* 2007;57(1-4):545-52.
61. Keipert S, Fedder J, Böhm A, Hanke B. Interactions between cyclodextrins and pilocarpine-as an example of a hydrophilic drug. *International Journal of Pharmaceutics* 1996;142(2):153-62.
62. Schuette JM, Warner IM. Structural considerations and fluorescence spectral definition of cyclodextrin/perylene complexes in the presence of 1-pentanol. *Talanta* 1994;41(5):647-9.
63. Yousef FO, Zughul MB, Badwan AA. The modes of complexation of benzimidazole with aqueous β -cyclodextrin explored by phase

- solubility, potentiometric titration, $^1\text{H-NMR}$ and molecular modeling studies. *Journal of Inclusion Phenomena and Macrocyclic Chemistry* 2007;57(1-4):519-23.
- 64.Mura P. Analytical techniques for characterization of cyclodextrin complexes in aqueous solution: a review. *Journal of Pharmaceutical and Biomedical Analysis* 2014;101:238-50.
- 65.Loftsson T, Másson M, Sigurdsson HH. Cyclodextrins and drug permeability through semi-permeable cellophane membranes. *International Journal of Pharmaceutics* 2002;232(1-2):35-43.
- 66.Mura P. Analytical techniques for characterization of cyclodextrin complexes in the solid state: A review. *Journal of Pharmaceutical and Biomedical Analysis* 2015;113:226-38.
- 67.Lahiani-Skiba M, Barbot C, Bounoure F, Joudieh S, Skiba M. Solubility and dissolution rate of progesterone-cyclodextrin-polymer systems. *Drug Development and Industrial Pharmacy* 2006;32(9):1043-58.
- 68.Loftsson T, Frikdriksdóttir H, Sigurkdardóttir AM, Ueda H. The effect of water-soluble polymers on drug-cyclodextrin complexation. *International Journal of Pharmaceutics* 1994;110(2):169-77.
- 69.Ammar HO, Salama HA, Ghorab M, Mahmoud AA. Implication of inclusion complexation of glimepiride in cyclodextrin-polymer systems on its dissolution, stability and therapeutic efficacy. *International Journal of Pharmaceutics* 2006;320(1-2):53-7.
- 70.Smith JS, MacRae RJ, Snowden MJ. Effect of SBE7- β -cyclodextrin complexation on carbamazepine release from sustained release

- beads. *European Journal of Pharmaceutics and Biopharmaceutics* 2005;60(1):73-80.
- 71.Do MP, Neut C, Delcourt E, Certo TS, Siepmann J, Siepmann F. In situ forming implants for periodontitis treatment with improved adhesive properties. *European Journal of Pharmaceutics and Biopharmaceutics* 2014;88(2):342-50.
- 72.Radvar M, Pourtaghi N, Kinane DF. Comparison of 3 periodontal local antibiotic therapies in persistent periodontal pockets. *Journal of Periodontology* 1996;67(9):860-5.
- 73.Cosyn J, Wyn I. A systematic review on the effects of the chlorhexidine chip when used as an adjunct to scaling and root planning in the treatment of chronic periodontitis. *Journal of Periodontology* 2006;77(2):257-64.
- 74.Soskolne WA. Subgingival delivery of therapeutic agents in the treatment of periodontal diseases. *Critical Reviews in Oral Biology & Medicine* 1997;8(2):164-74.
- 75.Drisko CH. The use of locally-delivered doxycycline in the treatment of periodontitis. *Journal of Clinical Periodontology* 1998;25(11):947-52.
- 76.Ruel-Gariepy E, Leroux JC. In situ-forming hydrogels-review of temperature-sensitive systems. *European Journal of Pharmaceutics and Biopharmaceutics* 2004;58(2):409-26.
- 77.Mayol L, Quaglia F, Borzacchiello A, Ambrosio L, La Rotonda MI. A novel poloxamers/hyaluronic acid in situ forming hydrogel for drug delivery: rheological, mucoadhesive and in vitro release properties. *European Journal of Pharmaceutics and Biopharmaceutics* 2008;70(1):199-206.

78. Li L, Guo D, Guo J, Song J, Wu Q, Liu D, Bi H, Xie X. Thermosensitive in-situ forming gels for ophthalmic delivery of tea polyphenols. *Journal of Drug Delivery Science and Technology* 2018;46:243-50.
79. Wang Y, Jiang S, Wang H, Bie H. A mucoadhesive, thermoreversible in situ nasal gel of geniposide for neurodegenerative diseases. *PloS one* 2017;12(12):e0189478.
80. Liu Y, Yang F, Feng L, Yang L, Chen L, Wei G, Lu W. In vivo retention of poloxamer-based in situ hydrogels for vaginal application in mouse and rat models. *Acta Pharmaceutica Sinica B*. 2017;7(4):502-9.
81. Ban E, Park M, Jeong S, Kwon T, Kim EH, Jung K, Kim A. Poloxamer-based thermoreversible gel for topical delivery of emodin: influence of P407 and P188 on solubility of emodin and its application in cellular activity screening. *Molecules*. 2017;22(2):246.
82. Bansal M, Mittal N, Yadav SK, Khan G, Gupta P, Mishra B, Nath G. Periodontal thermoresponsive, mucoadhesive dual antimicrobial loaded in-situ gel for the treatment of periodontal disease: Preparation, in-vitro characterization and antimicrobial study. *Journal of Oral Biology and Craniofacial Research* 2018;8(2):126-33.
83. Lehr CM, Bouwstra JA, Schacht EH, Junginger HE. In vitro evaluation of mucoadhesive properties of chitosan and some other natural polymers. *International Journal of Pharmaceutics* 1992;78(1-3):43-8.

- 84.Valenta C. The use of mucoadhesive polymers in vaginal delivery. *Advanced Drug Delivery Reviews* 2005;57(11):1692-712.
- 85.Ahmadi R, de Bruijn JD. Biocompatibility and gelation of chitosan-glycerol phosphate hydrogels. *Journal of Biomedical Materials Research* 2008;86(3):824-32.
- 86.Rattes AL, Oliveira WP. Spray drying conditions and encapsulating composition effects on formation and properties of sodium diclofenac microparticles. *Powder Technology* 2007;171(1):7-14.
- 87.Laokuldilok T, Kanha N. Effects of processing conditions on powder properties of black glutinous rice (*Oryza sativa* L.) bran anthocyanins produced by spray drying and freeze drying. *Food Science and Technology* 2015;64(1):405-11.
- 88.Gouin S. Microencapsulation: industrial appraisal of existing technologies and trends. *Trends in Food Science & Technology* 2004;15(7-8):330-47.
- 89.Poncelet D. Microencapsulation: fundamentals, methods and applications. In *Surface Chemistry in Biomedical and Environmental Science* 2006:23-34.
- 90.Xiao Z, Liu W, Zhu G, Zhou R, Niu Y. A review of the preparation and application of flavour and essential oils microcapsules based on complex coacervation technology. *Journal of the Science of Food and Agriculture* 2014;94(8):1482-94.
- 91.Reza Mozafari M, Johnson C, Hatziantoniou S, Demetzos C. Nanoliposomes and their applications in food nanotechnology. *Journal of Liposome Research* 2008;18(4):309-27.

92. Yeo Y, Baek N, Park K. Microencapsulation methods for delivery of protein drugs. *Biotechnology and Bioprocess Engineering* 2001;6(4):213-30.
93. Khan KA. The concept of dissolution efficiency. *Journal of Pharmacy and Pharmacology* 1975;27(1):48-9.
94. Gratieri T, Gelfuso GM, Rocha EM, Sarmiento VH, de Freitas O, Lopez RF. A poloxamer/chitosan *in situ* forming gel with prolonged retention time for ocular delivery. *European Journal of Pharmaceutics and Biopharmaceutics* 2010;75(2):186-93.
95. Koland M. Investigation of a biodegradable injectable *in situ* gelling implantable system of rivastigmine tartrate. *Asian Journal of Pharmaceutics* 2018;11(04):1-8.
96. Garala K, Joshi P, Shah M, Ramkishan A, Patel J. Formulation and evaluation of periodontal *in situ* gel. *International Journal of Pharmaceutical Investigation* 2013;3(1):29-41.
97. Abdelgawad WY, Mohamed MI, Gad MK, Ahmed E. Formulation, evaluation and clinical assessment of Gemifloxacin *in situ* gel for the treatment of chronic periodontitis. *International Journal of Pharmaceutical Sciences Review and Research* 2016;38(1):78-85.
98. Fülöp Z, Saokham P, Loftsson T. Sulfobutylether- β -cyclodextrin/chitosan nano- and microparticles and their physicochemical characteristics. *International Journal of Pharmaceutics* 2014;472(1-2):282-7.
99. Pakzad Y, Ganji F. Thermosensitive hydrogel for periodontal application: *in vitro* drug release, antibacterial activity and toxicity evaluation. *Journal of Biomaterials Applications* 2016;30(7):919-29.

100. Choi SG, Lee SE, Kang BS, Ng CL, Davaa E, Park JS. Thermosensitive and mucoadhesive sol-gel composites of paclitaxel/dimethyl- β -cyclodextrin for buccal delivery. PLoS One 2014;9(10):e109090.
101. Loftsson T, Brewster ME. Cyclodextrins as functional excipients: methods to enhance complexation efficiency. Journal of pharmaceutical sciences. 2012 Sep 1;101(9):3019-32.
102. Puttarak P, Brantner A, Panichayupakaranant P. Biological activities and stability of a standardized pentacyclic triterpene enriched *Centella asiatica* extract. Natural Product Sciences 2016;22(1):20-4.
103. Borhan MZ, Ahmad R, Rusop M, Abdullah S. Green extraction: enhanced extraction yield of asiatic acid from *Centella asiatica* (L.) nanopowders. Journal of Applied Chemistry 2013:1-7.
104. Wenz G. Influence of intramolecular hydrogen bonds on the binding potential of methylated β -cyclodextrin derivatives. Beilstein Journal of Organic Chemistry 2012;8(1):1890-5.
105. Higuchi T, & Connors, A. K. . Phase-solubility techniques. Advances in Analytical Chemistry and Instrumentation,. 1965:117–212.
106. Zia V, Rajewski RA, Bornancini ER, Luna EA, Stella VJ. Effect of alkyl chain length and degree of substitution on the complexation of sulfoalkyl ether β -cyclodextrins with steroids. Journal of Pharmaceutical Sciences 1997;86(2):220-4.
107. Zia V, Rajewski RA, Stella VJ. Thermodynamics of binding of neutral molecules to sulfobutyl ether β -cyclodextrins (SBE- β -CDs):

- the effect of total degree of substitution. *Pharmaceutical Research* 2000;17(8):936-41.
108. Faucci MT, Mura P. Effect of water-soluble polymers on naproxen complexation with natural and chemically modified beta-cyclodextrins. *Drug Development and Industrial Pharmacy* 2001;27(9):909-17.
109. Mahmoud AA, El-Feky GS, Kamel R, Awad GEA. Chitosan/sulfobutylether- β -cyclodextrin nanoparticles as a potential approach for ocular drug delivery. *International Journal of Pharmaceutics* 2011;413(1-2):229-36.
110. Patel AR, Vavia PR. Effect of hydrophilic polymer on solubilization of fenofibrate by cyclodextrin complexation. *Journal of Inclusion Phenomena and Macrocyclic Chemistry* 2006;56(1-2):247-51.
111. Valero M, Pérez-Revuelta BI, Rodríguez LJ. Effect of PVP K-25 on the formation of the naproxen: β -cyclodextrin complex. *International Journal of Pharmaceutics* 2003;253(1-2):97-110.
112. Garnero C, Zoppi A, Genovese D, Longhi M. Studies on trimethoprim: hydroxypropyl- β -cyclodextrin: aggregate and complex formation. *Carbohydrate Research* 2010;345(17):2550-6.
113. Panichpakdee J, Pavasant P, Supaphol P. Electrospinning of asiaticoside/2-hydroxypropyl- β -cyclodextrin inclusion complex-loaded cellulose acetate fiber mats: release characteristics and potential for use as wound dressing. *Polymer Korea* 2014;38(3):338-50.
114. Kulkarni AD, Belgamwar VS. Inclusion complex of chrysin with sulfobutyl ether- β -cyclodextrin (Captisol®): preparation,

- characterization, molecular modelling and *in vitro* anticancer activity. *Journal of Molecular Structure* 2017;1128:563-71.
115. Xu J, Zhang Y, Li X, Zheng Y. Inclusion complex of nateglinide with sulfobutyl ether β -cyclodextrin: Preparation, characterization and water solubility. *Journal of Molecular Structure* 2017;1141:328-34.
116. Meliana Y, Harmami SB, Restu WK. Characterization of nanoencapsulated *Centella asiatica* and *Zingiber officinale* extract using combination of malto dextrin and gum arabic as matrix. *Materials Science and Engineering* 2017;172:1-7.
117. Ribeiro LS, Ferreira DC, Veiga FJ. Physicochemical investigation of the effects of water-soluble polymers on vinpocetine complexation with β -cyclodextrin and its sulfobutyl ether derivative in solution and solid state. *European Journal of Pharmaceutical Sciences*. 2003;20(3):253-66.
118. Jain AS, Date AA, Pissurlenkar RR, Coutinho EC, Nagarsenker MS. Sulfobutyl Ether₇ β -cyclodextrin (SBE₇ β -CD) carbamazepine complex: preparation, characterization, molecular modeling, and evaluation of *in vivo* anti-epileptic activity. *American Association of Pharmaceutical Scientists, Pharmaceutical Science and Technology* 2011;12(4):1163-75.
119. Semcheddine F, Guissi NE, Liu X, Wu Z, Wang B. Effects of the preparation method on the formation of true nimodipine SBE- β -CD/HP- β -CD inclusion complexes and their dissolution rates enhancement. *Pharmaceutical Science and Technology* 2015;16(3):704-15.

120. Deng Y, Pang Y, Guo Y, Ren Y, Wang F, Liao X, Yang B. Host-guest inclusion systems of daidzein with 2-hydroxypropyl- β -cyclodextrin (HP- β -CD) and sulfobutyl ether- β -cyclodextrin (SBE- β -CD): Preparation, binding behaviors and water solubility. *Journal of Molecular Structure* 2016;1118:307-15.
121. Semcheddine F, Guissi NE, Liu X, Wu Z, Wang B. Effects of the preparation method on the formation of true nimodipine SBE- β -CD/HP- β -CD inclusion complexes and their dissolution rates enhancement. *Pharmaceutical Science and Technology* 2015;16(3):704-15.
122. Jug M, Bećirević-Laćan M. Multicomponent complexes of piroxicam with cyclodextrins and hydroxypropyl methylcellulose. *Drug Development and Industrial Pharmacy* 2004;30(10):1051-60.
123. Trapani G, Latrofa A, Franco M, Pantaleo MR, Sanna E, Massa F, Tuveri F, Liso G. Complexation of zolpidem with 2-hydroxypropyl- β -, methyl- β -, and 2-hydroxypropyl- β -cyclodextrin: effect on aqueous solubility, dissolution rate, and ataxic activity in rat. *Journal of Pharmaceutical Sciences* 2000;89(11):1443-51.
124. Ryzhakov A, Do TT, Stappaerts J, Bertoletti L, Kimpe K, Couto AR, Saokham P, Van MG, Augustijns P, Somsen GW, Kurkov S. Self-assembly of cyclodextrins and their complexes in aqueous solutions. *Journal of Pharmaceutical Sciences* 2016;105(9):2556-69.
125. Do TT, Van HR, Van MG. A study of the aggregation of cyclodextrins: determination of the critical aggregation concentration, size of aggregates and thermodynamics using isodesmic and K2-K models. *International Journal of Pharmaceutics* 2017;521(1-2):318-26.

126. Lourenco C, Teixeira M, Simões S, Gaspar R. Steric stabilization of nanoparticles: size and surface properties. *International Journal of Pharmaceutics* 1996;138(1):1-2.
127. Zhang P, Liu X, Hu W, Bai Y, Zhang L. Preparation and evaluation of naringenin -loaded sulfobutylether - β - cyclodextrin/chitosan nanoparticles for ocular drug delivery. *Carbohydrate Polymers* 2016;149:224-30.
128. Cui F, Qian F, Yin C. Preparation and characterization of mucoadhesive polymer-coated nanoparticles. *International Journal of Pharmaceutics* 2006;316(1-2):154-61.
129. Kawashima Y, Yamamoto H, Takeuchi H, Kuno Y. Mucoadhesive DL-lactide/glycolide copolymer nanospheres coated with chitosan to improve oral delivery of elcatonin. *Pharmaceutical Development and Technology* 2000;5(1):77-85.
130. Sreekumar S, Goycoolea FM, Moerschbacher BM, Rivera-Rodriguez GR. Parameters influencing the size of chitosan-TPP nano-and microparticles. *Scientific Reports* 2018;8(1):4695.
131. Danaei M, Dehghankhold M, Ataei S, Hasanzadeh Davarani F, Javanmard R, Dokhani A, Khorasani S, Mozafari M. Impact of particle size and polydispersity index on the clinical applications of lipidic nanocarrier systems. *Pharmaceutics* 2018;10(2):57.
132. Trapani A, Garcia-Fuentes M, Alonso MJ. Novel drug nanocarriers combining hydrophilic cyclodextrins and chitosan. *Nanotechnology* 2008;19(18):185101.
133. Kaur I, Suthar N, Kaur J, Bansal Y, Bansal G. Accelerated stability studies on dried extracts of *Centella asiatica* through chemical, HPLC, HPTLC, and biological activity analyses. *Journal of*

Evidence-based Complementary & Alternative Medicine 2016;21(4):NP127-37.

134. Mei L, Huang X, Xie Y, Chen J, Huang Y, Wang B, Wang H, Pan X, Wu C. An injectable in situ gel with cubic and hexagonal nanostructures for local treatment of chronic periodontitis. *Drug Delivery* 2017;24(1):1148-58.
135. Thongborisute J, Takeuchi H. Evaluation of mucoadhesiveness of polymers by biacore method and mucin-particle method. *International Journal of Pharmaceutics* 2008;354(1-2):204-9.
136. Haffajee AD, Socransky SS, Goodson JM. Subgingival temperature (I). Relation to baseline clinical parameters. *Journal of Clinical Periodontology* 1992;19(6):401-8.
137. Galgatte UC, Chaudhari PD. Preformulation study of poloxamer 407 gels: effect of additives. *International Journal of Pharmacy and Pharmaceutical Sciences* 2014;6(1):130-3.
138. Choi HG, Lee MK, Kim MH, Kim CK. Effect of additives on the physicochemical properties of liquid suppository bases. *International Journal of Pharmaceutics* 1999;190(1):13-9.
139. Ur-Rehman T, Tavelin S, Gröbner G. Chitosan in situ gelation for improved drug loading and retention in poloxamer 407 gels. *International Journal of Pharmaceutics* 2011;409(1-2):19-29.
140. Nogueiras-Nieto L, Alvarez-Lorenzo C, Sandez-Macho I, Concheiro A, Otero-Espinar FJ. Hydrosoluble cyclodextrin/poloxamer polypseudorotaxanes at the air/water interface, in bulk solution, and in the gel state. *The Journal of Physical Chemistry B*. 2009;113(9):2773-82.

141. Rodriguez-Perez AI, Rodriguez-Tenreiro C, Alvarez-Lorenzo C, Concheiro A, Torres-Labandeira JJ. Drug solubilization and delivery from cyclodextrin-pluronic aggregates. *Journal of Nanoscience and Nanotechnology* 2006;6(9-10):3179-86.
142. Shaker DS, Ghorab MK, Klingner AN, Teiama MS. In-situ injectable thermosensitive gel based on poloxamer as a new carrier for tamoxifen citrate. *International Journal of Pharmaceutics and Pharmaceutical Sciences* 2013;5(Suppl 4):429-37.
143. Singh NK, Lee DS. *In situ* gelling pH-and temperature-sensitive biodegradable block copolymer hydrogels for drug delivery. *Journal of Controlled Release* 2014;193:214-27.
144. Varshosaz J, Tabbakhian M, Salmani Z. Designing of a thermosensitive chitosan/poloxamer *in situ* gel for ocular delivery of ciprofloxacin. *The Open Drug Delivery Journal* 2008;2(1):61-70.
145. Oyarzun-Ampuero FA, Brea J, Loza MI, Torres D, Alonso MJ. Chitosan–hyaluronic acid nanoparticles loaded with heparin for the treatment of asthma. *International Journal of Pharmaceutics* 2009;381(2):122-9.
146. Dumortier G, Grossiord JL, Zuber M, Couarraze G, Chaumeil JC. Rheological study of a thermoreversible morphine gel. *Drug Development and Industrial Pharmacy* 1991;17(9):1255-65.
147. Szejtli J. Medicinal applications of cyclodextrins. *Medicinal Research Reviews* 1994;14(3):353-86.
148. Ikeda S, Nishinari K. “Weak gel”-type rheological properties of aqueous dispersions of nonaggregated κ -carrageenan helices. *Journal of Agricultural and Food Chemistry* 2001;49(9):4436-41.

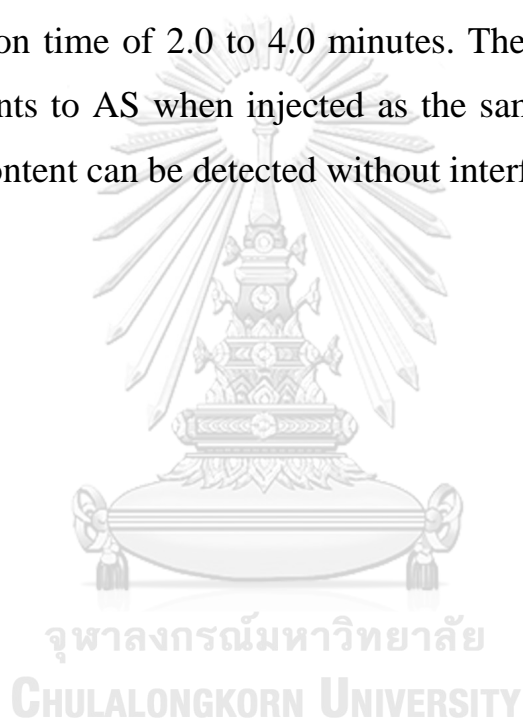
149. Ahuja A, Khar RK, Ali J. Mucoadhesive drug delivery systems. *Drug Development and Industrial Pharmacy* 1997;23(5):489-515.
150. Alhalaweh A, Vilinska A, Gavini E, Rassu G, Velaga SP. Surface thermodynamics of mucoadhesive dry powder formulation of zolmitriptan. *Pharmaceutical Science and Technology* 2011;12(4):1186-92.
151. Albers CN, Jacobsen OS, Aamand J. Using 2, 6-dichlorobenzamide (BAM) degrading *Aminobacter* sp. MSH1 in flow through biofilters—initial adhesion and BAM degradation potentials. *Applied Microbiology and Biotechnology* 2014;98(2):957-67.
152. Thongborisute J, Takeuchi H. Evaluation of mucoadhesiveness of polymers by biacore method and mucin-particle method. *International Journal of Pharmaceutics* 2008;354(1-2):204-9.
153. Alfaqeeh SA, Anil S. Gingival crevicular fluid flow rate and alkaline phosphatase level as potential marker of active tooth movement. *Oral Health and Dental Management* 2014;13(2):458-63.
154. Ritger PL, Peppas NA. A simple equation for description of solute release II. Fickian and anomalous release from swellable devices. *Journal of Controlled Release* 1987;5(1):37-42.

APPENDIX

HPLC VALIDATION

1. Specificity

The chromatograms of β CD, HP β CD, CM β CD, SBE β CD, CS, P407, SSF, PBS, BAC, mobile phase and various concentrations of AS standard solution are displayed in Fig. 22 and Fig. 23. AS was eluted with the retention time of 10.9 to 11.6 minutes and the solvent peak was found with the retention time of 2.0 to 4.0 minutes. There was no interference peak of excipients to AS when injected as the same condition. It can be seen that, AS content can be detected without interference.



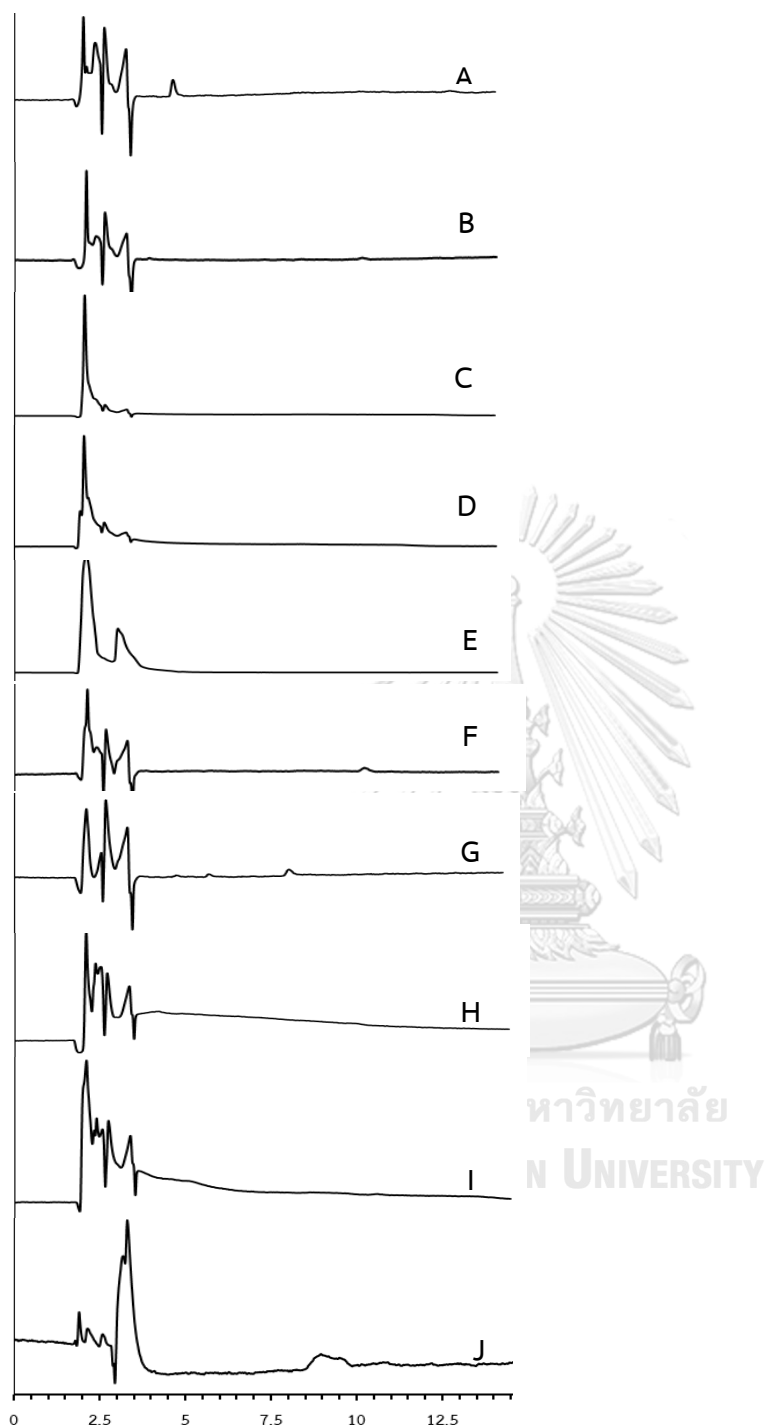


Figure 23 The HPLC chromatograms of (A) β CD, (B) HP β CD, (C) CM β CD, (D) SBE β CD, (E) CS, (F) P407, (G) SSF, (H) PBS, (I) BAC and mobile phase.

2. Linearity

The chromatograms of AS standard solution are shown in Fig. 23. The retention time of AS was about 10.8 to 11.2 minutes. The calibration curve was plotted between the peak area and concentration of AS ($\mu\text{g/mL}$). The results are presented in Table 19, 20, 21 and Fig.24, 25 and 26. The linear regression analysis was performed with coefficient of determination (R^2) and resulted as 0.9997-1.0000 This result indicated that HPLC condition was acceptable to determine the amount of AS in the formulation.



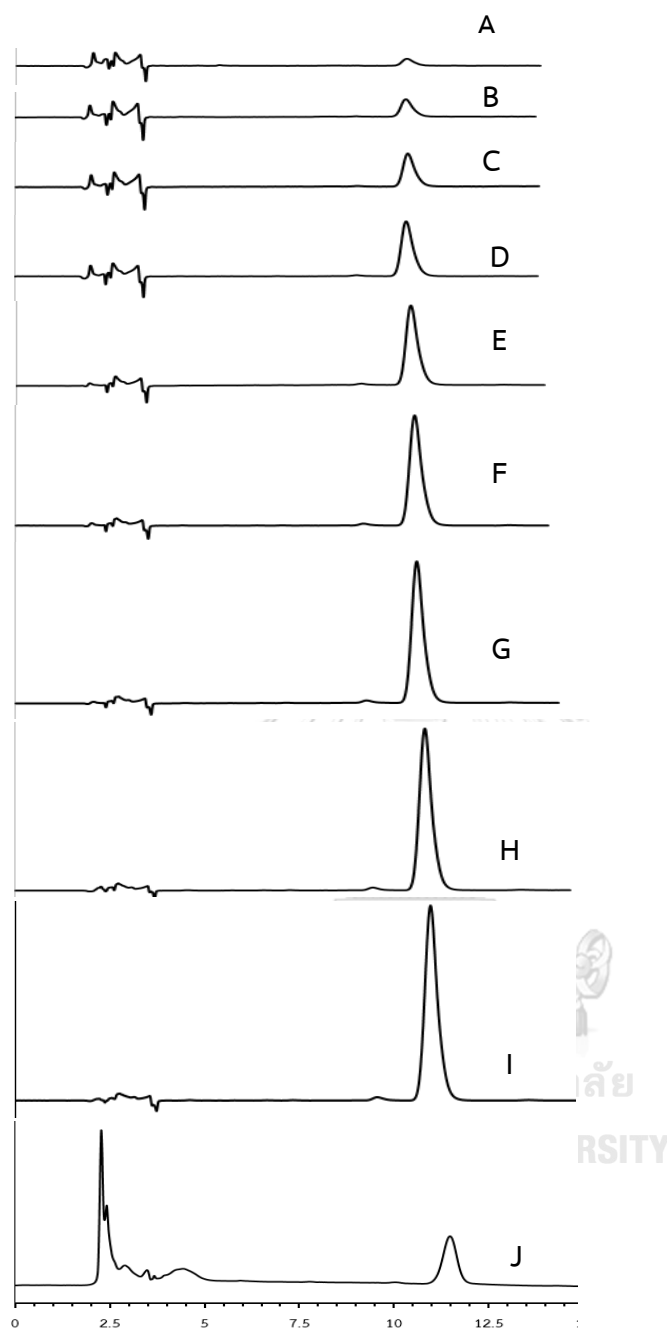


Figure 24 The HPLC chromatograms of AS standard solution (A) 12.5 $\mu\text{g/mL}$, (B) 25 $\mu\text{g/mL}$, (C) 50 $\mu\text{g/mL}$, (D) 100 $\mu\text{g/mL}$, (E) 200 $\mu\text{g/mL}$, (F) 400 $\mu\text{g/mL}$, (G) 600 $\mu\text{g/mL}$, (H) 800 $\mu\text{g/mL}$, (I) 1000 $\mu\text{g/mL}$ and (J) 1% w/w AS loaded in situ gel dissolved in methanol:water (30:70 v/v)

Table 17 Data of calibration curve of AS standard solutions (No.1)

AS conc. ($\mu\text{g/mL}$)	Peak area					
	n1	n2	n3	Mean	SD	%CV
12.62	23.6785	24.3176	24.3860	24.1274	0.3902	1.62
25.25	46.7062	45.9722	47.8072	46.8285	0.9235	1.97
50.50	92.7435	94.0294	91.9909	92.9213	1.0307	1.11
101.00	180.6033	180.6090	182.7555	181.3227	1.2409	0.68
202.00	360.7803	362.0335	362.9512	361.9217	1.0897	0.30
404.00	716.1889	718.4636	717.4448	717.3658	1.1394	0.15
606.00	1073.1868	1082.1151	1082.1123	1079.1380	5.1538	0.47
808.00	1441.3299	1411.9163	1441.7885	1431.6780	17.1158	1.19
1010.00	1784.9805	1784.8466	1791.8558	1787.2280	4.0086	0.22

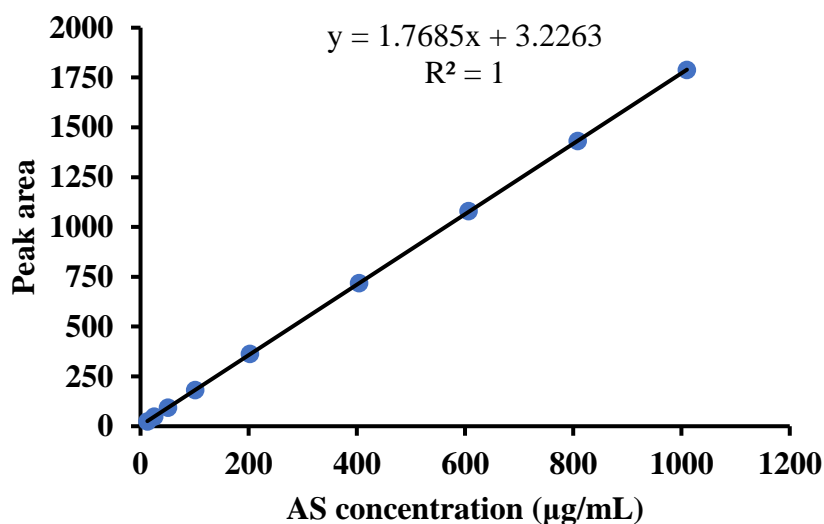


Figure 25 Calibration curve of AS standard solutions by HPLC method (No.1)

Table 18 Data of calibration curve of AS standard solutions (No.2)

AS conc. ($\mu\text{g/mL}$)	Peak area					
	n1	n2	n3	Mean	SD	%CV
12.57	22.0349	22.0254	22.8294	22.2966	0.4614	2.06
25.15	46.4160	46.9243	45.5240	46.2881	0.7088	1.53
50.30	93.7004	91.0680	93.9970	92.9218	1.6122	1.73
100.60	184.8556	183.8203	183.1402	183.9390	0.8637	0.46
201.20	363.9462	367.2551	367.5736	366.2580	2.0086	0.54
402.40	721.8720	721.4720	723.1424	722.1620	0.8721	0.12
603.60	1088.6881	1081.2844	1112.2402	1094.0700	16.1647	1.47
804.80	1446.0847	1421.0432	1426.1425	1431.0900	13.2336	0.92
1006.00	1798.5931	1800.7164	1814.1660	1804.4900	8.4450	0.46

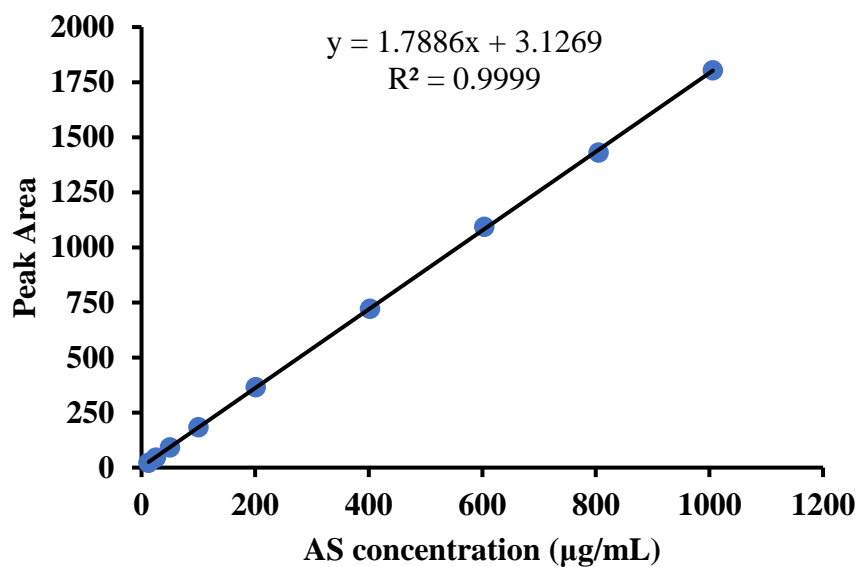


Figure 26 Calibration curve of AS standard solutions by HPLC method (No.2)

Table 19 Data of calibration curve of AS standard solutions (No.3)

AS conc ($\mu\text{g/mL}$)	Peak area					
	n1	n2	n3	Mean	SD	%CV
12.45	22.8705	22.3588	22.3716	22.5337	0.2917	1.29
24.90	44.4921	45.0240	44.1682	44.5615	0.4321	0.96
49.80	90.4530	88.4721	89.1708	89.3653	1.0046	1.12
99.60	179.7816	173.9479	178.8113	177.5140	3.1258	1.76
199.20	355.7941	348.0390	357.1390	353.6570	4.9118	1.38
398.40	711.9660	695.6764	713.6684	707.1040	9.9327	1.40
597.60	1025.3903	1081.2844	997.5273	1034.7300	42.6532	4.12
796.80	1414.5183	1378.9421	1384.2073	1392.5600	19.2013	1.37
996.00	1773.2096	1779.3139	1775.4849	1776.0028	3.0849	0.17

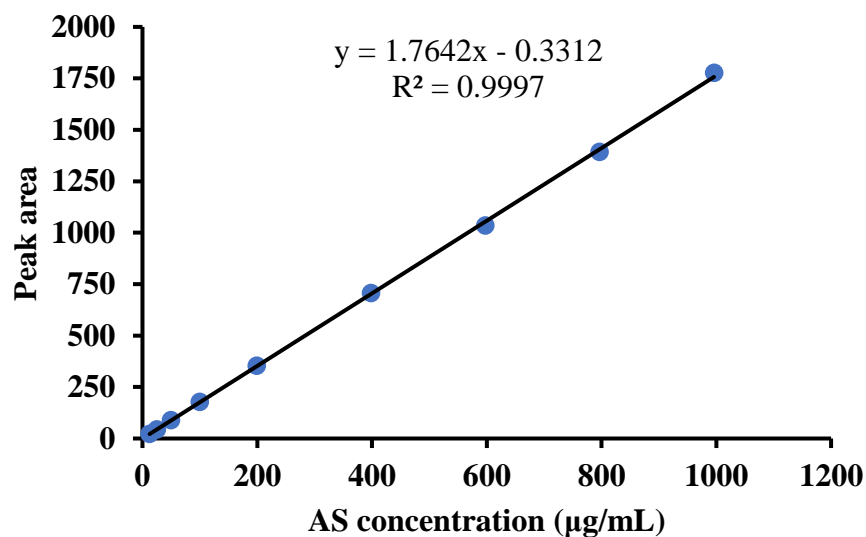


Figure 27 Calibration curve of AS standard solutions by HPLC method (No.3)

3. Precision

To validate precision, within run precision and between run precision were determined. The data of analysis are demonstrated in Table 22 and 23. The percentage of coefficient of variation (%CV) values of peak area in both within run and between run were low (0.45-1.55% and 0.62-2.95% respectively). Therefore, the HPLC condition could be used to analyze AS content over a period of time.

Table 20 Data of within run precision of AS analyzed by HPLC method

AS conc. ($\mu\text{g/mL}$)	Peak area					mean	SD	%CV
	n1	n2	n3	n4	n5			
12.62	24.1497	24.4998	24.2960	24.3826	24.0662	24.2788	0.1744	0.71
202.00	360.4747	362.2016	363.1097	363.2335	364.9644	362.7968	1.6381	0.45
1010.00	1786.3920	1784.3698	1791.0305	1804.7248	1851.9399	1803.6914	28.1153	1.55

4. Accuracy

The percentage of analytical recovery in each AS concentration with three determinations are shown in Table 24, 25 and 25. The mean percentage recoveries were 102.86%, 103.86% and 104.86% with low %CV values of 2.03%, 1.90% and 2.10% respectively. This result concluded that the HPLC method could be used to determine AS content within the concentration range of 12.5-1000 $\mu\text{g/mL}$.

Table 21 Data of between run precision of AS analyzed by HPLC method

AS conc. ($\mu\text{g/mL}$)	Peak area						
	N	Day 1	Day 2	Day 3	mean	SD	%CV
12.5	n1	24.4847	23.1906	23.5345	23.7366	0.67033	2.82
	n2	24.7824	23.7609	23.1241	23.8891	0.83657	3.50
	n3	24.7954	23.1779	23.6780	23.8838	0.82817	3.46
	n4	24.8161	23.6178	23.5636	23.9992	0.70797	2.94
	n5	24.4118	23.1954	23.5535	23.7202	0.62511	2.63
	Average	24.6581	23.3885	23.4907	23.8458	0.70533	2.95
202.00	n1	362.3245	364.9744	367.2977	364.8655	2.48842	0.68
	n2	364.8313	365.5012	368.1710	366.1678	1.76682	0.48
	n3	361.1984	364.5708	367.4594	364.4095	3.13361	0.85
	n4	365.1942	367.6294	372.6235	368.4823	3.78735	1.02
	n5	367.5836	371.5621	370.6640	369.9365	2.08663	0.56
	Average	364.2263	366.8475	369.2431	366.7723	2.50921	0.68
1010.00	n1	1801.2560	1798.9273	1811.9364	1804.0398	6.9370	0.38
	n2	1792.7301	1798.8469	1803.8757	1798.4840	5.5816	0.31
	n3	1796.5309	1805.7109	1814.6115	1805.6177	9.04065	0.50
	n4	1801.7787	1826.2025	1852.3259	1826.7690	25.2784	1.38
	n5	1852.9004	1868.4413	1876.2787	1865.8734	11.8988	0.63
	Average	1809.0392	1819.6257	1831.8056	1820.1568	11.3925	0.62

Table 22 Data of accuracy of AS analyzed by HPLC method (No.1)

Actual conc. (ug/mL)	Peak area			Mean	Mean analytical conc (ug/mL)	Percent discovery
	n1	n2	n3			
402.00	366.2490	364.5981	363.9654	364.9375	405.0063	100.75
523.00	498.1068	484.0508	497.8913	493.3496	548.7889	104.93
620.00	567.3511	573.8096	577.8068	572.9892	637.9609	102.90
					Mean	102.86
					SD	2.09
					%CV	2.03

Table 23 Data of accuracy of AS analyzed by HPLC method (No.2)

Actual conc. (ug/mL)	Peak area			Peak area	Mean analytical conc (ug/mL)	Percent discovery
	n1	n2	n3			
403.00	369.4244	366.8666	371.7329	369.3413	409.9373	101.72
525.00	491.4889	491.8709	511.8367	498.3988	554.4424	105.61
621.00	571.0460	581.2908	591.7548	581.3639	647.3380	104.24
					Mean	103.86
					SD	1.97
					%CV	1.90

Table 24 Data of accuracy of AS analyzed by HPLC method (No.3)

Actual conc. (ug/mL)	Peak area			Peak area	Mean analytical conc (ug/mL)	Percent discovery
	n1	n2	n3			
405.00	366.7828	365.9791	393.7480	375.5033	416.8368	102.92
526.00	486.9107	498.1558	495.8887	493.6517	549.1271	104.40
621.00	633.7080	579.5579	580.8177	598.0279	665.9966	107.25
					Mean	104.86
					SD	2.20
					%CV	2.10



VITA

NAME Ms. Hay Man Saung Hnin Soe
DATE OF BIRTH 25 December 1992
PLACE OF BIRTH Bago, Myanmar
INSTITUTIONS ATTENDED University of Pharmacy, Yangon, Myanmar
HOME ADDRESS 93 H, Pidauk Lane, Thuwanna, Yangon, Myanmar



จุฬาลงกรณ์มหาวิทยาลัย
CHULALONGKORN UNIVERSITY